TECHNISCHE UNIVERSITÄT MÜNCHEN

Klinik und Poliklinik für Kinder- und Jugendmedizin

Klinikum rechts der Isar

Direktor: Univ.-Prof. Dr. St. Burdach

Evaluation of potential biomarkers for Ewing´s sarcoma as cargo of tumor derived exosomes

Isabella Viktoria Miller

Vollständiger Abdruck der von der Fakultät für Medizin der Technischen Universität München zur Erlangung des akademischen Grades eines

Doktors der Medizin

genehmigten Dissertation.

Vorsitzender:		Univ.-Prof. Dr. E. J. Rummeny
Prüfer der Dissertation:	1.	Univ.-Prof. Dr. St. Burdach
	2.	Priv.-Doz. Dr. J. M. E. Teichert-von Lüttichau
	3.	Univ.-Prof. Dr. A. Krackhardt

Die Dissertation wurde am 31.10.2014 bei der Technischen Universität München eingereicht und durch die Fakultät für Medizin am 03.02.2016 angenommen.

Contents

List of Figures

List of Tables

List of Abbreviations

ALL	acute lymphoblastic leukemia
cDNA	complementary DNA
CM	confocal microscopy
CSF	cerebrospinal fluid
CTx	chemotherapy
ELISA	enzyme-linked immunosorbent assay
EM	electron microscopy
ES	Ewing's sarcoma
ESCRT	Endosomal sorting complex required for transport
ETS	E-twenty six
EV	extracellular vesicle
EWS	Ewing sarcoma breakpoint region 1
FBS	fetal bovine serum
FC	fold change
FCY	flow cytometry
FLI1	Friend leukemia virus integration 1
GEO	Gene Expression Omnibus
GSEA	gene-set enrichment analysis
ID	initial diagnosis
LC-MS	light chain mass spectrometry
MAA	microarray analysis
ML	magnetic ligation
mRNA	messenger RNA
miRNA	micro RNA
MRD	minimal residual disease
MSCs	mesenchymal stem cells
MV	microvesicle
MVB	multivesicular body
µNMR	micro nuclear magnetic resonance
NBL	neuroblastoma
NTC	no-template-control

PLA	proximity ligation assay
qRT-PCR	quantitative real-time polymerase chain reaction
RT	room temperature
SEM	standard error of the mean
siRNA	short interfering RNA
UC	ultracentrifugation
WB	western blot

Summary

The Ewing´s sarcoma (ES) is a highly malignant primary bone tumor of children and adolescents, which is characterized by early metastasis and high rates of relapse. The discovery of minimal residual disease (MRD) in peripheral blood by specific RNA based biomarkers is challenging, since, due to RNase degradation, free RNA is unstable in the blood. However, exosomes, 30-100 nm sized extracellular vesicles (EVs) implicated in intercellular communication, do, if released by ES, potentially protect ES specific RNA transcripts as circulating shuttles.

In this research project, for biomarker discovery ES specific transcripts were identified and detected in the cargo of the ES cell line derived EVs, this study gave first evidence of. Therefor, microarray analyses were re-evaluated, suggesting 12 highly expressed potential marker transcripts, of which five (STEAP1, LIPI, NR0B1, NKX2.2, EWS-FLI1) proved their specificity being undetectable by qRT-PCR in the blood of 20 healthy donors. These five transcripts are steadily expressed in ES cell line derived EVs, which hold features of exosomes, since they show a characteristic size and morphology in electron microscopy and bear the exosome specific surface proteins CD63 and CD81 in flow cytometry. Furthermore, ES cell line derived exosomes display a typical RNA spectrum and effectively protect their RNA cargo from RNase digestion. In order to develop a clinical application, in a pre-clinical *in vitro* model ES cell line derived exosomes were serially diluted in healthy donor plasma. After re-isolation, the marker transcripts were detected by qRT-PCR down to a concentration in the scope of the estimated exosome concentration in the blood of tumor patients. According to the results of this model, peripheral blood samples of seven ES patients were acquired. However, in the blood of ES patients no characteristic marker pattern separating them from healthy subjects was identified.

ES cell line derived exosomes were further examined for their potential functions, since tumor derived exosomes have been shown to serve as key players in tumor progression and metastasis. Therefore, exosomes of three ES cell lines underwent microarray analyses. ES cell line derived exosomes share a common transcriptional signature, which is implicated in g-protein coupled signaling, neurotransmitter signaling and stemness. Additionally, several oncogenic miRNAs are enriched in exosomes compared to their cells of origin. Since ES cell line derived exosomes appear to be taken up by other cell types, as shown for HEK293 cells in this study, it remains a deeply interesting question for future research, how tumor derived exosomes are involved in ES tumorigenesis.

1 Introduction

1.1 Ewing´s sarcoma

1.1.1 The Ewing family of tumors

The Ewing´s sarcoma (ES), a member of the Ewing family of tumors (ET), is the second most common primary bone cancer in children and adolescents after osteosarcoma. It arises with a peak incidence at the age of 15 (Riggi and Stamenkovic, 2007), approximately 80% of the patients are younger than 20 years (Lahl et al., 2008). Maintaining an incidence of 1-3 patients per million per year, ES is a rare, but, due to its high aggressiveness and early metastasis, fatal tumor. At diagnosis, 25% percent of ES have spread clinically detectable metastases (Bernstein et al., 2006; Schleiermacher et al., 2003) and it can be assumed, that an uncertainly higher number of patients already feature micrometastases. This contributes to the poor 5-year disease-free survival rate of 65-76% for localized ES patients treated multimodally with surgery, radiation and multi-agent chemotherapy (Miser et al., 2004; Burdach and Jürgens, 2002). All the worse, in a primarily metastatic situation, the 5-year disease-free survival rate is remarkably reduced to 27 % (Bernstein et al., 2006; Burdach et al., 1993, 2010).

The highly malignant phenotype of ES is in 85% driven by the specific translocation t(11;22)(q24;q12), which generates the aberrant transcription factor EWS-FLI1. EWS (Ewing sarcoma breakpoint region 1) is a strong transcription activator, while FLI1 (friend leukemia virus integration 1), as a member of the ETS (E-twenty six) family, provides a highly conserved DNA binding domain. 15% of the fusion products are combinations of EWS with alternative ETS family members, most commonly ERG (10%) (Delattre et al., 1992, 1994; Sorensen et al., 1994). This fusion oncoprotein induces the transcriptional dysregulation dictating the malignant behavior of ES. Thereby, thousands of genes are up- or downregulated by EWS-FLI1, some of which have been shown to be crucial for oncogenesis, such as NR0B1, NKX2.2, EZH2, PRKCB or STEAP1 (Toomey et al., 2010; Surdez et al., 2012; Grunewald et al., 2012).

Whereas the molecular origin of ES development is partly elucidated, the cellular origin remains unclear since the cell of origin could not be certainly determined yet. Firstly described as “diffuse endothelioma of the bone” by James Ewing in 1921, ES, which appears microscopically as a tumor of small blue round cells, has provoked many hypotheses about its histogenesis. Today, two of theses hypotheses dominate the ongoing debate: Whether the ES arises from a neural crest derived mesenchymal stem cell, according to the neural expres-

sion pattern in ES, or from a mesoderm-derived mesenchymal progenitor cell, which obtains a neural phenotype through EWS-FLI1 expression (Staege et al., 2004; von Levetzow et al., 2011; Tirode et al., 2007; Kauer et al., 2009).

1.1.2 RNA based markers for subclinical disease and their limitations

Caused by the late onset of specific symptoms, ES is mostly diagnosed in a progressive state. After multimodal therapy, 30-40% of ES patients incur a regression of the disease, despite intensive follow-up programs including MRI, FDG-PET/CT, technetium scintigraphy and bone marrow punctures (Stahl et al., 2011; Gerth et al., 2007). Due to the dismal outcome of relapsed disease (5-year overall survival after relapse is 13%), sensitive biomarkers, which provide an earlier detection of subclinical residual disease, are urgently required for a faster onset of rescue therapy (Stahl et al., 2011).

There have been several attempts to identify reliable markers in bone marrow or peripheral blood over the last two decades. Mostly, the detection of EWS-ETS fusion transcripts or proteins as the ontologically most specific marker was focus of research. In 1995, Peter et al. discovered circulating tumor cells in bone marrow and blood by nested RT-PCR, detecting one tumor cell in the scope of 10^6 blood cells (Peter et al., 1995). This observation was confirmed by other groups, which found in 20-30% of the patients with localized disease micrometastases in the bone marrow identifying EWS-ETS transcripts by RT-PCR. The record of these micrometastases is associated with an increased risk for recurrence and distant metastasis (Fagnou et al., 1998; Schleiermacher et al., 2003; Vermeulen et al., 2006). In some studies, tumor cells circulating in peripheral blood were found as well in up to 26% of ES patients, a correlation with patient outcome could only be proved for patients with localized disease (Fagnou et al., 1998; Schleiermacher et al., 2003).

Beyond EWS-FLI1, its highly overexpressed downstream targets suit as biomarker candidates, too. They are abundantly higher expressed in the ES cell transcriptome than EWS-FLI1, and additionally, they can be tested independently of the knowledge on the translocation type. Cheung et al. (2007) identified transcripts, which are highly specific for ES by gene expression array analysis. The undetectability of the designed marker panel, consistent of STEAP1, CCND1 and NKX2.2, in bone marrow could be strongly correlated with patients´ survival. Interestingly, the markers identified by Cheung et al. (2007) are included in the signature of 37 genes highly overexpressed in ES described in the study of Staege et al. (2004), which constituted the basis of this project.

Recapitulatory, sensitive detection of minimal residual disease (MRD) is possible, but limited in bone marrow and peripheral blood. Therefore, after-care is dominated by frequent imaging and bone marrow punctures. The identification of reliable markers in peripheral blood could partially replace radiation exposure and invasive procedures.

Adequate biomarkers, if RNA based, notably would have to fulfill two criteria: A high speci-

ficity for ES compared to all other human tissues and a conserved state in human peripheral blood.

1.2 Exosomes

Exosomes are small, 30-100 nm sized extracellular vesicles (EVs), which carry a functionally active cargo consistent of proteins, mRNAs and miRNAs (Bobrie et al., 2011; Pant et al., 2012). Thus, exosomes enable their cell of origin to transport their specifically sorted content to any other cell. This exchange of molecular information was postulated to constitute a new way of intercellular communication (Valadi et al., 2007).

1.2.1 Biogenesis and classification

Exosomes are produced by, as far as investigated, every cell type and can be found in most body liquids, such as plasma, urine, saliva, amniotic fluid, broncheoalveolar lavage, ascites and cerebrospinal fluid (Pant et al., 2012; Keller et al., 2011, 2009).

The hallmark of exosomes - in contrast to other, larger types of EVs (see table 1.1) - is their endosomal origin. In the cells´ late endosome, they are formed by inward budding of the endosomal membrane. During this process of invagination an endosomal sorting complex (either ESCRT- or ceramide-dependent) selectively loads the exosomal charge from the cytosol into the vesicles. At this point, the late endosome transforms into a multivesicular body, which will fuse later with the plasma membrane and release the exosomes into the extracellular space (figure 1.1).

Exosomes consist of a double lipid layer rich of cholesterol, sphingomyelin and ceramide. They bear numerous surface proteins, such as tetraspanins, including CD63 and CD81, antigen presentation proteins as MHC I and II, lipid raft associated proteins as flotillin 1 and adhesion molecules. Due to the process of double inward budding the orientation of the exosomal membrane proteins is the same as the cells. In their cargo characteristic proteins give evidence of their endosomal origin, such as components of the endosomal sorting complex (ESCRT, Alix and TSG101), heat shock proteins (especially Hsp70) and proteins involved in membrane transport and fusion, such as Rab and annexins (figure 1.2)(van der Pol et al., 2012).

Featuring these specific components, exosomes can clearly be distinguished from other types of EVs. Additionally, they exhibit different properties in electron microscopy, such as a size of 30-100 nm and the specific “cup shaped” morphology after fixation. They can further be characterized by their density on a sucrose gradient in the scope of 1.13-1.19 g/ml. In the past, the nomenclature of different types of EVs was often used unprecisely in literature. In this thesis the term exosomes or microvesicles is exclusively used for vesicles fulfilling the criteria listed in table 1.1. For vesicles which cannot definitely be classified, the term extracellular vesicles (EVs) will be utilized.

Figure 1.1: Biogenesis and components of exosomes

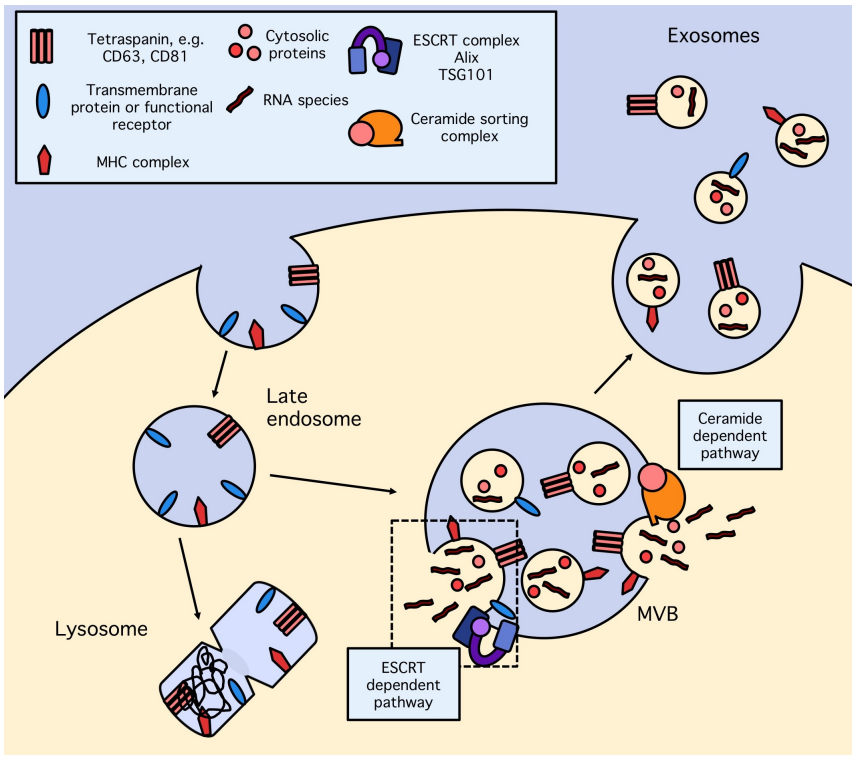

Lately evidence rises, that there are not only different types of EVs, but also several subclasses of exosomes. Methodologically, these subclasses cannot be separated so far, but the differentiation of exosome subclasses with distinct features and functions will be an important future field of research casting light upon the biological relevance of exosomes *in vivo*.

1.2.2 Communication pathways

Exosomes have been compared to a message in a bottle (Kharaziha et al., 2012), a trojan horse (Thébaud and Stewart, 2012) or an intercellular postal service - since the ways their message is delivered to the recipient cell are differential (figure 1.3).

Basically, exosomes use two distinct modalities of communication: surface receptor interaction and internalization.

As exosomes carry MHC receptors of both classes, they participate in antigen presentation and immunomodulation (Chaput and Thery, 2011). Yet, they bear a multitude of other membrane receptors that can activate specific pathways. In this context, it was reported that exosomes carry Wnt-proteins on their surface and induce Wnt signaling in the targeted cells (Gross et al., 2012).

The other mode of message delivery, internalization into the recipient cell, can occur through plasma membrane fusion or endozytosis of the exosome. In both cases a horizontal transfer of the exosomal content, which is functionally processed in the recipient cell, occurs. Intact RNA

Figure 1.2: Characteristic exosomal molecules

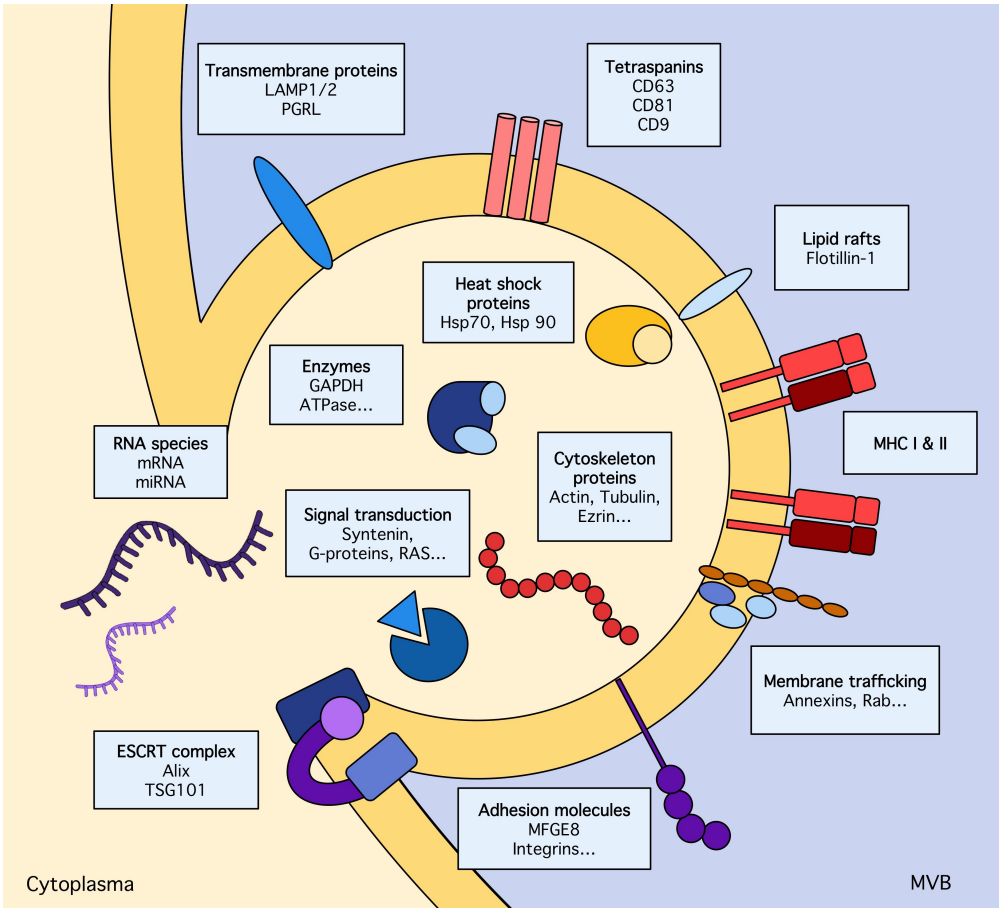

Table 1.1: Characteristics of the three main types of extracellular vesicles

Type	Origin	Diameter (nm)	Density (g/ml)	EM	Marker proteins
Exosomes	Endosome/ MVBs	30-100	1.13-1.19	cup shaped	CD63, CD81, Hsp70, Alix, TSG101
Microvesicles	membrane shedding	100-1000	Unknown	irregular	Integrins, selectins, CD40ligand
Apoptotic bodies	apoptotic blebbing	1000-5000	1.16-1.28	heterogenous	Histones, TSP, C3b

(van der Pol et al., 2012; Akers et al., 2013; Mathivanan et al., 2010; Taylor and Gercel-Taylor, 2013)

Figure 1.3: Exosomal communication pathways

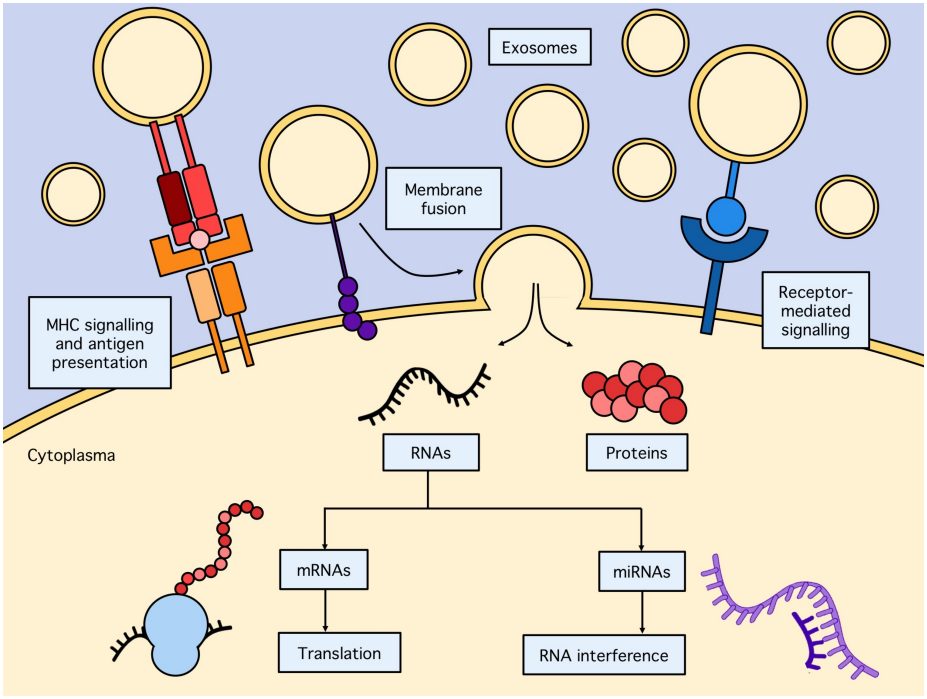

Figure modified from EL Andaloussi et al. (2013)

species including mRNAs and microRNAs proved to be transferred between cells modulating gene expression (Valadi et al., 2007). On protein level, it was shown that glioblastoma derived EVs deliver the oncogenic receptor EGVRvIII to glioblastoma cells lacking this mutation. In consequence they adapt the transformed phenotype (Al-Nedawi et al., 2008). Further research is required on the mechanism of recognition between exosome and target cell, navigating the selective exchange between defined cell types. It was hypothesized that tetraspanins contribute to these specific docking sites (Rana and Zöller, 2011).

Generally, exosomes can interact with cells in a juxtacrine - modulating the microenvironment - or a paracrine manner by release of exosomes into the circulation.

1.2.3 Roles in tumorigenesis

Exosomes fulfill pleiotropic physiological effects, as stem cell maintenance, tissue repair, immune surveillance and blood coagulation (EL Andaloussi et al., 2013). But they also play key roles in pathologic processes. Especially in cancerogenesis, there is increasing evidence that tumor derived exosomes influence the tumors environment in favor of tumor growth and metastasis via multiple mechanisms.

1.2.3.1 Immunosuppression

Tumor derived exosomes inherit immunosuppressive functions (Chaput and Thery, 2011). Thus, they are able to interact directly with CD8 positive T-cells and induce apoptosis via the Fas ligand. This was shown for several tumor cell lines, but also for tumor derived EVs gained from patient plasma and ascites (Kim et al., 2005; Andreola et al., 2002; Huber et al., 2005; Wieckowski et al., 2009; Peng et al., 2011). Furthermore, tumor derived exosomes induce the proliferation of regulatory T-cells (Szajnik et al., 2010), but inhibit the proliferation of T-cells dependent on interleukin 2 (Clayton et al., 2007). They suppress the function of natural killer cells via TGFβ (Szczepanski et al., 2011) and reduce their cytotoxicity by exposure of the NKG2D ligand on the exosomal surface (Ashiru et al., 2010; Clayton et al., 2008; Liu et al., 2006). EVs also affect dendritic cells by impairing their differentiation from myeloid precursors (Yu et al., 2007), while they promote the proliferation of myeloid suppressor cells instead (Liu et al., 2010; Chalmin et al., 2010). These interactions only display a part of the complex communication between tumor derived exosomes and the immune system, but they clearly contribute to the tumor´s undermining of immune surveillance.

On the other side, tumor derived exosomes also hold functions, which can promote immune response. Presenting antigens to DCs, tumor derived exosomes can provoke T-cell activation (Chaput and Thery, 2011).

1.2.3.2 Angiogenesis

Tumor growth requires angiogenesis, which is partly mediated by tumor derived exosomes. For instance, glioblastoma derived EVs were shown to induce massive growth of HUVEC cells in vitro (Skog et al., 2008). Some of the multiple underlying mechanisms of the activation of endothelial cells through tumor derived exosomes have been elucidated.

EGFR derived from cancer cells bound on the EV surface can activate endothelial cells via the autocrine VEGF/VEGFR-2 pathway (Al-Nedawi et al., 2009). Moreover, the uptake of tumor derived exosomes bearing tetraspanin 8 induces the expression of angiogenic genes in endothelial cells, such as Willebrand factor, Tspan8, VEGF and its receptor VEGFR-2, resulting in increased proliferation of endothelial cells (Nazarenko et al., 2010). Notch ligand Dll4 was shown to be delivered into endothelial cells by tumor exosomes, increasing the branching of vessels (Sheldon et al., 2010). Furthermore, exosomes can promote epigenetic changes in endothelial cells, for example by the exosomal transfer of miR-9 from melanoma cells to endothelial cells, inducing their migration and promoting angiogenesis *in vivo* by the JAK-STAT pathway (Zhuang et al., 2012).

1.2.3.3 Modulation of the microenvironment

Tumor cells can manipulate their environment by means of exosomes. Not only stromal cells are affected by tumor derived exosomes - neighbored tumor cells communicate among

themselves via exosomes. As mentioned in 1.2.2, glioblastoma cells harboring the mutated EGFRvIII receptor transfer this receptor towards glioblastoma cells lacking it. Subsequently, these glioblastoma cells develop the same, more malignant EGFRvIII dependent phenotype including morphological transformation and anchorage-independent growth (Al-Nedawi et al., 2008). In a similar manner, colon cancer cells expressing a mutant KRAS protein release exosomes with a significantly changed proteome, containing tumor-promoting proteins such as EGFR, SRC family kinases, integrin and the mutant KRAS itself. These exosomes were shown to be taken up by wild-type KRAS colon cancer cells, which adapt the behavior of the mutant KRAS cells, as enhanced cell growth and tumorigenicity (Demory Beckler et al., 2013).

However, the modulation of stromal cells by tumor derived exosomes seems to pave the way for progressive tumor development. It was reported on exosomes derived from different cancer cell lines, such as mesothelioma (Webber et al., 2010), gastric (Gu et al., 2012), mammary (Cho et al., 2012) and prostate carcinoma cells (Webber et al., 2014), that they convert stromal cells into tumor associated myofibroblasts, which support tumor growth, vascularization, and metastasis. Thereby, TGFβ associated with transmembrane proteoglycan betaglycan plays a key role by activating Smad-dependent signaling (Webber et al., 2010; Gu et al., 2012).

1.2.3.4 Metastasis

The transformation of stromal cells by exosomes, not in a juxtacrine, but in a paracrine manner, can furthermore prepare metastatic spread of the tumor.

Melanoma derived exosomes accumulate in sentinel lymph nodes and induce the recruitment of melanoma cells, angiogenesis and extracellular matrix remodeling in favor of metastasis (Hood et al., 2011). Peinado et al. (2012) showed that exosomes derived from highly metastatic melanoma cells are able to reprogram bone marrow progenitor cells by transfer of the oncoprotein MET. The exosomes induced a pro-vasculogenic phenotype, preparing a premetastatic niche. Metastatic burden was increased threefold in mice injected with melanoma cells and bone marrow progenitor cells which were primarily treated with melanoma exosomes compared to controls with untreated bone marrow progenitor cells.

Interestingly, in reverse stromal cells influence the tumor´s behavior with behalf of exosomes. This was shown for tumor associated fibroblasts in breast cancer, which produce exosomes stimulating breast cancer cell motility and metastatic spread activating the autocrine Wnt-PCP pathway (Luga et al., 2012). Contrarily, exosomes of bone marrow derived mesenchymal stem cells induce dormancy in breast cancer cells, reducing proliferation and chemosensitivity to docetaxel, probably to facilitate tumor cell survival in a metastatic niche (Ono et al., 2014).

1.2.3.5 Drug resistance

Historically exosomes were first described in their function as garbage shuttles, which transport cellular waste into the extracellular space. This function remains an important one, especially with regards to drug resistance mechanisms in tumor cells. Indeed, there is evidence that chemotherapy agents, such as cisplatin, are concentrated and removed from the cytosol by the release of exosomes (Safaei et al., 2005).

Beyond, there are several other exosome mediated mechanisms inducing tumor cell drug resistance. For instance, in breast cancer, exosomes from HER2-overexpressing cell lines as well as exosomes derived from patient plasma, bind trastuzumab and thus reduce the amount of the active antibody in the circulation (Ciravolo et al., 2012). The overexpression of drug transporters is crucial for the development of a tumor´s chemoresistance. Two studies revealed that exosomes enable tumor cells to exchange these drug transporters and hereby transfer their resistance (Gong et al., 2012; Corcoran et al., 2012). Prostate cancer cell lines, which are resistant towards docetaxel, release the responsible drug transporter MDR-, in their exosomes, which are taken up by sensitive cell lines resulting in chemoresistance (Corcoran et al., 2012). Similarly, adriamycin resistant breast cancer cells express high levels of TrpC5, which is required for adriamycin elimination via EV budding, and transfer TrpC5 mRNA to other cancer cells impairing their drug sensitivity (Ma et al., 2014).

1.2.4 Diagnostic implications as tumor markers

Since it has been investigated that extracellular vesicles carry a fingerprint of their cell of origin, that they are produced abundantly by some cancer entities and that they are released into the circulation, EVs arise as new opportunity for biomarker discovery. The idea of a "fluidome" or a "liquid biopsy" prompted an abundance of studies on exosomal biomarkers in cancer (Pant et al., 2012).

Conserving their nucleid acid cargo from degradation, EVs promised particularly to provide new potential in RNA diagnostics. In 2008, Skog et al. detected mRNA of the mutant EGFRvIII encapsulated in microvesicles in the plasma of glioblastoma patients (Skog et al., 2008). A year later, in exosome preparations of plasma of gastric cancer patients an abundantly higher amount of MAGE-1 and HER-2/neu transcripts than in healthy controls was found (Baran et al., 2010). In prostate cancer, the fusion transcript TM-PRSS2:ERG was detected in the urine of all individuals with a gleason score higher 7, PCA-3 transcript was found in all diseased subjects (Nilsson et al., 2009). Studies for specific transcripts, such as fusion proteins or their downstream targets, have in common that they share a high specificity, but a low sensitivity caused by the predominant background of EVs derived from normal tissues. To overcome this problem, new PCR techniques as BEAMing PCR and droplet PCR were applied. Hereby, the detection of tumor transcripts holding short mutations was considerably improved (Chen et al., 2013). In a different approach, whole transcriptome expression patterns

of patient plasma derived exosomes were compared to healthy controls by microarray analysis showing a definable signature in glioblastoma patients compared to healthy controls (Noerholm et al., 2012). Beyond mRNA, an abundance of other small RNAs, coding or non-coding, is element of the exosomal cargo. Great diagnostic value is foremost ascribed to miRNAs. In many cancer entities, as breast (Corcoran et al., 2011), lung (Rabinowits et al., 2009), ovarian (Taylor and Gercel-Taylor, 2008), prostate (Bryant et al., 2012), colorectal (Ogata-Kawata et al., 2014) and esophageal carcinoma (Takeshita et al., 2013; Tanaka et al., 2013), specific miRNA patterns were found within patient plasma derived exosomes.

On the protein level, interesting studies can be found especially in melanoma and ovarian cancer, where tumor derived proteins could not only be detected in plasma, but also in ascites (Logozzi et al., 2009; Peinado et al., 2012; Li et al., 2009; Keller et al., 2009).

The source of exosomes derived from urine, as a body fluid with easy, uninvasive and unlimited access to samples, is even more favorable. Contrarily to exosomes enriched from peripheral blood, these exosomes additionally have direct contact to the fluid. Thus, research on exosome tumor markers has partly focused on prostate and bladder cancer.

For a more detailed description of all mentioned exosomal tumor markers and an overview on all relevant studies in this field see table 1.2.

Despite the plethora of promising approaches, broad studies on the diagnostic or predictive value of exosomal biomarkers in plasma are lacking. Eminent reason is the remaining variety in the method of exosome isolation, ranging from different ultracentrifugation protocols over ELISA techniques to magnetic ligation assays. A further step towards the simplification of exosome diagnostics is a new method called ExoScreen developed by Yoshioka et al. (2014) for colorectal cancer, which renders the lossy step of exosome purification. Instead, tumor derived exosomes were identified by antibody coupled photosensitizer-beads, reducing preparation time and probe volume, but not impairing test sensitivity (Yoshioka et al., 2014).

Furthermore, the compound of the exosomal cargo underlies a fluctuation dependent on tumor state, therapy and unknown factors requiring a deeper understanding of these mechanisms for biomarker identification on the one side (Tickner et al., 2014), but, if closely monitored, reflecting treatment response on the other side (Shao et al., 2012; Ma et al., 2014).

Table 1.2: EVs as cancer biomarkers

Cancer entity	Fluid	Methods	Marker	Name	Outcome	Ref
Glioblastoma	Plasma	UC/ RT-PCR	miRNA, mRNA	miR-21, EGFRvIII	The tumor-specific EGFRvIII was detected in serum EVs from 7 of 25 glioblastoma patients.	Skog et al. (2008)
	Plasma	UC/ MAA	mRNA	up- or downregulated transcripts in patient exosomes	Unsupervised clustering separates GBM patients (n=9) from controls (n=7) in expression array analysis.	Noerholm et al. (2012)
	Plasma	µNMR	Protein	EGFR, EGFRvIII, PDPN, IDH1 R132H	Markers in combination: Sensitivity 92%, specificity 88%.	Shao et al. (2012)
	CSF	UC/ ddPCR, BEAMing PCR	mRNA	IDH1	Detection of mutant IDH1 in 5 of 8 CSF samples.	Chen et al. (2013)
Melanoma	Plasma	ExoTest/ WB	Protein	CD63, caveolin-1	Plasma exosome concentration significantly higher in melanoma patients (P=0.001 for both CD63+ and Cav1+ exosomes). Levels of Cav1+ exosomes significantly higher than levels of CD63+ exosomes in melanoma patients (P = 0.004). Sensitivity of caveolin-1 68%.	Logozzi et al. (2009)
	Plasma	UC/ WB	Protein	TYRP2, VLA-4, HSP90, MET	All increased at stage 4 disease, TYRP2 and MET also increased at stage 3 disease.	Peinado et al. (2012)
Ovarian cancer	Plasma	UC/ MS	Protein	Claudin-4	32 of 63 plasma samples positive, sensitivity 51%.	Li et al. (2009)
	Ascites, Plasma	UC/ MS	Protein	EpCAM, ADAM10, EMMPRIN, pro-herperanase	Each marker was detected in at least 3 of 6 patient ascites samples, ADAM 10 in 4 of 6 plasma samples.	Keller et al. (2009)

Cancer entity	Fluid	Methods	Marker	Name	Outcome	Ref
	Plasma	ML/ MAA	Protein/ miRNA	EpCAM, miR-21, miR-141, miR-200a, miR-200c, miR-200b, miR-203, miR-205 and miR-214	Amount of circulating EpCAM-positive extracellular vesicles increased with disease progression. Exosomal microRNA from ovarian cancer patients (n=50) exhibited similar profiles, which were significantly distinct from profiles observed in benign disease (n=10).	Taylor and Gercel-Taylor (2008)
Breast cancer	Plasma	nn/ RT-PCR	miRNA	miR-21	Upregulated in 10 patient samples.	Corcoran et al. (2011)
	Plasma	UC/RT-PCR	mRNA	TrpC5, flotillin 2, mdr1, and MUC1	All significantly elevated in EVs in 17 of 33 samples of patients under chemotherapy, not in 12 patients without chemotherapy.	Ma et al. (2014)
Lung cancer	Plasma	ML/ MAA	protein/ miRNA	EpCAM, miR-17-3p, miR-21, miR-106a, miR-146, hmiR-155, miR-191, miR-192, miR- 203, miR-205, miR-210, miR-212 and miR-214.	Mean EpCAM-positive exosome concentration of 2.85 mg/mL in lung adenocarcinoma group (n=27), 0.77 mg/mL in control group (n=9) (P < .001). Mean exosomal miRNA concentration 158.6 ng/mL versus 68.1 ng/mL in control group (P < .001). 12 miRNAs, which proved to be upregulated in lung cancer, could be detected in plasma derived exosomes.	Rabinowits et al. (2009)
	Plasma	ML/ RT-PCR	miRNA	let-7f, miR-30e-3p	Levels of let-7f, miR-20b and miR-30e-3p decreased in plasma EVs of NSCLC patients (n=78) compared to controls (n=48). (Levels of let-7f and miR-30e-3p distinguished between two groups of patients for stage of disease and therefore possibility of surgery and were associated with short disease-free survival and overall survival)	Silva et al. (2011)

Cancer entity	Fluid	Methods	Marker	Name	Outcome	Ref
Oral squamous cell carcinoma	Plasma	UC/ WB	Protein	FasL	FasL-positive EVs detected in sera of 21 of 27 patients, EV-bound FasL expression correlates with tumor burden and lymph node status.	Kim et al. (2005)
Esophageal squamous cell carcinoma	Plasma	UC/ RT-PCR	miRNA	miR-1246	71.3% sensitivity and 73.9% specificity for distinguishing ESCC patients from healthy controls, correlated with the TNM stage.	Takeshita et al. (2013)
	Plasma	Exo Quick/ RT-PCR	miRNA	miR-21	Expression of serum miR-21 in the patient group was significantly increased compared to control group (P= .0009); positive lymph node status and metastasis associated with higher exosomal miR-21 expression.	Tanaka et al. (2013)
Gastric cancer	Plasma	UC/ RT-PCR	mRNA	MAGE-1, HER-2/neu	MAGE-1 mRNA expression 2^{10}-fold higher in patient´s samples (n=5) than in controls (n=5), HER-2/neu expression 2^{3}-fold.	Baran et al. (2010)
Colorectal cancer	Plasma	UC/CM/ FCY/ WB	Protein	EpCAM, Flotillin for exosomal protein amount	Amount of exosomes in cancer patients (n=91) was statistically higher than in healthy controls (n=12) (mean rank = 53.93 vs. 24.35). High levels of exosomes are associated with low differenciation and poor overall survival.	Silva et al. (2012)
	Serum	Exo Screen	Protein	CD147	CD147 positive EVs significantly higher in patient serum (n=194) than in healthy serum (n=191)	Yoshioka et al. (2014)
	Serum	UC/MA	miRNA	let-7a, miR-1229, miR-1246, miR-150, miR-21, miR-223, miR-23a	All significantly higher in patients than controls, miR- 23a and miR-1246 sensitivity of 95% and 90% in stage I.	Ogata-Kawata et al. (2014)

Cancer entity	Fluid	Methods	Marker	Name	Outcome	Ref
	Ascites	UC /LC-MS	Protein	Set of colon cancer progression associated proteins	Detection of colon cancer progression associated proteins in ascites of 3 patients.	Choi et al. (2011)
Prostate cancer	Plasma	PLA/ RT-PCR	Protein	Prostasome surface antigens	The median prostasome levels in blood plasma of patients (n=20) were 2.5 to 7-fold higher compared to control samples (n=20), distinguished patients with high and medium Gleason scores.	Tavoosidana et al. (2011)
	Plasma	UC/WB	Protein	Survivin	Expression in patients (n=19) significantly higher than in BPH (n=20)/healthy (n=6) probes ($p<0.001$), independent from Gleason score ($p<0.05$).	Khan et al. (2012)
	Urine	UC	mRNA	PCA-3, TM-PRSS2: ERG	TMPRSS2:ERG detected in untreated patients with gleason score 7 to 9 (2/4), PCA-3 detected in all untreated patients (4/4). Both markers not detected in treated patients or patients after prostatectomy.	Nilsson et al. (2009)
	Urine	UC/WB	Protein	PSA, PSMA, 5T4	PSA in 8/20, PSMA in 9/20, 5T4 in 14/20 patient samples positive, all negative in 10 controls. No correlation between cancer stadium and quantity of exosomes in urine.	Mitchell et al. (2009)
	Urine	UC	Protein	delta-catenin	Immunoreactivity of delta-catenin associated with tumor activity: Sensitivity 87,5%, Specifity 83,3%.	Lu et al. (2009)
	Urine	Filtration/ RT-PCR	miRNA	miR-107 and miR-574-3p	miR-107 and miR-574-3p are significantly higher in urine of patients (n=115) than benign (n=17) controls ($p<0.001$ and $p<0.012$).	Bryant et al. (2012)

Cancer entity	Fluid	Methods	Marker	Name	Outcome	Ref
Bladder cancer	Urine	UC/ LC-MS/WB	Protein	mucin 4, EPS8L2, EPS8L1, Resistin, GTPase NRas, RAI3, and others	Nine proteins were differentially expressed between patient (n=4) and control(n=5) samples, verfied for mucin 4 and EPS8L2 in 2 more samples and controls.	Smalley et al. (2008)
	Urine	UC/ LC-MS	Protein	Basigin, 5T4, CD36, CD44, CD73	Elevated exosomal CD36, CD44, 5T4, basigin, and CD73 in cancer of 1 patient sample compared to 1 control.	Welton et al. (2010)

ExoTest	In-house sandwich ELISA for CD63 and Rab-5b
ExoScreen	Amplified luminescent proximity homogeneous assay
ExoQuick	Commercial precipitation assay

1.3 Research objectives

1.3.1 Aim of the project

It has been the underlying aim of this MD thesis to investigate biomarkers for ES in the form of specific transcripts in peripheral blood. The project was based on the hypothesis that the ES produces exosomes containing and thus protecting these transcripts from degradation. Furthermore, the encapsulation of transcripts in exosomes offers an approach to enrich them in human plasma.

In the present study the author selected biomarker transcripts highly specific for ES, proved the existence of ES derived exosomes, described their characteristic features and detected the elected transcripts in their functionally active RNA cargo. Moreover, the author showed that these transcripts can be effectively enriched *in vitro* via exosome preparation and that they are protected from RNase degradation. In a pre-clinical plasma model exosomes diluted in healthy donor plasma could be re-detected to a high degree of sensitivity. Nevertheless, the transcripts could not be detected in the exosome concentrate of seven patient plasma samples tested.

Furthermore, the author explored some of the biological roles of exosomes in ES tumorigenesis by direct immunofluorescence and microarray analysis.

1.3.2 Key questions

1. Which transcripts could serve as potential biomarkers for ES in peripheral blood?
2. How can the sensitivity of biomarker detection be increased?
3. Does the ES produce exosomes?
4. Do these exosomes contain ES specific transcripts?
5. Does exosome enrichment indeed increase the test sensitivity?
6. Do exosomes serve as vehicles for potential biomarkers in plasma?
7. What can further be mentioned about the possible biological role of exosomes in ES tumorigenesis?

2 Materials and Methods

2.1 Materials

2.1.1 List of Manufacturers

Manufacturer	Location
Abcam	Cambridge, UK
Abgent	San Diego, California, USA
AEG	Nürnberg, Germany
Agilent	Santa Clara, CA, USA
Ambion	Austin, Texas, USA
Amersham Biosciences	Piscataway, New Jersey, USA
Applied Biosystems	Darmstadt, Germany
ATCC	Rockyville, Maryland, USA
B. Braun Biotech Int.	Melsungen, Germany
BD Biosciences Europe	Leverkusen, Germany
Beckman Coulter	Brea, California, USA
Becton Dickinson (BD)	Heidelberg, Germany
Biochrom	Berlin, Germany
BioRad	Hercules, California, USA
Biozym	Hess. Olendorf, Germany
Brand	Wertheim, Germany
Branson	Dietzenbach, Germany
DSMZ	Braunschweig, Germany
Electron Microscopy Sciences	Hatfield, PA, USA
Eppendorf	Hamburg, Germany
Exiquon	Vedbaek, Denmark
Falcon	Oxnard, California, USA
FEI Company	Eindhoven, The Netherlands
Fermentas	St. Leon-Rot, Germany
GLW	Würzburg, Germany
Greiner	Nürtingen, Germany
Heraeus	Hanau, Germany

IBM Corporation	Armonk, New York, USA
Invitrogen	Darmstadt, Germany
Keen View	Münster, Germany
Kern	Balingen, Germany
Leica	Wetzlar, Germany
Lonza	Basel, Switzerland
Merck	Darmstadt, Germany
Millipore	Billerica, Massachusetts, USA
Molecular BioProducts, MbP	San Diego, California, USA
Nalgene	Rochester, New York, USA
Nikon	Düsseldorf, Germany
Nunc	Naperville, USA
Peske OHG	Munich, Germany
Philips	Hamburg, Germany
Qiagen	Hilden, Germany
R&D Systems	Minneapolis, Minnesota, USA
Roche	Mannheim, Germany
(Carl) Roth	Karlsruhe, Germany
Santa Cruz Biotechnology	Santa Cruz, CA, USA
Sarstedt	Nürnbrecht, Germany
Sartorius	Göttingen, Germany
Scotsman	Vernon Hills, IL, USA
Sempermed	Vienna, Austria
Siemens	Munich, Germany
Sigma	Deisenhofen, Germany
Syngene	Cambridge, UK
Taylor-Wharton	Theodore, AL, USA
Thermo Fisher Scientific	Ulm, Germany
TPP	Trasadingen, Switzerland
Zeiss	Jena, Germany

2.1.2 General materials

Material	Manufacturer
Cryovials	Nunc
Cuvettes	Roth
EDTA-coated collection tubes (9 ml)	Sarstedt
Filters for solutions (0.1, 0.2 and 0.45 µm)	Sartorius

Flasks for cell culture (25, 75 and 150 cm^2)	TPP
Gloves (nitrile, latex)	Sempermed
Hypodermic needle (23 and 30G)	B. Braun Biotech Int.
Pasteur pipettes	Peske OHG
Pipettes (2, 5, 10 and 25 ml)	Falcon
Pipette tips (10, 200 and 1,000 µl)	MbP
Pipette filter tips (10, 200 and 1,000 µl)	Biozym
Plates for cell culture (6-, 24- and 96-well)	TPP
Tubes for cell culture (polystyrene, 15 ml)	Falcon
Tubes for cell culture (polypropylene, 15 and 50 ml)	Falcon
Tubes for molecular biology, Safelock (1.5 and 2 ml)	Eppendorf
Tubes for flow cytometry (5 ml)	Falcon
Tubes for supercentrifugation (PP, 50 ml)	Sorvall
Tubes for ultracentrifugation rotor 70.1 Ti (PA, 13.5 ml)	Beckman Coulter
Tubes for ultracentrifuation rotor SW41 Ti (PA, 13.2 ml)	Beckman Coulter

2.1.3 Instruments and equipment

Device	Specification	Manufacturer
Bioanalyzer		Agilent
Ice maker	AF 100	Scotsman
Cell counting chamber	Neubauer	Brand
Centrifuge	Multifuge 3 S-R	Heraeus
Centrifuge	Biofuge fresco	Heraeus
Centrifuge	5417R	Eppendorf
Controlled-freezing box	Mr. Frosty	Nalgene
Electrophoresis chamber		BioRad
Flow cytometer	FACScalibur™	Becton Dickinson
Freezer (-80°C)	Hera freeze	Heraeus
Freezer (-20°C)	cool vario	Siemens
Fridge (+4°C)	cool vario	Siemens
Gel documentation	Gene Genius	Syngene
Heating block	Thermomixer Comfort	Eppendorf
Incubator	Hera cell 150	Heraeus
Liquid nitrogen reservoir	L-240 K series	Taylor-Wharton
Micropipettes	(0.5-10 µl, 10-100 µl, 20-200 µl, 100-1,000 µl)	Eppendorf

Microscope (fluorescence)	AxioVert 100	Zeiss
Microscope (electron)	CM120 Twin FEIelectron microscope	FEI Company
Microscope	Nikon Eclipse TS 100	Nikon
Microwave oven		Siemens, AEG
Multichannel pipette	(10-100 µl)	Eppendorf
Numeric camera	soft imaging system	Keen View
PCR cycler	iCycler	BioRad
Pipetting assistant	Easypet	Eppendorf
Precision balance	ABS/ABJ	Kern
Real-time PCR	7300 Real-Time PCR	Applied Biosystems
Rotator		GLW
Shaking incubator		Eppendorf
Spectrophotometer	GeneQuant II	Amersham Biosciences
Sonicator	Digital Sonifier®	Branson
Sterile bench		Heraeus
Supercentrifuge	RC 6	Sorvall
Ultracentrifuge	Optima XL-90	Beckman Coulter
Ultracentrifuge rotor	70.1 Ti	Beckman Coulter
Ultracentrifuge rotor	SW 41 Ti	Beckman Coulter
Water bath		GFL GmbH
Vortexer	Vortex-Genie 2	Scientific Industries

2.1.4 Chemical and biological reagents

Chemical or reagent	Manufacturer
Agarose	Invitrogen
AmpliTaq DNA Polymerase	Invitrogen
β-mercaptoethanol	Sigma
Blue Juice Gel Loading Buffer	Invitrogen
Bradford reagent	BioRad
BSA (bovine serum albumin)	Sigma
Calcein AM	Merck
DEPC (diethylpyrocarbonate)	Sigma
dNTPs	Roche
DMEM medium	Invitrogen
DMSO (dimethyl sulfoxide)	Merck
EDTA (ethylenediaminetetraacetate)	Merck

EtBr (ethidium bromide)	BioRad
Ethanol	Merck
FBS (fetal bovine serum)	Biochrom
Gentamicin	Biochrom
Glutaraldehyde	Electron microscopy sciences
Glycine	Merck
HCl (hydrochloric acid)	Merck
Isopropanol	Sigma
L-glutamine	Invitrogen
Methanol	Roth
Methylcellulose	Electron microscopy sciences
NaOH (sodium hydroxide)	Merck
PBS 10x (phosphate buffered saline)	Invitrogen
PCR buffer (10x)	Invitrogen
PFA (paraformaldehyde)	Invitrogen
Propidium iodide	Sigma
Ready-Load 1.0 and 0.1 Kb DNA Ladder	Invitrogen
RNaseZap®	Invitrogen
RPMI 1640 medium	Invitrogen
Tris	Merck
Trypan Blue	Sigma
Trypsin / EDTA	Invitrogen
Uranyl acetate	Electron microscopy sciences

All reagents were purchased from Sigma (Deisenhofen, Germany) if not otherwise specified.

2.1.5 Commercial reagent kits

Name	Manufacturer
High-Capacity cDNA Reverse Transcription Kit	Applied Biosystems
miRCURY RNA Isolation Kit	Exiquon
QIAamp® UltraSens™Virus Kit	Qiagen
RNeasy® Mini Kit	Qiagen
TRI Reagent RNA Isolation Kit	Ambion
TaqMan® Gene Expression Assays	Applied Biosystems
MycoAlert Mycoplasma Detection Kit	Lonza
GeneChip Whole Transcript Sense Target Labeling Kit	Affymetrix

2.1.6 Media, buffers and solutions

2.1.6.1 Cell culture media and universal solutions

Standard Medium	500 ml RPMI 1640 or DMEM, 10% fetal bovine serum (FBS), 2 mM L-glutamine, 1 mg gentamicin
PBS	10x PBS diluted 10 times in autoclaved water
4% paraformaldehyde	4% PFA in 1xPBS, adjusted to pH 7.4 with NaOH
Trypsin	
Freezing medium	10% DMSO in FCS

2.1.6.2 Buffer and gel for DNA/RNA electrophoresis

TAE running buffer	50xTAE: 2 M Tris, 10% EDTA (0.5 M), 5.71% HCl
Electrophoresis gel	200 ml TAE buffer (1x), 2% agarose, 4 µl EtBr

2.1.6.3 Buffers, solutions and antibodies for flow cytometry

Blocking buffer	Glycine 1M		
Staining buffer	PBS/0,5% BSA		
Latex beads	Aldehyd/sulfate latex 4% w/v 4µm		Invitrogen
Primary antibodies	CD63	sc-5275	Santa Cruz
	CD81	sc-7637	Santa Cruz
	Calnexin	sc-80645	Santa Cruz
	GM130	ab76154	Abcam
Secondary antibodies	goat anti mouse IgG1-FITC	sc-2078	Santa Cruz
	goat anti rabbit IgG1-FITC	sc-2012	Santa Cruz
Isotype antibodies	mouse IgG1		Santa Cruz
	rabbit IgG1		Santa Cruz

2.1.6.4 Human cell lines

All human cell lines were purchased from the German Collection of Microorganisms and Cell Cultures (DSMZ), except for the human A673 ET cell line, which was purchased from ATCC (LGC Standards). The human SB-KMS-KS1 ET cell line was established in the Laboratory of Functional Genomics of Department of Pediatrics (TU München).

The following human cancer cell lines were used:

Table 2.1: Human cancer cell lines

A673	ET cell line (type 1 translocation) established from the primary tumor of a 15-year-old girl
cALL2	Acute lymphoblastic leukemia (ALL) cell line established in 1993 from peripheral blood of a 15-year-old Caucasian girl
CHP126	Neuroblastoma cell line with N-MYC amplification established in 1973 from a stage III tumor of a 14-month-old girl
MHH-ES1	ET cell line (type 2 translocation) established from ascites of a 12-year-old Turkish boy with a pelvic ET and peritoneal metastases
MHH-NB11	Neuroblastoma cell line established from an adrenal metastasis of a 4-year-old Caucasian boy
Nalm6	B precursor leukemia cell line established in 1976 from peripheral blood of a 19-year-old man with relapsed ALL
RDES	ET cell line (type 2 translocation) established in 1984 from the primary tumor (humerus) of a 19-year-old Caucasian man
SB-KMS-KS1	ET cell line (type 1 translocation; initially designated SBSR-AKS) established from an inguinal metastasis of a 17-year-old girl
SHSY5Y	Neuroblastoma cell line established in 1970 from bone marrow of a 4-year-old girl
SIMA	Neuroblastoma cell line with N-MYC amplification established in 1991 from a stage III tumor of a 20-month-old Caucasian boy
SK-ES1	ET cell line (type 2 translocation) established in 1971 from an 18-year-old man
SK-N-MC	ET cell line (type 1 translocation) established in 1971 from a supraorbital metastasis of an Askin's tumor (ET of the chest) of a 14-year-old girl
TC-71	ET cell line (type 1 translocation) established in 1981 from a locally relapsed ET (humerus) of a 22-year-old man

2.1.6.5 Primer assays used for quantitative Real-Time PCR (qRT-PCR)

Primers were purchased as specific TaqMan Gene Expression Assays from Applied Biosystems:

STEAP1	Hs00185180_m1
LIPI	Hs01017703_m1
NR0B1	Hs00230864_m1
NKX2.2	Hs00159616_m1
GPR64	Hs00971379_m1
EZH2	Hs00544830_m1
NPY1R	Hs00168565_m1
ITM2A	Hs01011360_g1
DKK2	Hs00205294_m1
PRKCB	Hs00176998_m1
B2M	Hs00187842_m1
GAPDH	Hs99999905_m1
ACTB	Hs01060665_g1

For the detection of the EWS-FLI1 fusion transcript, the following primers were used:

sense	5'-TAGTTACCCACCCCAAACTGGAT-3'
antisense	5'-GGGCCGTTGCTCTGTATTCTTAC-3'
probe	5'-FAM-CAGCTACGGGCAGCA-TAMRA-3'

2.2 Methods

2.2.1 Cell culture conditions and cell cryoconservation

All cell lines were cultured in RPMI 1640 medium (Invitrogen) containing 10% FBS (Biochrom), 1% L-glutamine and 100 µg/ml gentamicin (Invitrogen). They were grown at 37°C in a humidified atmosphere containing 5% CO_2. Approximately every 4 days, cells were split 1:4 into larger culture flasks and cultured in 30 ml fresh medium.

For cell cryoconservation, $1 \cdot 10^6$cells per ml FBS/10% DMSO were frozen at -192°C in liquid nitrogen. Therefore, the harvested cell pellet was diluted in an adequate volume of cool FBS/10% DMSO. 1 ml aliquots of this suspension were transferred into cryovials, which were pre-cooled on ice. To avoid membrane rupture, for the first 24h the cryovials were stored in controlled freezing boxes at -80°C before they were placed in liquid nitrogen.

For re-culturing, the frozen cells were thawed at room temperature (RT) until the content was liquid enough to be quickly transferred into a tube containing 5 ml of standard media. Then, the cells were centrifuged 1,500 rpm for 5 min, resuspended in 1ml of media and transferred into T75 culture flasks containing 10 ml of pre-warmed standard medium.

The quantity of cells was determined using a Neubauer hemocytometer after the cells were stained with Trypan-Blue (Sigma) to check the cell viability.

Cell lines were routinely controlled for mycoplasma contamination using MycoAlertTM Mycoplasma Detection Kit according to the manufacturer's instructions (Lonza) and for purity (status of EWS-ETS fusion transcript in ES cell lines, checked by PCR).

Due to the fact that FBS contains bovine exosomes, for most of the experiments the media first had to be cleared from FBS-derived exosomes. Therefore, FBS was ultracentrifuged for 2 h at 100,000g to pellet and discharge the bovine serum exosomes, before it was collected and added to the RPMI 1640 media.

2.2.2 Provenience of blood samples and plasma preparation

Human blood samples were obtained with IRB approval from the Faculty of Medicine of the Technische Universität München (TUM) under the Neo-Ident study (approval no: 2562/09). All donors gave written informed consent. Peripheral blood samples were obtained from 23 healthy adult donors, whose health status was checked by a standardized questionnaire (see Appendix). Peripheral venous blood was drawn into 9 ml EDTA-coated collection tubes (Sarstedt) and centrifuged for 7 min at 2,200 rpm. Plasma was carefully transferred into a new tube, centrifuged for 15 min at 4,000 rpm to remove platelets. Then it was filtered through a 0.45 µm filter (Sartorius) and centrifuged again at 4,000 rpm for 3 min to clear it from debris. All centrifugation steps were performed at 4°C. Plasma samples were stored at -80°C if they were not used immediately for RNA extraction or exosome enrichment.

For negative controls (see section 3.1.3) two 9 ml tubes were required from each donor, for dilution experiments (see section 2.2.3.4) 15 9 ml tubes were taken and for exosome enrichment from patient or control plasma (see section 3.5.2) three 9 ml tubes were necessary.

In order to facilitate the co-operation with the clinic, to check the tumor stage and pre-treatment of the patient and for the sake of determining the dates of the blood withdrawal, a form to be filled in by the attending doctor was designed (see Appendix).

2.2.3 Exosome preparation

Exosomes were isolated from the cell culture supernatant of A673, SK-N-MC, and SB-KMS-KS1 ES cell lines using the ultracentrifugation protocol previously described by Thery et al. (2006) (figure 2.1).

2.2.3.1 Cell culture

ES cells at 80% confluency were washed thrice with PBS and cultured in fresh RPMI 1640 media containing 10% exosome-depleted FBS (see 2.2.1), 1% glutamine and 100 µg/ml gentamycin (both Invitrogen). The supernatant of at least four T150 cell culture flasks (or circa $250{\cdot}10^6$ cells, respectively) was used for exosome production of one cell line.

Figure 2.1: Procedure of exosome preparation

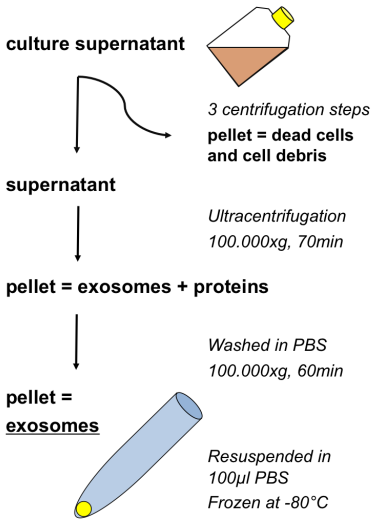

2.2.3.2 Ultracentrifugation

After 48 to 72 h the supernatant was collected and centrifuged in a Hereaus Multifuge 3 S-R at 300g for 10 min and at 2,000g for 10 min discarding the cell pellet. Then the supernatant was transferred into polypropylene supercentrifugation tubes (Nalgene) and centrifuged at 10,000g for 30 min in a Sorvall RC 6 supercentrifuge with a SS-34 rotor to clear it from cellular debris. Subsequently, the supernatant was transferred into polyallomer ultracentrifugation tubes (Beckman Coulter) and the filling volume was adjusted (up to 0.01 g) using a precision balance (Kern) before ultracentrifugation at 100,000g for 70 min was started to collect the exosomes. Afterwards, the supernatant was discharged by tipping it out quickly (this proved to be more preserving than taking it off with a pipet boy) and carefully removing remaining drops of medium with a pipette. In a second step, the mostly invisible exosome pellets were pooled, resuspended in PBS and once more ultracentrifuged at 100,000g for 60 min using an Optima XL-90 ultracentrifuge with a 70.1 Ti rotor (both Beckman Coulter).

Exosomes from human plasma samples were isolated by ultracentrifugation at 110,000g for 120 min using a SW 41 Ti rotor (Beckman Coulter).

The correct number of revolutions per minute at 100,000g or 110,000g for the respective rotor was calculated by means of the formula

$$rpm = \sqrt{\frac{g}{1.12 \times 10^{-6} \times r}}$$

The final exosome pellet was resuspended in 10 to 100 ml PBS. All centrifugation steps were carried out at 4°C.

2.2.3.3 Quantification and storage

The amount of harvested exosomes was estimated by measuring the protein content with a commercial Bradford assay (Bio-Rad). For this purpose, 5 µl of the resuspended exosome pellet were diluted with 5 µl of PBS. Then 1 ml of 1:5 diluted Bradford solution (Bio-Rad) was added. After 3 min, protein concentrations were measured photometrically at 595 nm and referenced to nine defined BSA standards (1. PBS, 2. 15.5 µg/ml, 3. 31 µg/ml, 4. 62 µg/ml, 5. 125 µg/ml, 6. 500 µg/ml, 7. 1,000 µg/ml, 8. 2,000 µg/ml, 9. 4,000 µg/ml). The average amount of exosomes harvested from supernatant of $1{\cdot}10^6$ A673 and SK-N-MC cells after 48 h incubation was 0.8 µg.

Figure 2.2: Amount of exosomes harvested from $1{\cdot}10^6$cells

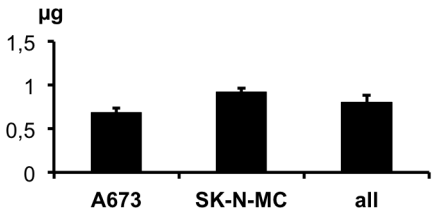

All exosome pellets were stored at -80°C if they were not used immediately for subsequent analyses.

2.2.3.4 Dilution experiments

As a pre-clinical plasma model, ES cell line derived exosomes were diluted in healthy donor plasma. It was based on a calculation that involved data of the usual exosome yields (0.8 µg protein equivalent of $1{\cdot}10^6$ cells in 48 h) as well as estimates about the possible behavior of ES exosomes *in vivo*. Based on previously published data it can be assumed that exosomes could be stable in blood for 8 days (Thery et al., 2006) and that more than 2% of the exosomes of a clinical ES would be released into the circulation. If a given ES comprised about $1{\cdot}10^9$ cells, which corresponds to a tumor volume of 1 cm^3 (James et al., 1999), and the plasma volume was 2.7 l, we can calculate that the amount of exosomes in 10 ml plasma would account 0.24 µg.

$$\frac{\frac{0.8\mu g}{10^6} \times 10^9 \times \frac{2d}{8d} \times 0.02}{2.7l} = 24\frac{\mu g}{l} = 0.24\frac{\mu g}{10\mu l}$$

Accordingly, for the preclinical model, ES cell line-derived exosomes were serially diluted (range: 30 to 0.1 µg exosome equivalent) in 10 ml of plasma of a healthy donor and then isolated by ultracentrifugation as described in 2.2.3.2 followed by RNA extraction, qRT-PCR and DNA gel electrophoresis.

Figure 2.3: Procedure of dilution experiments

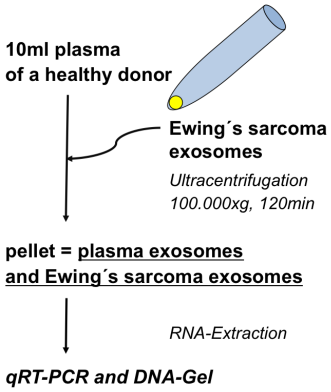

2.2.4 RNA isolation

There are several ways extracting RNA from exosomes. Because exosomes differ from their donor cells not only in protein and lipid composition, but also in their RNA content, different methods are eligible for RNA isolation from cells and exosomes (Eldh et al., 2012). As there exists no specific exosomal RNA isolation kit up to date, properties of other methods or kits have to be utilized to receive optimal results. For example, exosomes have a more rigid membrane than cells have due to a decreased phosphatidylcholine content and enrichment in sphingomyelin and cholesterol (Laulagnier et al., 2004; Trajkovic et al., 2008; Mitchell et al., 2009) and therefor a stronger lysing buffer (as in the miRCURY RNA Isolation Kit) is conducive, whereas phenol based lyzation is less valuable. Besides, exosomes contain a high amount of small RNAs, which are marginally filtered by some of the column based methods as the RNeasy Mini Kit. Moreover, the selection of the extraction method depends on the liquid the exosomes are soluted in and its protein content (Plasma or PBS), on the exosome or RNA concentration (high sensitivity required, e.g. for transcript detection in peripheral blood) and on what the RNA is supposed to be used for (high quality required, e.g. for microarrays).

2.2.4.1 RNA isolation from cells

RNeasy Mini Kit RNA from cultured cells was extracted with the RNeasy Mini Kit according to the manufacturer's instructions (Qiagen Handbook 04/2006). This procedure does not provide an enrichment of RNAs smaller than 200 bases, because they are sequestered under given high-salt conditions. Up to $1{\cdot}10^7$ cells were lysed in an appropriate volume of RLT buffer (containing 10 µl ß-mercaptoethanol/ml RLT), mixed with an equal amount of 70% ethanol and vortexed. The lysate was transferred onto RNeasy spin columns and centrifuged for 1 min at 10,000 rpm. This step enabled binding of the RNA to the silica-gel membrane within the RNeasy spin column. The membranes were washed three times with wash buffers

with a final centrifugation step at 12,000 rpm for 2 min to dry the membranes. Elution of RNA was carried out with 30-40 µl RNAse-free water.

TRI Reagent RNA Isolation Kit This RNA isolation procedure was used to extract total RNA from cultured cells for microarray experiments, because RNA isolation by RNeasy Mini Kit is not sufficient for the isolation of RNA molecules smaller than 200 bases. RNA isolation was performed with the TRI Reagent RNA Isolation Kit according to manufacturer's instructions (Ambion Manual Version 06/10). Up to $1{\cdot}10^7$trypsinated cells were homogenized in 1 ml TRI Reagent and centrifuged at 12,000g for 10 min. After addition of 200 µl BCP (1-bromo-3-chloropropane) per ml TRI Reagent, samples were vigorously vortexed for 20 sec and centrifuged at 12,000g for 15 min at 4°C. The aqueous RNA phase was transferred into a new reaction tube and RNA was precipitated by adding 500 µl isopropanol per ml TRI Reagent. The sample was vortexed and centrifuged at 12,000g for 8 min at 4°C. Then the RNA pellet was washed with 500 µl 75% ethanol and centrifuged at 7,500g for 5 min at 4°C. After removal of ethanol the pellet was air-dried for 7 min and dissolved in 50-100 µl RNAse-free water.

2.2.4.2 RNA isolation from exosomes and plasma

QIAamp Ultra Sens Virus Kit This kit uses a carrier RNA to detect very small amounts of RNA or RNA fragments in blood and other body fluids. RNA was isolated from plasma as well as exosomes diluted in and enriched from plasma using the QIAamp Ultra Sens Virus kit following the manufacturer's instructions (Qiagen Handbook 01/2003). To 1 ml of Plasma or exosome concentrate diluted in PBS up to a volume of 1 ml an adequate volume of Buffer AC and 5,6 µl carrier RNA were added. After 10 min incubation the mixture was centrifuged at 660g for plasma and at 830g for exosomes in order to receive optimal results. The precipitates were resuspended with proteinase K and buffer AR during shaking incubation at 40°C for 10 min. The lysate was mixed with binding buffer and transferred into the QIAamp spin columns, centrifuged at 4300g and washed twice with two different washing buffers. The RNA was eluted with 40µl of buffer AVE and subsequent centrifugation at 6000g for 1 min. To further increase the gain of RNA, the eluate was pipetted once more on the membrane of the column and centrifuged as described above. To avoid RNase contamination during the RNA isolation process, the sterile bench and all instruments were pre-cleaned with RNaseZap® (Invitrogen). All centrifugation steps were carried out at RT.

miRCURY RNA Isolation Kit To isolate RNA from exosomes for microarray analysis the miRCURY RNA isolation kit (Exiquon, Vedbaek, Denmark) was used according to the manufacturer's protocol and as described previously by Eldh et al. (2012). To 200 µg exosomes 350 µl lysis solution (containing 10 µl ß-mercaptoethanol/ml) were given. After vortexing, 200 µl of 99% ethanol were added. The vortexed lysate was transferred into spin columns, washed

thrice with wash solution (centrifugation at each washing step with 14,000g, 1 min) before 50 µl elution buffer were pipetted carefully on the membrane to elute the RNA in a final centrifugation step at 200g for 2 min and thereafter at 14,000g for 1 min. All centrifugation steps were carried out at RT.

RNA concentration and quality were checked photometrically at 260 nm before RNA was stored at -80°C.

2.2.5 RNase treatment

To prove that the exosomal RNA is protected from RNases, RNase-treatment was carried out. Therefore, freshly prepared exosomes or supernatant were incubated with 0.1 µg/µl RNase A (Fermentas) for 10 min at 37°C. As a control, exosomes were sonicated to disrupt their membrane before RNase-treatment as it was described previously (Keller et al., 2011). The Sonication of exosomes was conducted three times successively for 10 sec at 80% amplitude with a digital sonicator (Branson).

2.2.6 Reverse transcription

To examine gene expression by qRT-PCR, isolated RNA was reversely transcribed into complementary DNA (cDNA) using the High-Capacity cDNA Reverse Transcription Kit (Applied Biosystems). According to the manufacturer's instructions (Applied Biosystems Insert P/N 4375222 REV A) 5.8µ l of reverse transcription master mix containing 0.8 µl dNTPs, 1 µl MultiScribe™ Reverse Transcriptase, 2 µl reverse transcription random primers and 2 µl buffer were mixed with 14.2 µl RNA solution (containing 1 µg purified RNA). The cDNA was synthesized under the following thermal cycling conditions: 10 min at 25°C, 120 min at 37°C, 5 min at 85°C, and terminal hold at 4°C.

2.2.7 Quantitative Real-Time PCR (qRT-PCR)

Quantification of synthesized cDNA by qRT-PCR allows examination of differential gene expression as the amount of cDNA corresponds to the amount of mRNA. Gene-specific primer assays were obtained from Applied Biosystems (see 2.1.6.5), which consisted of a FAM™ dye-labeled TaqMan® MGB probe and two unlabeled PCR primers. All analyses were carried out in 96-well format. 1 µl of specific primer assays and 1 µl of cellular, 2 µl of exosomal or 4 µl of plasma derived cDNA template were added to 10 µl TaqMan Universal PCR Master Mix (Applied Biosystems) and adjusted to a final volume of 20 µl with RNAse-free water. Fluorescence was measured with an AB 7300 Real-Time PCR System (Applied Biosystems). Gene expression values were normalized to those of the housekeeping genes *glyceraldehyde 3-phosphate dehydrogenase* (GAPDH) or *beta-2-microglobulin* (B2M) using the 2^{-ddCt} method. Mean values and standard deviations of duplicate measurements were calculated using Microsoft Excel.

2.2.8 Detection of EWS/FLI1

There are no inventoried TaqMan Gene Expression Assays for the detection of EWS/FLI1 type 1 mRNA levels available. Thus, primers detecting EWS (sense) and FLI1 (antisense) of the fusion transcript and a probe detecting type 1 translocation were designed. The master mix was prepared by adding 10 µl of TaqMan Universal PCR Master Mix, 0.6 µl of each primer and 0.4 µl of FAM probe and the required volume of cDNA to a final volume of 19.5 µl Master Mix per well. Fluorescence was measured with an AB 7300 Real-Time PCR System (Applied Biosystems). Gene expression values were normalized to those obtained for GAPDH or B2M and calculated using the 2^{-ddCt} method.

2.2.9 Agarose gel electrophoresis

DNA fragments were separated in a 2% agarose gel at 10 V/cm. Therefore, 4 g agarose were dissolved in 200 ml TAE buffer and boiled before 4 µl EtBr were added. After the gel was casted and cooled, a mix of 20 µl of cDNA and 2 µl of 6x Blue Juice Gel Loading Buffer (Invitrogen) were loaded in each lane. A 0.1 kb or 1 kb, respectively, DNA ladder (Invitrogen) was appended as a size standard. The gel ran for 1 h at 70 V. DNA amplicons were visualized with a Gene Genius Bio imaging system (Syngene).

2.2.10 Microarrays

Experiments were done in cooperation with Olivia Prazeres da Costa, M.Sc. (Expression Core Facility at the Institute for Medical Microbiology, Immunology and Hygiene of the TU München). At least ten 150T cell culture flasks of A673, SK-N-MC, and SB-KMS-KS1 cells were cultivated for 48 h before exosome preparation as described in 2.2.3. Thereafter, RNA was extracted separately from the cells via TRI Reagent RNA Isolation Kit and from the respective exosomes via miRCURY RNA Isolation Kit. RNA quality was checked by using a Bioanalyzer (Agilent). Total RNA (200 ng) was amplified and labeled using Affymetrix GeneChip Whole Transcript Sense Target Labeling Kit. cRNA was hybridized to Affymetrix Human Gene 1.0 ST arrays. Arrays were RMA-normalized. Quality assessment consisted of RNA degradation plots, Affymetrix control metrics, sample cross-correlation, and probe-level visualizations. Normalization incorporated (separately for each RNA type data-set) background correction, quantile normalization, and probe-level summation by RMA.

The microarray data were analyzed with the GENE-E software package (http://www.broadinstitute.org/cancer/software/GENE-E/) and deposited at the Gene Expression Omnibus (GEO; GSE42282). Gene-set enrichment analysis (GSEA) was performed with the GSEA tool (http://www.broad.mit.edu/gsea) using a preranked list and 1,000 permutations.

For the interrogation of publicly available microarray data, data-sets were retrieved from the GEO and the Array Express platform of the EMBL-EBI (http://www.ebi.ac.uk/arrayexpress),

manually revised for their correct annotations, and then simultaneously RMA-normalized using brainarray custom CDF files (v15 ENTREZG). Individual data accession codes are given in the results section.

2.2.11 Flow cytometry

Exosomes are too small to be analyzable events in flow cytometric assessment. To overcome this obstacle, exosomes were bound to 4 µm aldehyde/sulfate latex beads (Invitrogen). Therefore, 20-40 µl exosomes derived from A673 and SK-N-MC ES cells were incubated with 1.5 µl latex beads overnight on a rotator wheel at 4°C and blocked with 1M glycine and 0.5% BSA in PBS before they were transferred into a 96-well-plate. Then, continuously blocking with 0.5% BSA in PBS, the exosomes were incubated with 2 µl CD63 (sc-5275), CD81 (sc-7637) or corresponding isotype control antibodies (all Santa Cruz) for 30 min at 4°C. The same procedure was applied for testing ES cell line-derived exosomes for the markers Calnexin (sc-80645, Santa Cruz) and GM130 (ab76154, Abcam). Before as well as after incubation with 2 µl of the secondary antibody (goat anti mouse IgG1 FITC (sc-2078) and goat anti rabbit IgG1 FITC (sc-2012); both Santa Cruz) three washing/blocking steps with 0.5% BSA in PBS and centrifugation at 4,000 rpm were carried out. The incubation with the secondary antibody (30 min at 4°C), all following washing and centrifugation steps and the transfer into FACS tubes (Falcon) were carried out in darkness.

For positive control of the Calnexin and GM130 antibodies, intact A673 and SK-N-MC cells were fixed with 4% paraformaldehyde for 20 min and permeabilized by the addition of 100% ice-cold methanol to a final concentration of 90% methanol. After 30 min incubation and three washing steps with 1·PBS the cells were blocked for 1 h at RT with 0.5% BSA in PBS before they were incubated with 2 µl of the specific antibodies for 30 min at RT. Before the cells were incubated with 2 µl of the secondary antibody (30 min at RT), three more washing steps were performed. Finally, the cells were washed three more times, resuspended in 1xPBS and transferred into flow cytometry tubes.

Samples were analyzed on a FACScalibur flow cytometer using Cellquest Pro software (both Becton Dickinson). At least 30,000 events/sample were recorded. Data were saved in *.fcs format and analyzed with Cellquest software (Beckton Dickinson).

2.2.12 Fluorescence microscopy

For fluorescence microscopy, first ES derived exosomes were stained with Calcein AM. Therefor, cell culture supernatant from A673 cells grown in exosome depleted medium was harvested and pre-centrifuged at 300g, 2,000g and 10,000g. Then 2 µg/ml Calcein AM (Merck) were added and the supernatant was incubated 30 min at 37 °C. Subsequently, the supernatant was ultracentrifuged thrice at 100,000g and resuspended in PBS each time in order to enrich

exosomes and wash out Calcein AM molecules, which did not get trapped into the exosomes. The isolated exosomes were resuspended in 2 ml PBS. For a negative control, 2 ml of the supernatant after the last ultracentrifugation step were taken to check that the the fluorescence effect was not caused by contamination. Calcein is a small molecule, obtaining a molecular mass of 0,99 kDa (http://www.anaspec.com/products/product.asp?id=29713). One single exosomal marker protein, in contrast, has a molecular mass of 50-100kDa. Exosomes were reported to have a molecular weight of more than 50,000 kDa (Taylor et al., 2011). Hence, it is not expectable that Calcein AM is co-pelleted with the exosome fraction at 100,000g.

The stained exosome preparation, the supernatant, 2 ml PBS or 2 ml PBS containing 2 µg/ml Calcein AM were given to $4{\cdot}10^6$ pre-cultured HEK293 cells. A fluorescence microscopy was carried out after 3 h and after 24 h. Images were recorded with a Zeiss AxioCam MRm camera attached on a Zeiss Axiovert 100 microscope and analyzed with NIH ImageJ software.

2.2.13 Electron microscopy

Electron microscopy studies were performed in cooperation with Graça Raposo, PhD (Institut Curie, Centre de Recherche and Structure and Membrane Compartments CNRS, UMR144, Paris, France) as previously described (Raposo et al., 1996). Exosomes resuspended in PBS were deposited for 20 min at RT on formvar-carbon coated electron microscopy grids. The samples were fixed for 20 min in PBS-2% PFA (Electron Microscopy Sciences), and quenched in PBS 50 mM glycine. After fixation in glutaraldehyde 1% (Electron Microscopy Sciences) grids were rinsed in water and contrast and embedding was performed with an ice-cold mixture of methylcellulose and uranyl acetate (both Electron Microscopy Sciences) for 10 min. Grids were air-dried before observation. Samples were observed at 80 kV with a CM120 Twin FEIelectron microscope (FEI Company).

2.2.14 Statistical analyses

Differences in proportions between groups were evaluated by two-tailed chi-square test, unpaired t-test with Welch's correction, or unpaired two-tailed student's t-test. Statistical significance level was set at $p < 0.05$.

3 Results

3.1 Selection of ES specific transcripts as potential biomarkers in plasma

3.1.1 Evaluation of microarray data

In order to select highly specific transcripts for biomarker discovery, microarray data of us and others was re-evaluated. The aim was to find marker candidate transcripts, which are highly expressed in ES and show concomitantly a very low expression in normal tissue. Therefor, genes fulfilling these criteria were identified in a two-step process using microarray data obtained from Affymetrix HGU133A chips as a discovery cohort (n=63 ES and n=36 normal tissues; GSE1825 (Staege et al., 2004), GSE15757 (Burdach et al., 2009), GSE7007 (Tirode et al., 2007), E-MEXP-1142 (Schaefer et al., 2008) and GSE2361 (Ge et al., 2005)) and published microarray data derived from Affymetrix HG-U133plus2.0 chips as a validation cohort (n=161 ES, n=353 normal tissues; GSE34620 (Postel-Vinay et al., 2012), GSE12102 (Scotlandi et al., 2009), GSE17679 (Savola et al., 2011), and GSE3526 (Roth et al., 2006)).

First, in the discovery cohort, genes were ranked in order of their linear fold change (FC) of the median expression levels in primary ES compared to normal tissue. The median was chosen as statistical method because it is more robust to outliers than the mean. The 30 genes with the highest FC in median gene expression (corresponding to the top 0.25% of probe-sets) in the discovery cohort were then reassessed in the validation cohort using the same method (figure 3.1 A). A few marker candidates, which appeared very promising due to their high FC in the discovery cohort, as KIAA0090 and CSPG5, could not be confirmed in the validation cohort. As final criteria for the marker selection, a mean FC higher than 10 and a previous implication in ES pathology were determined. 10 transcripts complying these conditions were finally selected as potential biomarkers (table 3.1).

In addition to those 10 genes, the analysis of the validation cohort also qualified LIPI with an FC of 44.4 as a promising candidate since the HG-U133plus2.0 microarrays contain probes for this gene, whereas the HG-U133A microarrays do not. Beyond that, EWS-FLI1 as the constitutionally most specific marker for ES was examined in all continuative experiments. Thus, 12 transcripts were selected for further analysis of their suitability as potential biomarkers.

Table 3.1: Overview on the selected genes based on their median fold changes (FC) in the discovery and validation cohort

			FCs ES versus normal tissue		
Entrez ID	Gene symbol	Description	Discovery	Validation	Mean FC
4886	NPY1R	Neuropeptide Y receptor Y1	64.8	105.6	85.2
10149	GPR64	G protein-coupled receptor	35.9	89.6	62.8
27123	DKK2	dickkopf 2 homolog	20.5	78.8	49.7
4821	NKX2.2	NK2 homeobox 2	62.0	29.5	45.8
149998	LIPI	Lipase, member 1	NA	44.4	44.4
2146	EZH2	Enhancer of zeste homolog 2	17.8	59.9	38.9
26872	STEAP1	Six transmembrane epithelial antigen of the prostate 1	17.6	51.6	34.6
190	NR0B1	Nuclear receptor subfamily 0, group B, member 1	16.8	30	23.4
595	CCND1	Cyclin D1	10.7	19.5	15.1
5579	PRKCB	Protein kinase C, beta	19.7	6.7	13.2
9452	ITM2A	Integral membrane protein 2A	13.1	8.5	10.8

Figure 3.1: Evaluation of the potential marker transcripts

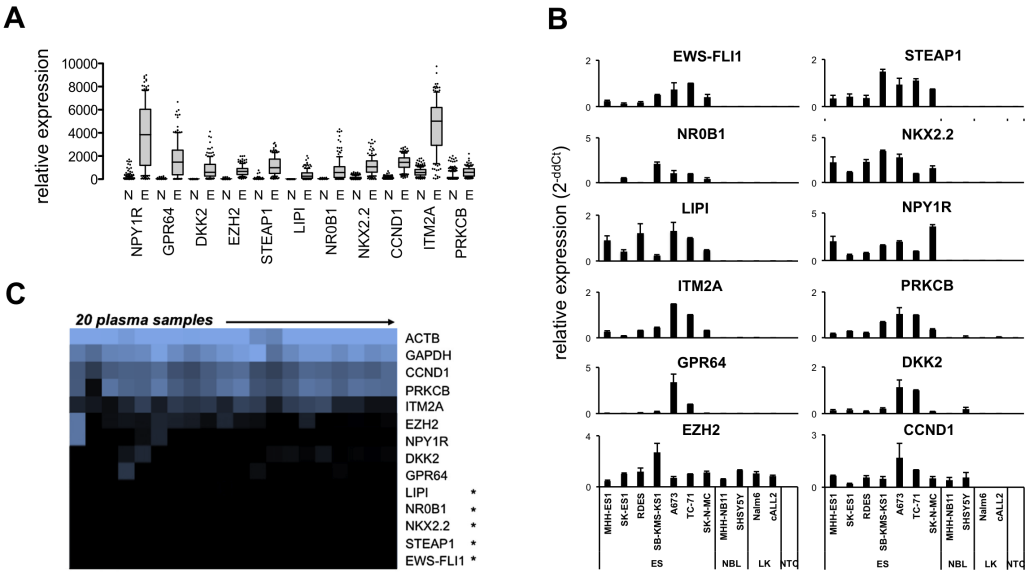

(A) Microarray analysis of the expression of candidate marker transcripts in 353 normal tissues (N) compared to 161 primary ES (E). (B) Evaluation of the specific marker transcripts. qRT-PCR of the 12 candidate transcripts in 7 ES, 2 neuroblastoma and 2 leukemia cell lines. Mean ± SEM of 2 experiments (duplicates/group). (C) Heatmap of marker transcript expression as measured by qRT-PCR normalized to B2M in 20 healthy plasma samples. Blue color represents delta-Ct values equal or greater than 0, whereas black colour represents no detection of the corresponding transcript in 50 PCR cycles (triplicate measurements). The housekeeping genes ACTB and GAPDH were used as positive controls. Asterisks mark transcripts that were undetectable in all plasma samples.

3.1.2 Validation of high expression

Accordingly the high expression of the marker candidate transcripts had to be validated. Therefor the expression of the transcripts in seven ES cell lines was compared to two neuroblastoma and two leukemia cell lines as negative controls by qRT-PCR. qRT-PCR confirmed a high expression level of all marker candidates (figure 3.1 B). Additionally, they are rather specific for ES (compared to leukemia and neruroblastoma), apart from the three transcripts EZH2, CCND1 and DKK2. EZH2 (Chang and Hung, 2012) and CCND1 (Diehl, 2002) are known to be expressed in many cancer entities, whereas DKK2 was described to be upregulated in neuroblastoma (Revet et al., 2010).

3.1.3 Limitation of transcript specificity

To further assess the specificity of these marker transcripts, their presence was tested in plasma samples from healthy donors. The analysis of 20 plasma samples revealed that most of the transcripts are detectable in plasma of healthy individuals due to their low but universal expression in normal tissue. Only five markers, including EWS-FLI1 as it was anticipated, were negative in all plasma samples and thus eligible for further investigation (figure 3.1 C), namely STEAP1, NR0B1, NKX2.2 and LIPI.

Having identified marker transcripts holding a specificity of 100% so far, the next step was the development of a method which allows the most sensitive detection of these marker transcripts. Because mRNAs are promptly degraded in plasma, where RNases are present ubiquitously, compartments were focused in which transcripts could potentially be protected. Since tumor cell derived exosomes have this property, their enrichment from patient plasma could be a source for marker transcript detection - provided that Ewing´s sarcomas, as it was shown for many other cancer entities, but not yet for sarcomas, produce exosomes.

3.2 Identification and description of ES derived exosomes

3.2.1 Elevated expression of exosome related genes in ES

The first indication that ES potentially releases exosomes was given by re-analysis of published microarray data. In the data of 353 normal tissues and 161 primary ES (GSE3526 (Roth et al., 2006), GSE34620 (Postel-Vinay et al., 2012), GSE12102 (Scotlandi et al., 2009) and GSE17679 (Savola et al., 2011)) a high expression of CD63 and CD81, the genes coding for the most specific exosomal surface marker proteins (Thery et al., 2006), was observed (figure 3.2 A). Coincidentally, several genes necessary for exosome production and release (which are exosomal markers as well) show an elevated expression in ES compared to normal tissue. Especially genes belonging to the Syntenin/ALIX pathway, which have been recently reported to participate in exosome biogenesis and secretion (Baietti et al., 2012), proved to be highly

Figure 3.2: Identification of ES derived exosomes

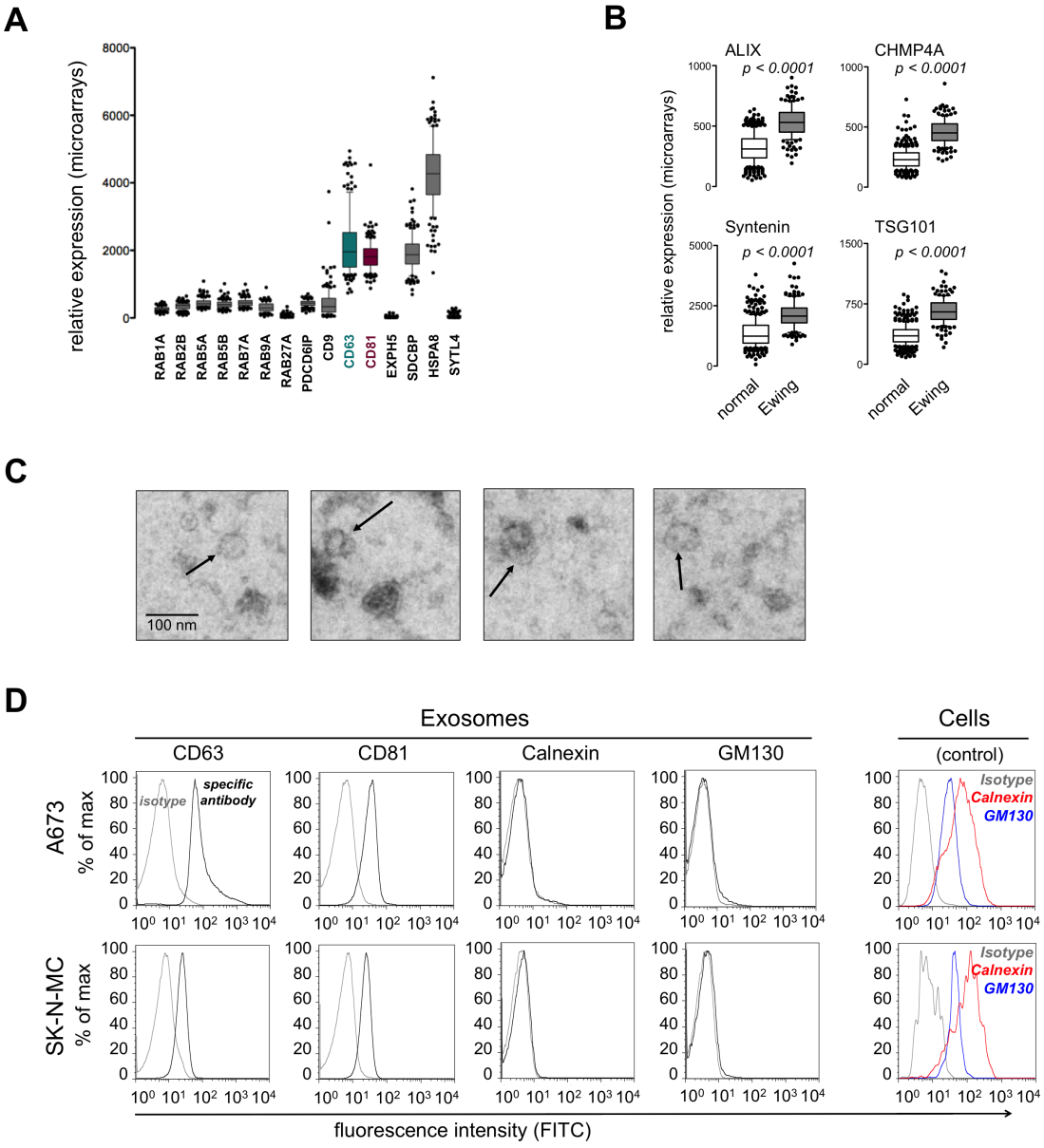

(A) ES highly express the canonical exosome markers CD63 and CD81. Microarray data of 161 ES were retrieved from GEO and derive from publicly available microarray data (GSE34620, GSE12102, GSE17679). Microarrays were simultaneously RMA-normalized using brainarray custom CDF files (v15 ENTREZG). (B) ES cell lines highly express enzymes necessary for exosome generation such as ALIX, CHMP4A, Syntenin, and TSG101 (Baietti et al., 2012). Microarray data of 353 normal tissues and 161 primary ES are represented as box-plots. Whiskers indicate the 10th and 90th percentiles. Outliers are displayed as dots. Unpaired t-test with Welch's correction. (C) Electron microscopy shows vesicles of 30-100 nm diameter corresponding to exosomes (arrows). (D) Flow cytometric analysis of the exosomal surface markers CD63 and CD81, as well as the endoplasmic reticulum marker Calnexin and the Golgi marker GM130. Exosomes were bound on 4 µm latex beads before incubation with isotype control (gray color) or specific antibodies (black color), respectively. As a control, intracellular staining and flow-cytometric assessment of Calnexin and GM130 of ES cells was carried out. At least 30,000 events per group were recorded; 2 experiments/cell line.

expressed (figure 3.2 B). These observations raise the prospect that there is active exosome production in ES.

3.2.2 Electron microscopy shows exosome-sized vesicles

To evidence this hypothesis, EVs were isolated from the cell culture supernatant of the ES cell lines A673, SK-N-MC and SK-KMS-KS1 as described in 2.2.3. The enriched EVs appeared in electron microscopy as 30-100 nm sized, concavely round-shaped, membrane limited vesicles (figure 3.2 C). Hence, the isolated vesicles fulfilled the established electron microscopy criteria for exosomes in size and morphology (characteristic concave "cup-shape") (Raposo et al., 1996; Thery et al., 2006).

3.2.3 Flow cytometric assessment reveals exosome characteristic surface proteins

In order to validate this investigation, flow cytometric assessment of the exosomal surface proteins CD63 and CD81 was performed. It revealed a strong expression of these two tetraspanins on the surface of the isolated ES derived EVs compared to the isotype. Cellular components, in contrast, as the endoplasmic reticulum marker Calnexin (Williams, 2006) and the Golgi matrix protein GM130 (Nakamura, 2010) could not be detected on the EVs, but, as a positive control, in their cells of origin (figure 3.2 D). This further confirms the endosomal (and not endoplasmic or Golgi) origin of the isolated vesicles and thus their identification as exosomes.

3.3 Detection of ES specific transcripts in the exosomal cargo

3.3.1 ES derived exosomes contain a characteristic spectrum of RNAs

Having explored the configuration of the exosomal surface, next, the content of the ES derived exosomes was studied. As a Bioanalyzer profile of the product of a RNA isolation won from exosome concentrate showed, ES derived exosomes contain an abundance of RNA (figure 3.3 A). Whereas total cellular RNA contains high amounts of ribosomal RNAs, which are displayed by the two characteristic peaks of 18s and 28s in the RNA profile, ribosomal RNA can only be found marginally in exosomes. Another difference between the cellular and the exosomal RNA profile is the size distribution of RNAs. Exosomes carry a broad spectrum of RNA, but especially small RNAs. The parental cells, in contrast, show an equal distribution of RNAs with different lengths (apart from the rRNA peaks).

Of note, the observed RNA profile appears very similar to previously described exosomal RNA bioanalyzer profiles, as that from murine mast cells described by Valadi et al. (2007).

Figure 3.3: Detection of functional mRNA in ES derived exosomes

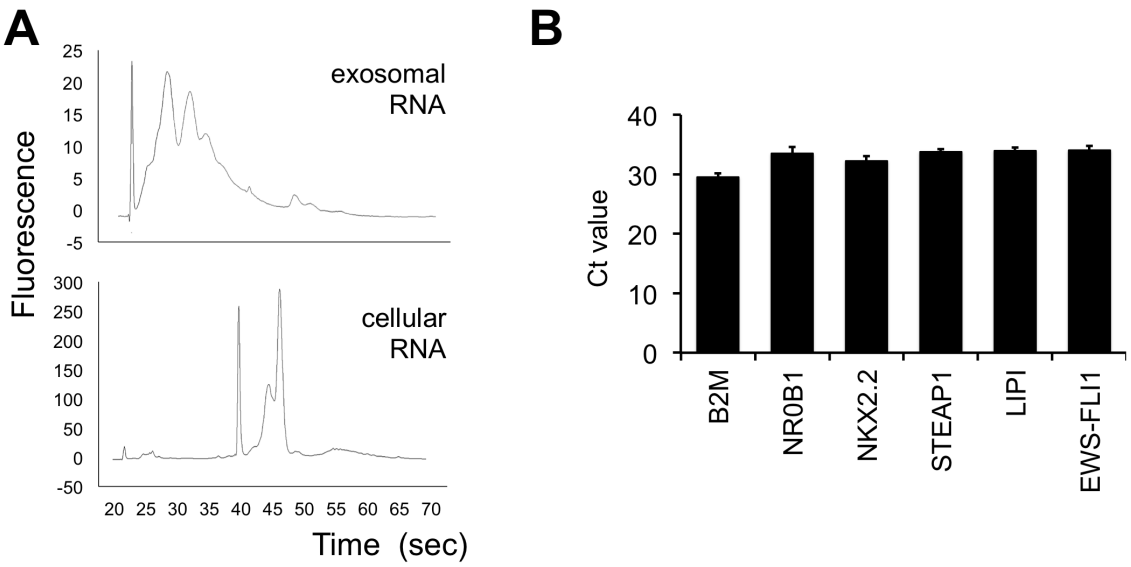

(A) Representative images of Bioanalyzer profiles of exosomal and cellular RNA from A673 cells. The spectrum of exosomal RNA contains a high amount of small RNAs, but few ribosomal RNAs. (B) Representative qRT-PCR results of five potential marker transcripts and the housekeeping gene B2M showing their stable expression in ES cell line-derived exosomes. Data are mean ± SEM of three experiments (duplicates/group).

3.3.2 Potential marker transcripts can be reliably found in ES derived exosomes

In the next step, it was surveyed whether the isolated exosomal RNA contains the marker transcripts selected in 3.1.3 by qRT-PCR. Strikingly, all five top marker transcripts could be found in the exosomal RNA preparation and the detection proved to be remarkably stable and reliable (figure 3.3 B). Furthermore the qRT-PCR shows, that ES derived exosomes contain functionally intact mRNAs, which could presumably be translated into proteins.

3.4 Increase of transcript yield by exosome enrichment

3.4.1 Gain of transcripts through exosome enrichment

Having demonstrated that the ES cell culture derived exosomes apparently contain the selected marker transcripts, the author investigated subsequently, whether the yield of transcripts can be increased by exosome enrichment. In order to evaluate the use of this methodology to increase the sensitivity for biomarker detection, the amount of transcripts in exosome preparations was compared to the latter cell culture supernatant. More precisely, it was tested, by which factor the gain of exosomal transcripts would rise, if RNA was isolated from an equal volume of exosomes enriched from cell culture supernatant or the untreated supernatant they

derived from. Thereby a median 2.5-fold increase (range: 1.9 to 3.8) of detectable transcripts at a relation of supernatant volume to exosomal concentration volume of 30 to 1 (figure 3.4 A, upper panel) was observed.

3.4.2 Efficacy of exosome enrichment procedure

To further examine how large the fraction of exosomes and thus transcripts, that can be harvested through the exosome enrichment process, is (and hence, how effective the exosome enrichment method works), the amount of transcripts isolated from exosome concentrate was compared to the supernatant that remained after ultracentrifugation. The yield of RNA in exosome preparations compared to the supernatant after ultracentrifugation was here considerably higher at the same relation of supernatant to exosome concentrate volume as described above (median: 17.8-fold; range: 9.4 to 40,835.6). This result confirms that the applied exosome enrichment process is efficient and that the majority of the RNA containing exosomes is pelleted during ultracentrifugation (figure 3.4 A, lower panel). However, it is questionable, why the amount of transcripts is so drastically diminished in supernatant after ultracentrifugation, since in untouched cell culture supernatant the harvest of transcripts is 7-fold higher, but only 2.5-fold increased when exosomes are isolated. The discrepancy of these two differential results could be caused by free or protein-bound RNA in cell culture supernatant, which might be degraded in the possibly RNase-contaminated setting of ultracentrifugation (figure 3.4 B). But considering that a certain amount of RNA is stable despite the assumed contamination could provide an indication that the exosomal RNA is protected from RNases by the exosome membrane.

3.4.3 Protection of the exosomal cargo from RNase degradation

To give evidence to this hypothesis, freshly prepared exosomes were treated with 0.1 µg/µl RNase A (see 2.2.5). As expected, exosomal RNA was protected from RNase-mediated degradation in intact exosomes (figure 3.4 C). In contrast, the RNA of exosomes, whose membranes were disrupted by sonication prior to RNase-treatment, was completely degraded. This experiment suggests that a considerable amount of RNA harvested from the supernatant of ES cells by ultracentrifugation is packed within exosomes and thus conserved and stabilized.

Supplementary, exosomes were enriched from cell culture supernatant in the presence of RNase (figure 3.4 D). Despite the continuous presence of RNAse, the specific transcripts could still be enriched by a remarkable factor, further confirming that these transcripts are indeed exosomal cargo. Interestingly, the obtained result is similar to the experiment described previously in 3.4.2, providing another indication that cell culture supernatant contains free, vulnerable to RNase and protected, exosome-loaded RNA.

Considering that human plasma contains active RNase (Reddi and Holland, 1976; Tsui et al., 2002), the substantial gain of transcripts by exosome enrichment and their protection

Figure 3.4: Enrichment effect and RNase protection of exosomal transcripts

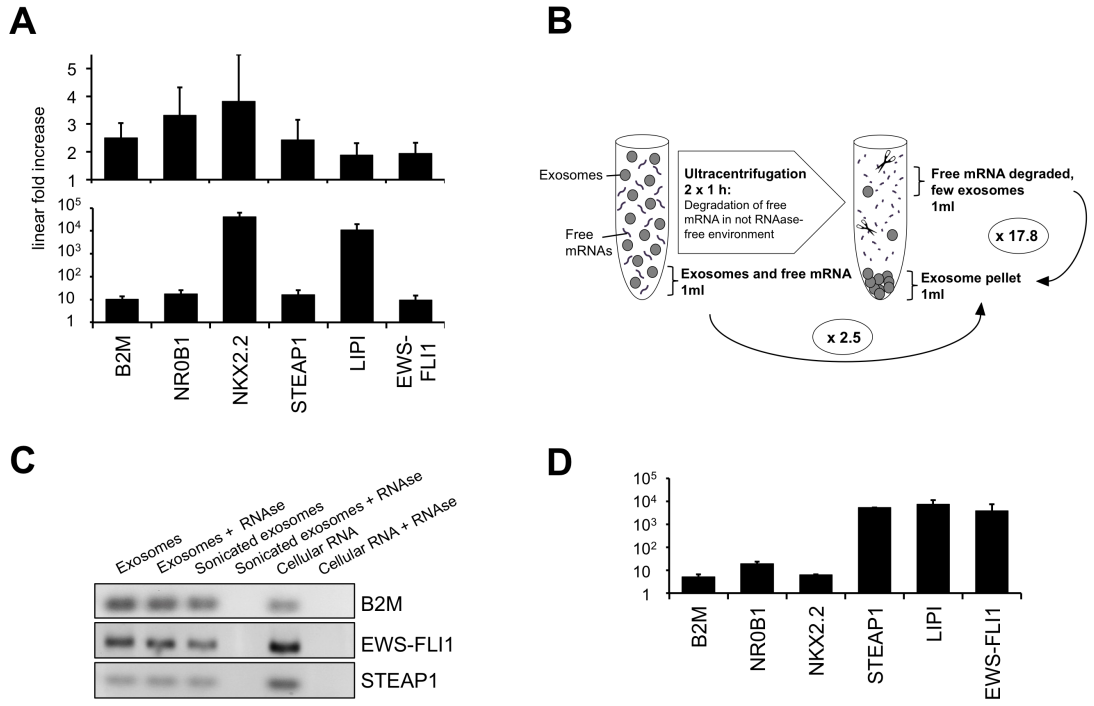

(A) Upper panel: Gain of transcripts through exosome enrichment compared with an equal volume of supernatant measured by qRT-PCR. Lower panel: Yield of exosomal transcripts through exosome enrichment compared to an equal volume of supernatant after ultracentrifugation measured by qRT-PCR. Both experiments: mean ± SEM of three experiments (duplicates/group). (B) Illustration of potential degradation of free mRNA during ultracentrifugation. (C) RNase-treatment revealed no degradation of mRNA inside intact exosomes, but within exosomes which were sonicated to disrupt their membranes prior to RNase-treatment. As an additional control, isolated cellular RNA was treated with RNase to demonstrate full RNase activity. Representative DNA gel image of B2M, EWS-FLI1 and STEAP after 50 cycles of PCR. (D) Enrichment of ES cell-line derived exosomes from supernatant in the presence of RNase. qRT-PCR of marker transcripts and the housekeeping gene B2M gained through exosome enrichment from cell culture supernatant compared to an equal volume of supernatant without exosome enrichment, both in the presence of 0.1 µg/µl RNase A. All experiments shown in this figure were performed with A673-derived exosomes.

from RNase within exosomes suggest that this method could be a valuable approach to use ES specific transcripts as stable biomarkers in peripheral blood.

3.5 Exosomes as vehicles for potential biomarkers in human plasma

3.5.1 Development of a pre-clinical plasma model

Since exosomes abound in human body fluids such as blood plasma, the enrichment protocol was applied on plasma of healthy subjects in a first step. Hereby, it was shown that the housekeeping gene B2M is increased 22-fold after exosome isolation compared to the analysis of untreated plasma, supporting the presumption that exosome enrichment enhances the possibility of ES transcript detection (figure 3.5 A).

In a second step, in order to assess the sensitivity of the elected five markers in a pre-clinical setting, a plasma model based on serial dilution of ES cell line derived exosomes in healthy donor plasma was designed. According to preliminary considerations (see section 2.2.3.4), exosomes were diluted in 10 ml healthy donor plasma in range from 30µg to 0.1 µg protein equivalent.

Strikingly, all marker transcripts could be detected by qRT-PCR down to a concentration of 0.3 µg/10 ml plasma at least once in two experiments (figure 3.5 B) and to some extent even down to 0.1 µg/10 ml (not shown).

3.5.2 Clinical testing of exosome enrichment in patient plasma

First, the minimal plasma volume required for marker detection was determined for the sake of avoiding to induce or aggravate iatrogenic anemia. With regards to the calculation described in 2.2.3.4, it can be estimated that at least 0.24 µg of tumor derived exosomes are present in the patients´ plasma. Since 0.3 µg of ES cell line derived exosomes were still steadily detectable in the pre-clinical plasma model, 10 ml were considered to be enough plasma to isolate tumor derived exosomes.

Before patient plasma samples were tested, eight plasma samples of healthy donors were analyzed after exosome enrichment to further confirm the specificity of the five marker transcripts. Therefore, 10 ml of healthy donor plasma were ultracentrifuged as described in section 2.2.3.2, RNA was extracted and qRT-PCR on the five markers was performed. Consistently, the markers were negative in all healthy samples, except STEAP1, which was positive in the samples of two subjects (one probe of duplicates) and LIPI, which was positive in one probe of one individual.

Nevertheless, in the plasma of seven ES patients, no evidence for a positive marker pattern could be provided (see figure 3.6). However, one positive STEAP1 sample out of duplicates appeared positive. Interestingly, this patient was one out of two, who did not receive

Figure 3.5: Specific transcripts in ES derived exosomes are detectable in human plasma *in vitro*

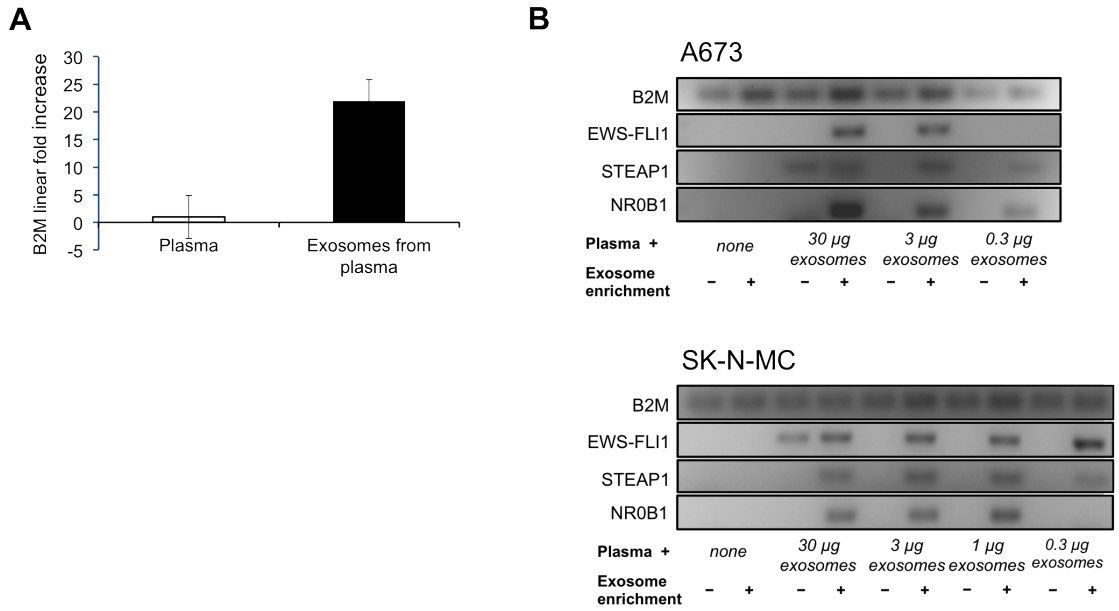

(A) Gain of B2M transcripts achieved by exosome enrichment from healthy donor patients. Duplicates of seven subjects were measured by qRT-PCR ± SEM. (B) A673 and SK-N-MC cell line derived exosomes were progressively diluted in healthy donor plasma. Representative DNA gel images of qRT-PCR products of B2M, EWS-FLI1, STEAP1 and NR0B1 with or without exosome enrichment via ultracentrifugation. Similar results were obtained for LIPI and NKX2.2 (not shown).

chemotherapy or any other therapeutic regime at time of probe assessment. All other samples of ES patient plasma were negative for all the potential marker transcripts.

3.6 Further investigations on the possible biological role of exosomes in ES tumorigenesis

Even though ES derived exosomes could not be detected in patient plasma via isolation of ES specific mRNA, the results of this study still provide evidence that the ES releases exosomes containing a functionally active cargo. To gain a tentative insight into their behavior, cargo and therefor their potential implications in ES tumorigenesis, some continuative experiments were carried out.

3.6.1 Uptake of ES derived exosomes by other cell types

First it was investigated, if exosomes derived from ES cell culture are functional and hence able to mediate their uptake by other cell types to deliver their cargo. For this purpose, exosomes were stained with Calcein AM, a fluorescent dye containing a acetomethoxy group that is transported through membranes. After the uptake of the labeled exosomes into the cell

Figure 3.6: Comparative heat maps of healthy donor and ES patient plasma

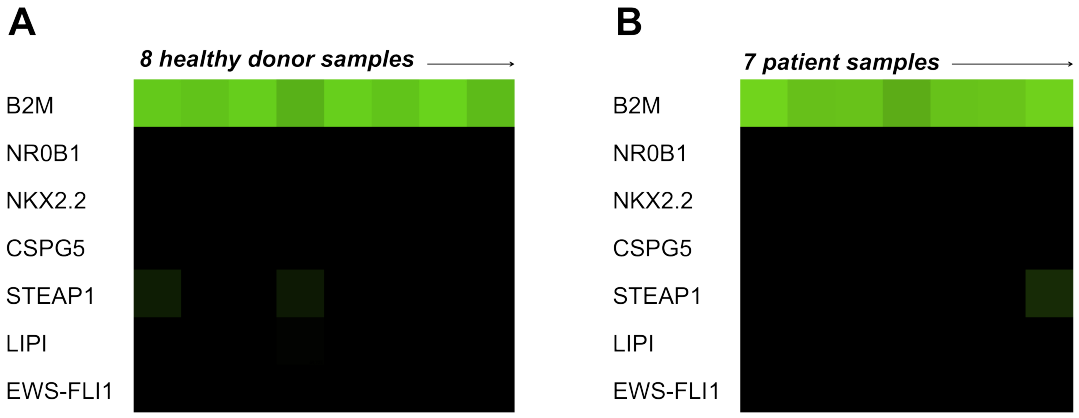

(A) Heat map of exosome preparations of 8 healthy donor plasma samples. 50 cycles of qRT-PCR were carried out. Positive signals were detected for two STEAP1 probes and one LIPI (each one of duplicates). (B) Heat map of ES patient plasma derived exosomes. All markers were negative except one positive STEAP1 sample of duplicates. 50 cycles of qRT-PCR.

and the decomposition of the exosomal membrane, intracellular unspecific esterases remove the Calcein's acetomethoxy group, which covered the calcium binding site of Calcein. Thus, Calcein chelates calcium ions and gives out strong green fluorescence (Gatti et al., 1998; Uggeri et al., 2004).

The Calcein labeled exosomes were then given to cultured cells of a different cell types, human embryonic kidney cells HEK293. To provide controls, cells were directly stained with an equal volume of Calcein AM (positive control), incubated with pure PBS (negative control) or supernatant of the stained exosomes added after washing them thrice with PBS by ultracentrifugation (negative control).

Fluorescent exosomes caused unlike an equal volume of washing supernatant a strong fluorescence of HEK 293 cells after 3h. This effect was visible for 24h at most. The induction of intense fluorescence only by pre-stained exosomes, but not by the negative controls, strongly suggests that the ES cell line derived exosomes are indeed taken up by different cell types (figure 3.7).

3.6.2 Microarrays show a common transcriptional signature of ES derived exosomes towards G-protein-coupled signaling, neurotransmitter signaling and stemness

To further specify what cargo ES derived exosomes could transfer into other cells and to gain insight into their the potential (patho-)biological function, RNA isolated from exosomes and their parental ES cell lines (A673, SK-N-MC, and SB-KMS-KS1) was subjected to microarray analysis (Affymetrix Human Gene ST 1.0). First the microarray data was filtered for probe-sets annotating known genes that are at least minimally expressed (minimal average

Figure 3.7: Uptake of ES derived exosomes by HEK293 cells

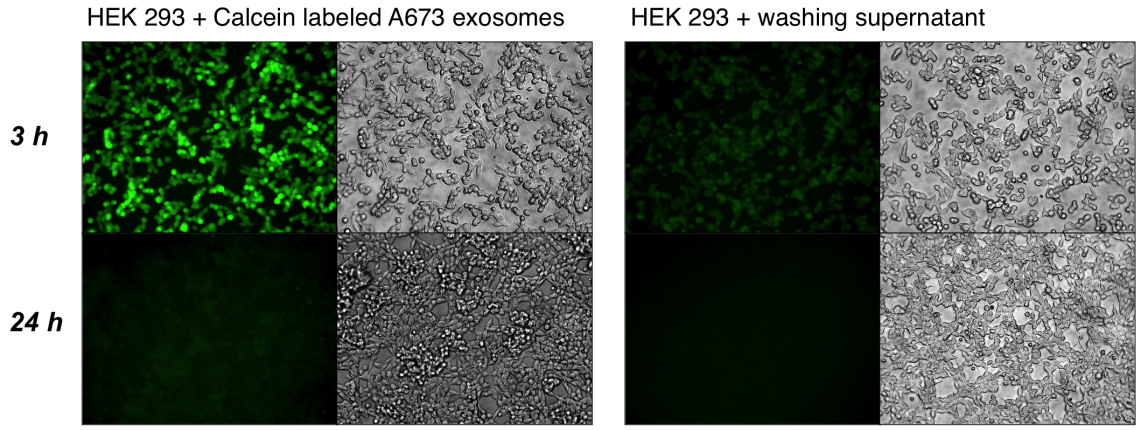

A673 derived exosomes are taken up by other cell types as HEK293. Cells were incubated with A673 exosomes, which were primarily labeled with the fluorescent dye Calcein AM, and examined after 3h and 24h. As a negative control, cells were incubated with an equal volume of washing supernatant of Calcein labeled exosomes, resulting in a significantly decreased fluorescence intensity.

expression intensity $\geq$10 in natural scale across all 6 samples) yielding a total of 13,610 different probe-sets. This list of probe-sets was then filtered for those probe-sets which show an at least log2-fold differential regulation between exosomes and their corresponding parental cell line. As seen in the Venn diagram in 3.8 A, exosomes from all three cell lines display a significant degree of overlap of in total 1,382 strongly regulated probe-sets (10.15% of all probe-sets) corresponding to 1,288 individual genes. Unsupervised hierarchical clustering of the samples and probe-sets further confirmed a strong match of the exosomal and the cellular RNA samples, respectively (3.8 B). We then performed a gene-set enrichment analysis (GSEA) with these commonly differentially regulated 1,382 probe-sets and the remaining non-regulated probe-sets. GSEA demonstrated a significant enrichment of transcripts in exosomes that are involved in G-protein-coupled signaling, neurotransmitter signaling, and stemness (3.8 C). For instance, the "MIKKELSEN_MEF_ICP_WITH_H3K27ME3" gene-set (Mikkelsen et al., 2008) describes a set of transcripts differentially expressed in murine embryonic fibroblasts with induced pluripotent stem cell characteristics that is associated with histone 3 lysine 27 tri-methylation, which has been previously reported to be implicated in the maintenance of a more immature phenotype of ES (Richter et al., 2009). In synopsis, these results indicate that ES cell line-derived exosomes are significantly enriched for a common set of transcripts involved in signal transduction and stemness.

Furthermore, a plethora of miRNAs was detected in the exosomal cargo (see Appendix V). Notably, 98% of the miRNAs are enriched in exosomes compared to the cellular expression level, 28% are more than 2-fold higher (figure 3.9).

Figure 3.8: ES cell line-derived exosomes share a common transcriptional signature.

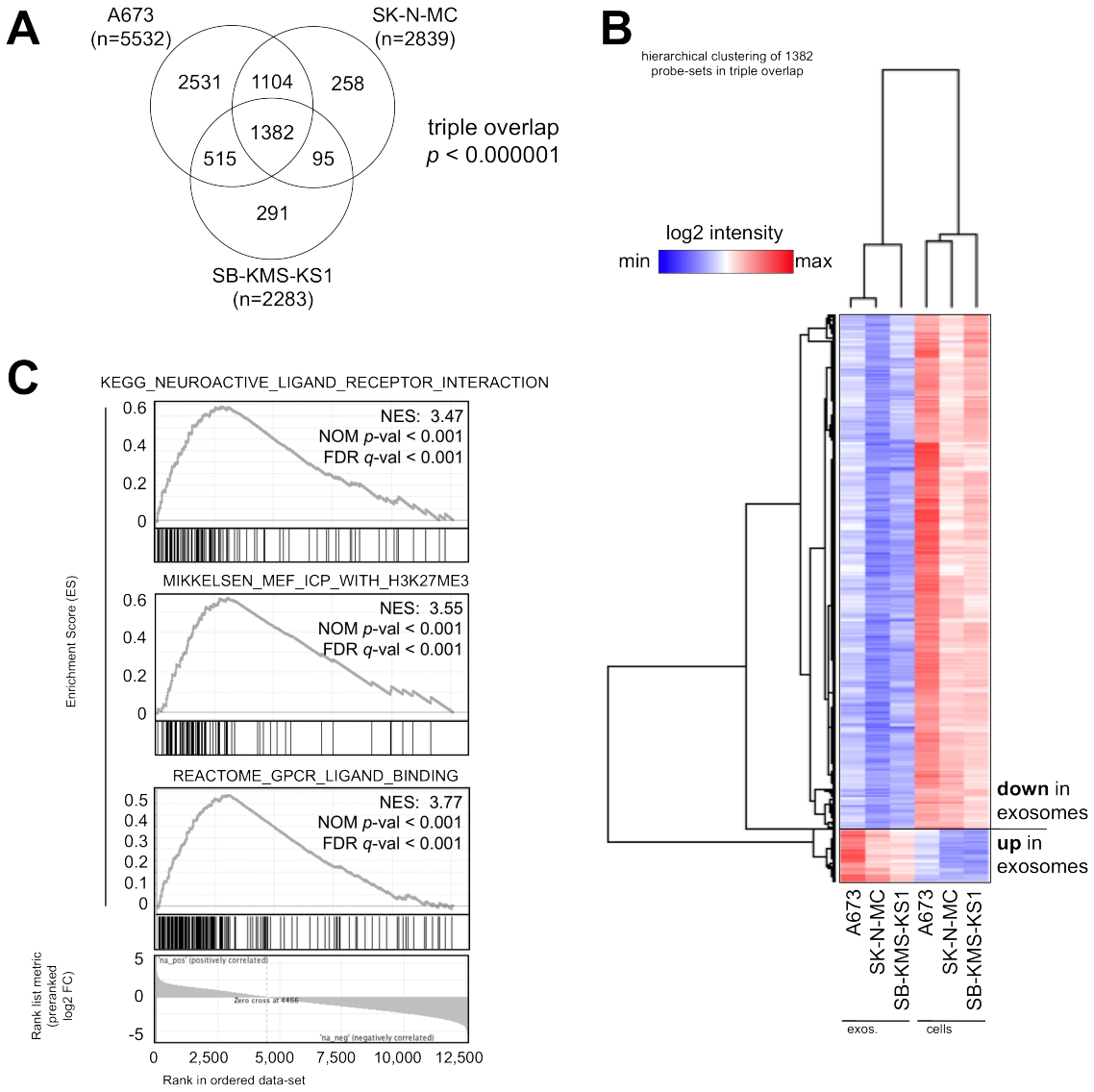

(A) Venn diagram of gene annotating probe-sets, which are differentially regulated between exosomes and their corresponding parental cell line (min. log2 FC $\geq$ 2), showing a significant degree of overlap (two-tailed chi-square test). (B) Unsupervised hierarchical clustering (average linkage) of the individual samples and the commonly differentially regulated 1,382 probe-sets. Data were log2-transformed and median-centered for depiction in a heatmap. (C) Gene-set enrichment analysis (GSEA) of the 1,382 commonly differentially regulated and non-regulated probe-sets. NES: Normalized Enrichment Score; NOM: nominal p value; FDR: False Discovery Rate.

Figure 3.9: miRNAs in ES cell line derived exosomes

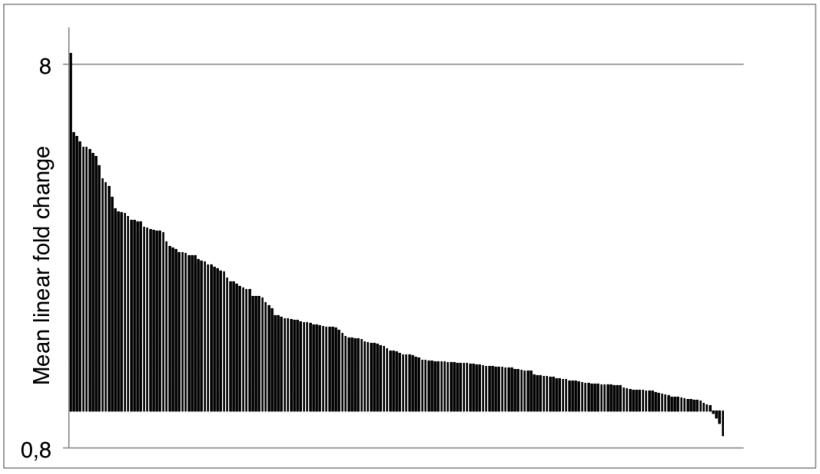

Fold change of miRNAs in ES cell line derived exosomes compared to their parental cells investigated by microarrays of three ES cell lines and corresponding exosomes. Nearly all miRNAs (except 4 of 205) showed a higher expression in the exosomes than in the cell they derived of. 58 miRNAs exhibited a fold change higher 2.

4 Discussion

It has been the aim of this study to assess if tumor specific transcripts can serve as biomarkers for ES in peripheral blood. Therefore, highly expressed ES transcripts were filtered on their expression in healthy human tissue, to evaluate the 12 most specific biomarker candidates. Based on the hypothesis that transcripts in human peripheral blood are only stable if they are associated with RNA binding proteins or extracellular vesicles (Redzic et al., 2014), it was investigated whether the ES releases vesicles containing these transcripts. In a third step, a model for patient plasma was designed, to assess the sensitivity of the enrichment method and to determine the conditions for testing ES patient blood plasma.

Challenge of biomarker identification

Indeed, the author could describe ES cell line derived extracellular vesicles holding the characteristics of exosomes, a subclass of EVs, for which pleiotropic roles in tumorigenesis were shown. These ES derived exosomes proved to carry the transcripts, which were priorly determined as highly ES specific, in their molecular cargo.

These selected transcripts are interesting biomarker candidates, not only for sensitive disease detection, but also for outcome prediction. Strikingly, the author´s selection of ES specific mRNAs is almost congruent to the set of biomarkers suggested by Cheung et al. (2007) for the detection of subclinical disease in bone marrow. By exosome enrichment, the amount of these transcripts could be increased effectively and steadily compared to the amount of transcripts found in cell culture supernatant and human plasma. Underpinned by the observation that ES derived exosomes save these transcripts from RNase digestion, exosome enrichment from peripheral blood of ES patients is a promising tool for biomarker discovery. Given the high sensitivity of this method shown in the patient plasma model, it remains unclear for which reasons the transcripts could not be detected in exosomes won from ES patient blood samples. The only positive sample, STEAP1, could, as well as the positive probes within the healthy donor samples, be caused by contamination, since for the probe only one sample of duplicates is positive. Alternatively, this result can be ranged as unspecific, since STEAP1 transcript was shown to be a marker for different classes of carcinomas as well as occasionally positive in the plasma of subjects lacking a malignant disease (Valenti et al., 2009).

The potential underlying mechanisms of the fail of significant transcript detection could, in spite of methodic accuracy and the proven high sensitivity of the detection method, root in different steps of the methodology used, as it will be pointed out closer in 5.2. In this chapter,

Table 4.1: Expression of biomarker transcripts in exosomes compared to cells of origin

	SK-N-MC		SB-KMS-KS1		A673		Mean	
Gene symbol	Exo	Cell	Exo	Cell	Exo	Cell	Exo	Cell
NPY1R	4.26	17.11	5.18	9.03	9.62	201.14	6.35	75.76
GPR64	4.82	4.03	4.58	11.87	24.20	357.26	11.20	124.39
DKK2	5.31	6.02	4.88	31.89	17.71	203.60	9.30	80.50
NKX2.2	7.14	22.71	8.51	48.92	25.59	154.51	13.75	75.38
LIPI	3.27	5.08	4.85	7.75	8.45	203.88	5.52	72.24
EZH2	10.27	103.81	70.60	335.60	9.97	242.59	30.28	227.34
STEAP1	10.98	32.74	15.26	77.62	16.50	221.01	14.25	110.46
NR0B1	5.02	9.58	10.95	51.78	13.26	102.57	9.74	54.64
CCND1	34.65	177.18	49.91	160.12	123.61	1508.92	69.39	615.41
PRKCB	13.26	108.66	53.65	224.98	28.29	371.16	31.73	234.93
ITM2A	8.70	77.82	27.03	112.10	17.75	292.29	17.82	160.74
DUX4	192.24	22.95	65.62	19.84	486.19	45.58	248.02	29.46

I would like to critically examine the basic approach of this thesis.

As described in 3.1, the first step was the election of potential marker transcripts, not from exosome preparations, but from ES cell lines and primary tumors. At this point, it was unclear, whether the ES indeed secretes exosomes serving as biomarker vehicles or not. When ES derived exosomes could be identified and furthermore contained the preliminary selected marker transcripts, these transcripts where adopted due to their proven stability in ES cell line derived exosomes and high specificity for ES. It was not considered that transcripts highly expressed in the parental cells are potentially not as highly expressed in the derived exosomes due to the cell´s selective sorting machinery. Finally, at the last stage of this project, the microarray analysis comparing the exosomal RNA content to the one of the cells, shed light on the actual amount of the marker transcripts in exosomes. It showed that all marker transcripts are highly expressed in the cell lines, but surprisingly comparatively lowly expressed in the derived exosomes (see table 4.1).

Implications of exosomal cargo RNA in ES tumorigenesis

Contrarily, having achieved the microarrays, transcripts highly enriched in ES derived exosomes could be identified (see Appendix VI and VII). The abundance of these RNAs in ES derived exosomes is not only notable due to their use as potential future biomarkers, but also for the functions they might inherit being transferred into other cells. One of the highly enriched candidates is, interestingly, DUX4. DUX4 is a transcription factor usually expressed in pluripotent germ lineage cells, whereas it underlies epigenetic silencing in somatically differentiated cells (Young et al., 2013). CIC-DUX4 fusion protein driven soft tissue sarcomas, which were primarily discussed as a EWS-ETS negative ES family member due

to their similar immunophenotype, do not generally share a common transcription signature with ES, but overexpress three ETS transcription factors (ETV4, ETV1, and ETV5) (Specht et al., 2014; Mariño Enríquez and Fletcher, 2014). A potential role of the unfused DUX4 in ES pathogenesis was not surveyed to present. Recently it was reported that DUX4 induces a neuroectodermal expression pattern in embryonic stem cells (Dandapat et al., 2013). Considering that ES display neuroectodermal features and a neuroectodermal transcriptional signature (von Levetzow et al., 2011; Staege et al., 2004), DUX4 transport via exosomes might contribute to a neuroectodermal differentiation within the tumor cell complex.

Additionally, a remarkably high amount of miRNAs was discovered in the cargo of ES cell line exosomes. 98% of the detected miRNAs were enriched in the exosomes compared to the cellular expression level, 28% holding a FC higher than 2. Interestingly, members of the miRNA cluster 106a˜363, which obtains oncogenic functions in ES, are enriched in ES derived exosomes (see table in Appendix) (Dylla and Jedlicka, 2013). Since it was shown that tumor derived exosomes deliver functionally active oncogenic miRNAs (Zomer et al., 2010; Umezu et al., 2012) and miRNAs promote tumorigenesis in ES, this is another field of research further studies should focus on.

Nevertheless, even if not in a quantity as large as expected, it remains mentionable, that the originally selected marker transcripts, encoding proteins which are known for holding key functions in ES oncogenesis, are present in ES derived exosomes and perhaps delivered between tumor cells.

For instance, EZH2 acts as an inhibitor of tumor cell differentiation and drives metastasis (Richter et al., 2009). NR0B1 and NKX2.2 are EWS-FLI1 mediated key transcription factors increasing the proliferative capacity of ES (Kinsey et al., 2006; Garcia-Aragoncillo et al., 2008; Smith et al., 2006). Furthermore, EWS-FLI1 itself as master transcription factor and inductor of endothelial gene expression in ES cells is contained in ES derived exosomes (Staege et al., 2004; Tirode et al., 2007). DKK2 is critical for osteolysis and bone infiltration (Hauer et al., 2013), whereas GPR64 promotes tumor invasion and metastasis via PGF and MMP1 (Richter et al., 2013). STEAP1 induces an oxidative stress phenotype in ES increasing invasiveness (Grunewald et al., 2012). Interestingly, STEAP3, another member of the STEAP family, is involved in exosome secretion (Lespagnol et al., 2008).

All these effects could be transferred between tumor cells either to keep a metabolic and transcriptional balance within the tumor or to distribute distinct features to tumor cell subclasses. As Tsugita et al. (2013) recently showed, ES cell line derived EVs containing EWS-FLI1 are present in the plasma of a xenograft model and EWS-FLI1 is transferred to other ES cells in vitro. Thus, it can be speculated if ES derived exosomes are a means of communication within the tumor network sending genetic information to push tumor subpopulations towards a specific differentiation. Interestingly, gene-set enrichment analysis revealed an implication of the exosomal RNA in G-protein-coupled signaling, neurotransmitter signaling and stemness, supporting the thesis of the maintenance of tumor promoting cellular features through

exosomal RNA transfer within the tumor network, but rather suggesting the upkeep of an undifferentiated phenotype. Taken together, exosomal genetic communication could serve to balance the degree of differentiation and the maintenance of stemness properties in different tumor subpopulations to sustain the tumors inner heterogenicity.

Beyond an autocrine tumor self-promoting effect, ES derived exosomes could as well communicate in a paracrine or endocrine manner with their micro- and macroenvironment.

Interestingly, the study of Tsugita et al. (2013) revealed that ES cell line derived EVs deliver EWS-FLI1 to other ES cells, but not to HOS cells. Contrarily, in this study the internalization of A673 derived exosomes HEK293 was observed, suggesting that ES derived exosomes are taken up by different cell types, too. Horizontal transfer of genetic information, epigenetic regulators and functional proteins opens an unforeseen spectrum of potential communication pathways and modulation between the ES and its stroma, as it was shown for many other cancer entities (see Introduction). Since EWS-FLI1, which proved to induce an endothelial gene expression not only in ES, but also in mesenchymal stem cells (Staege et al., 2004; Tirode et al., 2007), it could be conjectured whether ES exosomes co-induce angiogenesis. Beyond neo-vascularisation, ES derived exosomes could take part in stromal reprogramming. Recent studies showed that exosomes are key players in the preparation of premetastatic niches and the initiation of metastasis (Peinado et al., 2012; Hood et al., 2011; Luga et al., 2012). Since ES is an early metastasizing tumor, it is tempting to speculate whether exosomes possess a role in metastatic spread. If so, a new therapeutic strategy for ES treatment was to interrupt this process by blocking exosome production and uptake pathways, furthermore disturbing the other potential tumor promoting effects of ES derived exosomes discussed here.

ES derived exosomes as therapeutic vehicles

Though the crucial influence and biological relevance of exosomes in tumor progression was shown for several cancer entities, the evaluation of tumor treatment by exosome inhibition requires future studies (Bobrie et al., 2012b; Vader et al., 2014). But beyond, tumor derived exosomes inherit potential themselves as therapeutic vehicles. Since it was shown that exosomes are transporters of functional siRNA and miRNA, which can be internalized into exosomes by electroporation and unroll their function intracellularily, they could be used for efficient silencing of tumor promoting genes in cancer treatment (Kosaka et al., 2013). Ohno et al. (2013) succeeded to address exosomes selectively to EGFR expressing breast cancer cells and deliver the tumorsuppressive miRNA let7-a into the cell. In ES, let7-a was shown to be directly repressed by EWS-FLI, promoting tumor progression, while treatment of tumor bearing mice with synthetically produced let-7a decelerated tumor growth (De Vito et al., 2011). Using let-7a loaded exosomes, which are selectively internalized by ES cells, might distinctly intensify the anti tumor effect of let-7a treatment.

As another clinical application for ES, it could be considered to transfer short interfering RNAs directed against EWS-FLI1 via exosomes inwards ES cells. Considering the importance

of selective internalization of EWS-FLI1 siRNA into the tumor cell for treatment response, as it was shown by Hu-Lieskovan et al. (2005), who designed EWS-FLI1 siRNA containing microparticles bearing transferrin which proved to be taken up specifically by tumor cells, "re-programmed" exosomes could serve as a reliable carrier for EWS-FLI1 siRNA.

Furthermore, as immunogenic microparticles, exosomes can be used as primers for immunotherapy. Interacting with to T-cells and DCs, antigens primary coupled to an exosomal surface protein can induce an anti tumor response by CD8+-cells, decreasing tumor growth *in vivo* (Zeelenberg et al., 2008). Accordingly, customized exosomes bearing antigens typical for ES, such as EZH2, could be used to stimulate T-cells for immunotherapy or anti tumor vaccination.

5 Conclusions, limitations and perspectives

5.1 Conclusions

This study revealed first evidence of exosomes derived from ES. Even though the author could not identify ES derived exosomes and their encapsulated ES specific transcripts in the peripheral blood of ES patients, this investigation offers other approaches for the detection of ES specific biomarkers, e.g. based on proteomics, miRNA or microarray signatures. Furthermore, the evidence of ES derived exosomes suggests that the ES uses exosomes to communicate with its environment and manipulate stromal cells. Thus, exosomes derived from ES might contribute to tumor growth, angiogenesis and metastasis.

Altogether, the identification of ES derived exosomes may have future relevance for the research on biomarkers and new therapeutic strategies on ES. The results of this MD thesis were published in an international peer-reviewed journal.

5.2 Limitations and perspectives

This M.D. thesis focused on the detection of specific mRNA biomarkers for ES in peripheral blood. During the course of this project, the author observed, that ES cell lines synthesize exosomes, which carry the transcripts pre-selected as potential biomarkers. This investigation led to further analyses on the characterization and potential role of ES derived exosomes. Nevertheless, in this field remain unresolved questions, which are beyond the scope of this thesis and require future studies to define the actual implications and biological relevance of tumor derived exosomes in ES tumorigenesis.

- This study shows that ES cell line derived exosomes are taken up by cells of another species, HEK293. A more in-depth question was whether ES derived exosomes are taken up by MSCs as the notional cell of origin as well as neighbored stromal cell in the bone marrow. Moreover, beyond the physical uptake, the procession of the exosomal cargo and its impact on the cells gene expression require further analysis.

- EVs were concentrated by serial ultracentrifugation and characterized on behalf of their size, morphology and surface proteins. An additional experiment to confirm their affiliation to the group of exosomes is density measurement assessed by a sucrose gradient. The latter was not performed because it requires overnight centrifugation, which was

not possible to arrange due to technical security issues. Thus, it remains unclear, if the detected EVs possibly descend from different subclasses, which cannot be separated by ultracentrifugation. The identification of diverse subclasses within the group of exosomes, holding different functions, and the methodic insufficiency to separate them is matter of discussion in current exosome research (Bobrie et al., 2012a).

- In the present study, ES cell line derived exosomes were exclusively examined for their mRNA and partly for their miRNA, but not for their protein content. The crucial question, if EWS-FLI1 protein or other key players in oncogenic transformation are transferred by ES derived exosomes and enroll their functional activity in other cells, is addressed to future research.

Despite excessive preparatory work and methodical optimization, the author could not detect ES derived exosomes and transcripts in patient plasma. Beyond the re-evaluation of the basic approach, which was discussed above, additional experiments as well as potentially remedial changes in the methodology can be proposed:

- First of all, the plasma of only seven patients was tested, a relatively small number. Moreover, except two, all of the patients were already after or under treatment (surgery, chemotherapy or radiotherapy) when the plasma samples were achieved. It is unclear, how chemo- or radiotherapy influences exosome production *in vivo*, since the behavior of tumor derived exosomes *in vivo* is generally unpredictable. Multiple interactions are described, such as uptake by the reticuloendothelial system (Ohno et al., 2013). A higher volume of plasma would have increased the chance of a marker detection, but considering that the patients are mostly children, impaired by advanced cancer, multimodal treatment and invasive diagnostics, this appeared ethically unjustifiable.

- In this study, for transcript detection conventional qRT-PCR was used. In the intention to reach an even more sensitive scope, nested PCR can be tried. However, the latter goes along with an increased risk for erroneous results caused by minimal contamination. To avoid a distortion of the results by contamination or unspecific reactions, more replicates, at least triplicates, of each sample would be necessary. Due to the limited plasma volume, in this study only duplicates were carried out for marker detection in patient and healthy subject plasma. Hence, it remains unclear, if the detected STEAP1 and LIPI transcripts have any informative value or not.

- Even though RNase should not have any effect on exosomal RNA, a distinct decrease of detectable transcripts was seen after RNase treatment. This could be caused by degradation of additional free RNA released from apoptotic tumor cells or ruptured exosomes. Though all steps were performed at 4°C and the environment was tried to be kept RNase free, the loss of RNA should be further minimized, for instance by adding RNase inhibitors at all steps.

- This study was exclusively focused on marker positivity, but not on negativity as positive outcome predictor.
- As discussed above, the marker transcripts were elected as a result of of their expression in the cell of origin, not of their abundance in the derived exosomes. For further studies on RNA based exosomal biomarker detection for ES, I would suggest to further evaluate the microarray data of ES cell line derived exosomes provided by this study. Now that this study has given the evidence, that the exosomal RNA content is disproportioned to the cells RNA spectrum, potential new marker transcripts should be elected by the criteria of ES specificity and high expression in ES derived exosomes.
- In the present study, the exosomes analyzed were all derived from ES cell lines in vitro, not from primary tissues. As the different genetic profiles and conditions might impact on exosome production and packing, the RNA signature of native ES derived exosomes might diverge from cell line derived exosomes. Currently, the only option to acquire native tumor derived exosomes is isolation from patients blood. According to Noerholm et al. (2012), comparative microarrays of patient derived exosomes and healthy donor derived exosomes isolated from plasma could provide insight into the actual RNA composition of ES derived exosomes.
- Furthermore, the analysis of the protein and miRNA spectrum in the exosomal cargo could provide new biomarker candidates, since these molecules meanwhile play the leading role in exosomal biomarker research. Especially the detection of ews-fli1 protein in ES derived exosomes would be of great value as a unique biomarker.

Bibliography

Akers, J. C., Gonda, D., Kim, R., Carter, B. S., and Chen, C. C. (2013). Biogenesis of extracellular vesicles (ev): exosomes, microvesicles, retrovirus-like vesicles, and apoptotic bodies. *J Neurooncol*, 113(1):1–11.

Al-Nedawi, K., Meehan, B., Kerbel, R. S., Allison, A. C., and Rak, J. (2009). Endothelial expression of autocrine vegf upon the uptake of tumor-derived microvesicles containing oncogenic egfr. *Proc Natl Acad Sci U S A*, 106(10):3794–9.

Al-Nedawi, K., Meehan, B., Micallef, J., Lhotak, V., May, L., Guha, A., and Rak, J. (2008). Intercellular transfer of the oncogenic receptor egfrviii by microvesicles derived from tumour cells. *Nat Cell Biol*, 10(5):619–24.

Andreola, G., Rivoltini, L., Castelli, C., Huber, V., Perego, P., Deho, P., Squarcina, P., Accornero, P., Lozupone, F., Lugini, L., Stringaro, A., Molinari, A., Arancia, G., Gentile, M., Parmiani, G., and Fais, S. (2002). Induction of lymphocyte apoptosis by tumor cell secretion of fasl-bearing microvesicles. *J Exp Med*, 195(10):1303–16.

Ashiru, O., Boutet, P., Fernández-Messina, L., Agüera-González, S., Skepper, J. N., Valés-Gómez, M., and Reyburn, H. T. (2010). Natural killer cell cytotoxicity is suppressed by exposure to the human nkg2d ligand mica*008 that is shed by tumor cells in exosomes. *Cancer Res*, 70(2):481–9.

Baietti, M. F., Zhang, Z., Mortier, E., Melchior, A., Degeest, G., Geeraerts, A., Ivarsson, Y., Depoortere, F., Coomans, C., Vermeiren, E., Zimmermann, P., and David, G. (2012). Syndecan-syntenin-alix regulates the biogenesis of exosomes. *Nat Cell Biol*, 14(7):677–85.

Baran, J., Baj-Krzyworzeka, M., Weglarczyk, K., Szatanek, R., Zembala, M., Barbasz, J., Czupryna, A., Szczepanik, A., and Zembala, M. (2010). Circulating tumour-derived microvesicles in plasma of gastric cancer patients. *Cancer Immunol Immunother*, 59(6):841–50.

Bernstein, M., Kovar, H., Paulussen, M., Randall, R. L., Schuck, A., Teot, L. A., and Juergens, H. (2006). Ewing's sarcoma family of tumors: current management. *Oncologist*, 11(5):503–19.

Bobrie, A., Colombo, M., Krumeich, S., Raposo, G., and Théry, C. (2012a). Diverse subpopulations of vesicles secreted by different intracellular mechanisms are present in exosome

preparations obtained by differential ultracentrifugation. *Journal of extracellular vesicles*, 1.

Bobrie, A., Colombo, M., Raposo, G., and Thery, C. (2011). Exosome secretion: molecular mechanisms and roles in immune responses. *Traffic*, 12(12):1659–68.

Bobrie, A., Krumeich, S., Reyal, F., Recchi, C., Moita, L. F., Seabra, M. C., Ostrowski, M., and Théry, C. (2012b). Rab27a supports exosome-dependent and -independent mechanisms that modify the tumor microenvironment and can promote tumor progression. *Cancer Res*, 72(19):4920–30.

Bryant, R. J., Pawlowski, T., Catto, J. W., Marsden, G., Vessella, R. L., Rhees, B., Kuslich, C., Visakorpi, T., and Hamdy, F. C. (2012). Changes in circulating microrna levels associated with prostate cancer. *Br J Cancer*, 106(4):768–74.

Burdach, S. and Jürgens, H. (2002). High-dose chemoradiotherapy (hdc) in the ewing family of tumors (eft). *Crit Rev Oncol Hematol*, 41(2):169–89.

Burdach, S., Jürgens, H., Peters, C., Nürnberger, W., Mauz-Körholz, C., Körholz, D., Paulussen, M., Pape, H., Dilloo, D., and Koscielniak, E. (1993). Myeloablative radiochemotherapy and hematopoietic stem-cell rescue in poor-prognosis ewing's sarcoma. *J Clin Oncol*, 11(8):1482–8.

Burdach, S., Plehm, S., Unland, R., Dirksen, U., Borkhardt, A., Staege, M. S., Muller-Tidow, C., and Richter, G. H. (2009). Epigenetic maintenance of stemness and malignancy in peripheral neuroectodermal tumors by ezh2. *Cell Cycle*, 8(13):1991–6.

Burdach, S., Thiel, U., Schöniger, M., Haase, R., Wawer, A., Nathrath, M., Kabisch, H., Urban, C., Laws, H. J., Dirksen, U., Steinborn, M., Dunst, J., Jürgens, H., and Meta-EICESS Study Group (2010). Total body mri-governed involved compartment irradiation combined with high-dose chemotherapy and stem cell rescue improves long-term survival in ewing tumor patients with multiple primary bone metastases. *Bone Marrow Transplant*, 45(3):483–9.

Chalmin, F., Ladoire, S., Mignot, G., Vincent, J., Bruchard, M., Remy-Martin, J.-P., Boireau, W., Rouleau, A., Simon, B., Lanneau, D., De Thonel, A., Multhoff, G., Hamman, A., Martin, F., Chauffert, B., Solary, E., Zitvogel, L., Garrido, C., Ryffel, B., Borg, C., Apetoh, L., Rébé, C., and Ghiringhelli, F. (2010). Membrane-associated hsp72 from tumor-derived exosomes mediates stat3-dependent immunosuppressive function of mouse and human myeloid-derived suppressor cells. *J Clin Invest*, 120(2):457–71.

Chang, C. J. and Hung, M. C. (2012). The role of ezh2 in tumour progression. *Br J Cancer*, 106(2):243–7.

Chaput, N. and Thery, C. (2011). Exosomes: immune properties and potential clinical implementations. *Semin Immunopathol*, 33(5):419–40.

Chen, W. W., Balaj, L., Liau, L. M., Samuels, M. L., Kotsopoulos, S. K., Maguire, C. a., Loguidice, L., Soto, H., Garrett, M., Zhu, L. D., Sivaraman, S., Chen, C., Wong, E. T., Carter, B. S., Hochberg, F. H., Breakefield, X. O., and Skog, J. (2013). BEAMing and Droplet Digital PCR Analysis of Mutant IDH1 mRNA in Glioma Patient Serum and Cerebrospinal Fluid Extracellular Vesicles. *Molecular therapy. Nucleic acids*, 2(May):e109.

Cheung, I. Y., Feng, Y., Danis, K., Shukla, N., Meyers, P., Ladanyi, M., and Cheung, N. K. (2007). Novel markers of subclinical disease for ewing family tumors from gene expression profiling. *Clin Cancer Res*, 13(23):6978–83.

Cho, J. A., Park, H., Lim, E. H., and Lee, K. W. (2012). Exosomes from breast cancer cells can convert adipose tissue-derived mesenchymal stem cells into myofibroblast-like cells. *Int J Oncol*, 40(1):130–8.

Choi, D.-S., Park, J. O., Jang, S. C., Yoon, Y. J., Jung, J. W., Choi, D.-Y., Kim, J.-W., Kang, J. S., Park, J., Hwang, D., Lee, K.-H., Park, S.-H., Kim, Y.-K., Desiderio, D. M., Kim, K. P., and Gho, Y. S. (2011). Proteomic analysis of microvesicles derived from human colorectal cancer ascites. *Proteomics*, 11(13):2745–51.

Ciravolo, V., Huber, V., Ghedini, G. C., Venturelli, E., Bianchi, F., Campiglio, M., Morelli, D., Villa, A., Della Mina, P., Menard, S., Filipazzi, P., Rivoltini, L., Tagliabue, E., and Pupa, S. M. (2012). Potential role of her2-overexpressing exosomes in countering trastuzumab-based therapy. *J Cell Physiol*, 227(2):658–67.

Clayton, A., Mitchell, J. P., Court, J., Linnane, S., Mason, M. D., and Tabi, Z. (2008). Human tumor-derived exosomes down-modulate nkg2d expression. *J Immunol*, 180(11):7249–58.

Clayton, A., Mitchell, J. P., Court, J., Mason, M. D., and Tabi, Z. (2007). Human tumor-derived exosomes selectively impair lymphocyte responses to interleukin-2. *Cancer Res*, 67(15):7458–66.

Corcoran, C., Friel, A. M., Duffy, M. J., Crown, J., and O'Driscoll, L. (2011). Intracellular and extracellular micrornas in breast cancer. *Clin Chem*, 57(1):18–32.

Corcoran, C., Rani, S., O'Brien, K., O'Neill, A., Prencipe, M., Sheikh, R., Webb, G., McDermott, R., Watson, W., Crown, J., and O'Driscoll, L. (2012). Docetaxel-resistance in prostate cancer: evaluating associated phenotypic changes and potential for resistance transfer via exosomes. *PLoS One*, 7(12):e50999.

Dandapat, A., Hartweck, L. M., Bosnakovski, D., and Kyba, M. (2013). Expression of the human FSHD-linked DUX4 gene induces neurogenesis during differentiation of murine embryonic stem cells. *Stem cells and development*, 22(17):2440–8.

De Vito, C., Riggi, N., Suvà, M.-L., Janiszewska, M., Horlbeck, J., Baumer, K., Provero, P., and Stamenkovic, I. (2011). Let-7a is a direct EWS-FLI-1 target implicated in Ewing's sarcoma development. *PloS one*, 6(8):e23592.

Delattre, O., Zucman, J., Melot, T., Garau, X. S., Zucker, J. M., Lenoir, G. M., Ambros, P. F., Sheer, D., Turc-Carel, C., Triche, T. J., and et al. (1994). The ewing family of tumors–a subgroup of small-round-cell tumors defined by specific chimeric transcripts. *N Engl J Med*, 331(5):294–9.

Delattre, O., Zucman, J., Plougastel, B., Desmaze, C., Melot, T., Peter, M., Kovar, H., Joubert, I., de Jong, P., and Rouleau, G. (1992). Gene fusion with an ets dna-binding domain caused by chromosome translocation in human tumours. *Nature*, 359(6391):162–5.

Demory Beckler, M., Higginbotham, J. N., Franklin, J. L., Ham, A.-J., Halvey, P. J., Imasuen, I. E., Whitwell, C., Li, M., Liebler, D. C., and Coffey, R. J. (2013). Proteomic analysis of exosomes from mutant kras colon cancer cells identifies intercellular transfer of mutant kras. *Mol Cell Proteomics*, 12(2):343–55.

Diehl, J. A. (2002). Cycling to cancer with cyclin d1. *Cancer Biol Ther*, 1(3):226–31.

Dylla, L. and Jedlicka, P. (2013). Growth-promoting role of the miR-106a˜363 cluster in Ewing sarcoma. *PloS one*, 8(4):e63032.

EL Andaloussi, S., Mäger, I., Breakefield, X. O., and Wood, M. J. A. (2013). Extracellular vesicles: biology and emerging therapeutic opportunities. *Nat Rev Drug Discov*, 12(5):347–57.

Eldh, M., Lotvall, J., Malmhall, C., and Ekstrom, K. (2012). Importance of rna isolation methods for analysis of exosomal rna: evaluation of different methods. *Mol Immunol*, 50(4):278–86.

Fagnou, C., Michon, J., Peter, M., Bernoux, A., Oberlin, O., Zucker, J. M., Magdelenat, H., and Delattre, O. (1998). Presence of tumor cells in bone marrow but not in blood is associated with adverse prognosis in patients with ewing's tumor. société française d'oncologie pédiatrique. *J Clin Oncol*, 16(5):1707–11.

Garcia-Aragoncillo, E., Carrillo, J., Lalli, E., Agra, N., Gomez-Lopez, G., Pestana, A., and Alonso, J. (2008). Dax1, a direct target of ews/fli1 oncoprotein, is a principal regulator of cell-cycle progression in ewing's tumor cells. *Oncogene*, 27(46):6034–43.

Gatti, R., Belletti, S., Orlandini, G., Bussolati, O., Dall'Asta, V., and Gazzola, G. C. (1998). Comparison of annexin v and calcein-am as early vital markers of apoptosis in adherent cells by confocal laser microscopy. *J Histochem Cytochem*, 46(8):895–900.

Ge, X., Yamamoto, S., Tsutsumi, S., Midorikawa, Y., Ihara, S., Wang, S. M., and Aburatani, H. (2005). Interpreting expression profiles of cancers by genome-wide survey of breadth of expression in normal tissues. *Genomics*, 86(2):127–41.

Gerth, H. U., Juergens, K. U., Dirksen, U., Gerss, J., Schober, O., and Franzius, C. (2007). Significant benefit of multimodal imaging: PET/CT compared with PET alone in staging and follow-up of patients with Ewing tumors. *Journal of nuclear medicine : official publication, Society of Nuclear Medicine*, 48(12):1932–9.

Gong, J., Jaiswal, R., Mathys, J.-M., Combes, V., Grau, G. E. R., and Bebawy, M. (2012). Microparticles and their emerging role in cancer multidrug resistance. *Cancer Treat Rev*, 38(3):226–34.

Gross, J. C., Chaudhary, V., Bartscherer, K., and Boutros, M. (2012). Active wnt proteins are secreted on exosomes. *Nat Cell Biol*, 14(10):1036–45.

Grunewald, T. G., Diebold, I., Esposito, I., Plehm, S., Hauer, K., Thiel, U., da Silva-Buttkus, P., Neff, F., Unland, R., Muller-Tidow, C., Zobywalski, C., Lohrig, K., Lewandrowski, U., Sickmann, A., Prazeres da Costa, O., Gorlach, A., Cossarizza, A., Butt, E., Richter, G. H., and Burdach, S. (2012). Steap1 is associated with the invasive and oxidative stress phenotype of ewing tumors. *Mol Cancer Res*, 10(1):52–65.

Gu, J., Qian, H., Shen, L., Zhang, X., Zhu, W., Huang, L., Yan, Y., Mao, F., Zhao, C., Shi, Y., and Xu, W. (2012). Gastric cancer exosomes trigger differentiation of umbilical cord derived mesenchymal stem cells to carcinoma-associated fibroblasts through tgf-beta/smad pathway. *PLoS One*, 7(12):e52465.

Hauer, K., Calzada-Wack, J., Steiger, K., Grunewald, T. G. P., Baumhoer, D., Plehm, S., Buch, T., Prazeres da Costa, O., Esposito, I., Burdach, S., and Richter, G. H. S. (2013). DKK2 mediates osteolysis, invasiveness, and metastatic spread in Ewing sarcoma. *Cancer research*, 73(2):967–77.

Hood, J. L., San, R. S., and Wickline, S. A. (2011). Exosomes released by melanoma cells prepare sentinel lymph nodes for tumor metastasis. *Cancer Res*, 71(11):3792–801.

Hu-Lieskovan, S., Heidel, J. D., Bartlett, D. W., Davis, M. E., and Triche, T. J. (2005). Sequence-specific knockdown of EWS-FLI1 by targeted, nonviral delivery of small interfering RNA inhibits tumor growth in a murine model of metastatic Ewing's sarcoma. *Cancer research*, 65(19):8984–92.

Huber, V., Fais, S., Iero, M., Lugini, L., Canese, P., Squarcina, P., Zaccheddu, A., Colone, M., Arancia, G., Gentile, M., Seregni, E., Valenti, R., Ballabio, G., Belli, F., Leo, E., Parmiani, G., and Rivoltini, L. (2005). Human colorectal cancer cells induce t-cell death

through release of proapoptotic microvesicles: role in immune escape. *Gastroenterology*, 128(7):1796–804.

James, K., Eisenhauer, E., Christian, M., Terenziani, M., Vena, D., Muldal, A., and Therasse, P. (1999). Measuring response in solid tumors: unidimensional versus bidimensional measurement. *J Natl Cancer Inst*, 91(6):523–8.

Kauer, M., Ban, J., Kofler, R., Walker, B., Davis, S., Meltzer, P., and Kovar, H. (2009). A molecular function map of ewing's sarcoma. *PLoS One*, 4(4):e5415.

Keller, S., Konig, A. K., Marme, F., Runz, S., Wolterink, S., Koensgen, D., Mustea, A., Sehouli, J., and Altevogt, P. (2009). Systemic presence and tumor-growth promoting effect of ovarian carcinoma released exosomes. *Cancer Lett*, 278(1):73–81.

Keller, S., Ridinger, J., Rupp, A. K., Janssen, J. W., and Altevogt, P. (2011). Body fluid derived exosomes as a novel template for clinical diagnostics. *J Transl Med*, 9:86.

Khan, S., Jutzy, J. M. S., Valenzuela, M. M. A., Turay, D., Aspe, J. R., Ashok, A., Mirshahidi, S., Mercola, D., Lilly, M. B., and Wall, N. R. (2012). Plasma-derived exosomal survivin, a plausible biomarker for early detection of prostate cancer. *PloS one*, 7(10):e46737.

Kharaziha, P., Ceder, S., Li, Q., and Panaretakis, T. (2012). Tumor cell-derived exosomes: a message in a bottle. *Biochim Biophys Acta*, 1826(1):103–11.

Kim, J. W., Wieckowski, E., Taylor, D. D., Reichert, T. E., Watkins, S., and Whiteside, T. L. (2005). Fas ligand-positive membranous vesicles isolated from sera of patients with oral cancer induce apoptosis of activated t lymphocytes. *Clin Cancer Res*, 11(3):1010–20.

Kinsey, M., Smith, R., and Lessnick, S. L. (2006). Nr0b1 is required for the oncogenic phenotype mediated by ews/fli in ewing's sarcoma. *Mol Cancer Res*, 4(11):851–9.

Kosaka, N., Takeshita, F., Yoshioka, Y., Hagiwara, K., Katsuda, T., Ono, M., and Ochiya, T. (2013). Exosomal tumor-suppressive microRNAs as novel cancer therapy. "Exocure" is another choice for cancer treatment. *Advanced Drug Delivery Reviews*, 65(3):376–382.

Lahl, M., Fisher, V. L., and Laschinger, K. (2008). Ewing's sarcoma family of tumors: an overview from diagnosis to survivorship. *Clin J Oncol Nurs*, 12(1):89–97.

Laulagnier, K., Motta, C., Hamdi, S., Roy, S., Fauvelle, F., Pageaux, J. F., Kobayashi, T., Salles, J. P., Perret, B., Bonnerot, C., and Record, M. (2004). Mast cell- and dendritic cell-derived exosomes display a specific lipid composition and an unusual membrane organization. *Biochem J*, 380(Pt 1):161–171.

Lespagnol, A., Duflaut, D., Beekman, C., Blanc, L., Fiucci, G., Marine, J.-C., Vidal, M., Amson, R., and Telerman, A. (2008). Exosome secretion, including the DNA damage-induced p53-dependent secretory pathway, is severely compromised in TSAP6/Steap3-null mice. *Cell death and differentiation*, 15(11):1723–33.

Li, J., Sherman-Baust, C. A., Tsai-Turton, M., Bristow, R. E., Roden, R. B., and Morin, P. J. (2009). Claudin-containing exosomes in the peripheral circulation of women with ovarian cancer. *BMC Cancer*, 9:244.

Liu, C., Yu, S., Zinn, K., Wang, J., Zhang, L., Jia, Y., Kappes, J. C., Barnes, S., Kimberly, R. P., Grizzle, W. E., and Zhang, H.-G. (2006). Murine mammary carcinoma exosomes promote tumor growth by suppression of nk cell function. *J Immunol*, 176(3):1375–85.

Liu, Y., Xiang, X., Zhuang, X., Zhang, S., Liu, C., Cheng, Z., Michalek, S., Grizzle, W., and Zhang, H.-G. (2010). Contribution of myd88 to the tumor exosome-mediated induction of myeloid derived suppressor cells. *Am J Pathol*, 176(5):2490–9.

Logozzi, M., De Milito, A., Lugini, L., Borghi, M., Calabro, L., Spada, M., Perdicchio, M., Marino, M. L., Federici, C., Iessi, E., Brambilla, D., Venturi, G., Lozupone, F., Santinami, M., Huber, V., Maio, M., Rivoltini, L., and Fais, S. (2009). High levels of exosomes expressing cd63 and caveolin-1 in plasma of melanoma patients. *PLoS One*, 4(4):e5219.

Lu, Q., Zhang, J., Allison, R., Gay, H., Yang, W.-X., Bhowmick, N. A., Frelix, G., Shappell, S., and Chen, Y.-H. (2009). Identification of extracellular delta-catenin accumulation for prostate cancer detection. *Prostate*, 69(4):411–8.

Luga, V., Zhang, L., Viloria-Petit, A. M., Ogunjimi, A. A., Inanlou, M. R., Chiu, E., Buchanan, M., Hosein, A. N., Basik, M., and Wrana, J. L. (2012). Exosomes mediate stromal mobilization of autocrine wnt-pcp signaling in breast cancer cell migration. *Cell*, 151(7):1542–56.

Ma, X., Chen, Z., Hua, D., He, D., Wang, L., Zhang, P., Wang, J., Cai, Y., Gao, C., Zhang, X., Zhang, F., Wang, T., Hong, T., Jin, L., Qi, X., Chen, S., Gu, X., Yang, D., Pan, Q., Zhu, Y., Chen, Y., Chen, D., Jiang, L., Han, X., Zhang, Y., Jin, J., and Yao, X. (2014). Essential role for TrpC5-containing extracellular vesicles in breast cancer with chemotherapeutic resistance. *Proceedings of the National Academy of Sciences of the United States of America*, 111(17):6389–6394.

Mariño Enríquez, A. and Fletcher, C. D. M. (2014). Round cell sarcomas - Biologically important refinements in subclassification. *The international journal of biochemistry & cell biology*.

Mathivanan, S., Ji, H., and Simpson, R. J. (2010). Exosomes: extracellular organelles important in intercellular communication. *J Proteomics*, 73(10):1907–20.

Mikkelsen, T. S., Hanna, J., Zhang, X., Ku, M., Wernig, M., Schorderet, P., Bernstein, B. E., Jaenisch, R., Lander, E. S., and Meissner, A. (2008). Dissecting direct reprogramming through integrative genomic analysis. *Nature*, 454(7200):49–55.

Miser, J. S., Krailo, M. D., Tarbell, N. J., Link, M. P., Fryer, C. J. H., Pritchard, D. J., Gebhardt, M. C., Dickman, P. S., Perlman, E. J., Meyers, P. A., Donaldson, S. S., Moore, S., Rausen, A. R., Vietti, T. J., and Grier, H. E. (2004). Treatment of metastatic ewing's sarcoma or primitive neuroectodermal tumor of bone: evaluation of combination ifosfamide and etoposide–a children's cancer group and pediatric oncology group study. *J Clin Oncol*, 22(14):2873–6.

Mitchell, P. J., Welton, J., Staffurth, J., Court, J., Mason, M. D., Tabi, Z., and Clayton, A. (2009). Can urinary exosomes act as treatment response markers in prostate cancer? *J Transl Med*, 7:4.

Nakamura, N. (2010). Emerging new roles of gm130, a cis-golgi matrix protein, in higher order cell functions. *J Pharmacol Sci*, 112(3):255–64.

Nazarenko, I., Rana, S., Baumann, A., McAlear, J., Hellwig, A., Trendelenburg, M., Lochnit, G., Preissner, K. T., and Zoller, M. (2010). Cell surface tetraspanin tspan8 contributes to molecular pathways of exosome-induced endothelial cell activation. *Cancer Res*, 70(4):1668–78.

Nilsson, J., Skog, J., Nordstrand, A., Baranov, V., Mincheva-Nilsson, L., Breakefield, X. O., and Widmark, A. (2009). Prostate cancer-derived urine exosomes: a novel approach to biomarkers for prostate cancer. *Br J Cancer*, 100(10):1603–7.

Noerholm, M., Balaj, L., Limperg, T., Salehi, A., Zhu, L. D., Hochberg, F. H., Breakefield, X. O., Carter, B. S., and Skog, J. (2012). Rna expression patterns in serum microvesicles from patients with glioblastoma multiforme and controls. *BMC Cancer*, 12:22.

Ogata-Kawata, H., Izumiya, M., Kurioka, D., Honma, Y., Yamada, Y., Furuta, K., Gunji, T., Ohta, H., Okamoto, H., Sonoda, H., Watanabe, M., Nakagama, H., Yokota, J., Kohno, T., and Tsuchiya, N. (2014). Circulating Exosomal microRNAs as Biomarkers of Colon Cancer. *PloS one*, 9(4):e92921.

Ohno, S.-i., Takanashi, M., Sudo, K., Ueda, S., Ishikawa, A., Matsuyama, N., Fujita, K., Mizutani, T., Ohgi, T., Ochiya, T., Gotoh, N., and Kuroda, M. (2013). Systemically injected exosomes targeted to EGFR deliver antitumor microRNA to breast cancer cells. *Molecular therapy : the journal of the American Society of Gene Therapy*, 21(1):185–91.

Ono, M., Kosaka, N., Tominaga, N., Yoshioka, Y., Takeshita, F., Takahashi, R.-u., Yoshida, M., Tsuda, H., Tamura, K., and Ochiya, T. (2014). Exosomes from bone marrow mesenchy-

mal stem cells contain a microRNA that promotes dormancy in metastatic breast cancer cells. *Science Signaling*, 7(332):ra63–ra63.

Pant, S., Hilton, H., and Burczynski, M. E. (2012). The multifaceted exosome: biogenesis, role in normal and aberrant cellular function, and frontiers for pharmacological and biomarker opportunities. *Biochem Pharmacol*, 83(11):1484–94.

Peinado, H., Aleckovic, M., Lavotshkin, S., Matei, I., Costa-Silva, B., Moreno-Bueno, G., Hergueta-Redondo, M., Williams, C., Garcia-Santos, G., Ghajar, C., Nitadori-Hoshino, A., Hoffman, C., Badal, K., Garcia, B. A., Callahan, M. K., Yuan, J., Martins, V. R., Skog, J., Kaplan, R. N., Brady, M. S., Wolchok, J. D., Chapman, P. B., Kang, Y., Bromberg, J., and Lyden, D. (2012). Melanoma exosomes educate bone marrow progenitor cells toward a pro-metastatic phenotype through met. *Nat Med*, 18(6):883–91.

Peng, P., Yan, Y., and Keng, S. (2011). Exosomes in the ascites of ovarian cancer patients: origin and effects on anti-tumor immunity. *Oncol Rep*, 25(3):749–62.

Peter, M., Magdelenat, H., Michon, J., Melot, T., Oberlin, O., Zucker, J. M., Thomas, G., and Delattre, O. (1995). Sensitive detection of occult ewing's cells by the reverse transcriptase-polymerase chain reaction. *Br J Cancer*, 72(1):96–100.

Postel-Vinay, S., Veron, A. S., Tirode, F., Pierron, G., Reynaud, S., Kovar, H., Oberlin, O., Lapouble, E., Ballet, S., Lucchesi, C., Kontny, U., Gonzalez-Neira, A., Picci, P., Alonso, J., Patino-Garcia, A., de Paillerets, B. B., Laud, K., Dina, C., Froguel, P., Clavel-Chapelon, F., Doz, F., Michon, J., Chanock, S. J., Thomas, G., Cox, D. G., and Delattre, O. (2012). Common variants near tardbp and egr2 are associated with susceptibility to ewing sarcoma. *Nat Genet*, 44(3):323–7.

Rabinowits, G., Gercel-Taylor, C., Day, J. M., Taylor, D. D., and Kloecker, G. H. (2009). Exosomal microrna: a diagnostic marker for lung cancer. *Clin Lung Cancer*, 10(1):42–6.

Rana, S. and Zöller, M. (2011). Exosome target cell selection and the importance of exosomal tetraspanins: a hypothesis. *Biochem Soc Trans*, 39(2):559–62.

Raposo, G., Nijman, H. W., Stoorvogel, W., Liejendekker, R., Harding, C. V., Melief, C. J., and Geuze, H. J. (1996). B lymphocytes secrete antigen-presenting vesicles. *J Exp Med*, 183(3):1161–72.

Reddi, K. K. and Holland, J. F. (1976). Elevated serum ribonuclease in patients with pancreatic cancer. *Proc Natl Acad Sci U S A*, 73(7):2308–10.

Redzic, J. S., Balaj, L., van der Vos, K. E., and Breakefield, X. O. (2014). Extracellular RNA mediates and marks cancer progression. *Seminars in cancer biology*.

Revet, I., Huizenga, G., Koster, J., Volckmann, R., van Sluis, P., Versteeg, R., and Geerts, D. (2010). Msx1 induces the wnt pathway antagonist genes dkk1, dkk2, dkk3, and sfrp1 in neuroblastoma cells, but does not block wnt3 and wnt5a signalling to dvl3. *Cancer Lett*, 289(2):195–207.

Richter, G. H., Plehm, S., Fasan, A., Rossler, S., Unland, R., Bennani-Baiti, I. M., Hotfilder, M., Lowel, D., von Luettichau, I., Mossbrugger, I., Quintanilla-Martinez, L., Kovar, H., Staege, M. S., Muller-Tidow, C., and Burdach, S. (2009). Ezh2 is a mediator of ews/fli1 driven tumor growth and metastasis blocking endothelial and neuro-ectodermal differentiation. *Proc Natl Acad Sci U S A*, 106(13):5324–9.

Richter, G. H. S., Fasan, A., Hauer, K., Grunewald, T. G. P., Berns, C., Rössler, S., Naumann, I., Staege, M. S., Fulda, S., Esposito, I., and Burdach, S. (2013). G-Protein coupled receptor 64 promotes invasiveness and metastasis in Ewing sarcomas through PGF and MMP1. *The Journal of pathology*, 230(1):70–81.

Riggi, N. and Stamenkovic, I. (2007). The biology of ewing sarcoma. *Cancer Lett*, 254(1):1–10.

Roth, R. B., Hevezi, P., Lee, J., Willhite, D., Lechner, S. M., Foster, A. C., and Zlotnik, A. (2006). Gene expression analyses reveal molecular relationships among 20 regions of the human cns. *Neurogenetics*, 7(2):67–80.

Safaei, R., Larson, B. J., Cheng, T. C., Gibson, M. A., Otani, S., Naerdemann, W., and Howell, S. B. (2005). Abnormal lysosomal trafficking and enhanced exosomal export of cisplatin in drug-resistant human ovarian carcinoma cells. *Mol Cancer Ther*, 4(10):1595–604.

Savola, S., Klami, A., Myllykangas, S., Manara, C., Scotlandi, K., Picci, P., Knuutila, S., and Vakkila, J. (2011). High expression of complement component 5 (c5) at tumor site associates with superior survival in ewing's sarcoma family of tumour patients. *ISRN Oncol*, 2011:168712–168712.

Schaefer, K. L., Eisenacher, M., Braun, Y., Brachwitz, K., Wai, D. H., Dirksen, U., Lanvers-Kaminsky, C., Juergens, H., Herrero, D., Stegmaier, S., Koscielniak, E., Eggert, A., Nathrath, M., Gosheger, G., Schneider, D. T., Bury, C., Diallo-Danebrock, R., Ottaviano, L., Gabbert, H. E., and Poremba, C. (2008). Microarray analysis of ewing's sarcoma family of tumours reveals characteristic gene expression signatures associated with metastasis and resistance to chemotherapy. *Eur J Cancer*, 44(5):699–709.

Schleiermacher, G., Peter, M., Oberlin, O., Philip, T., Rubie, H., Mechinaud, F., Sommelet-Olive, D., Landman-Parker, J., Bours, D., Michon, J., Delattre, O., and Société Française d'Oncologie Pédiatrique (2003). Increased risk of systemic relapses associated with bone

marrow micrometastasis and circulating tumor cells in localized ewing tumor. *J Clin Oncol*, 21(1):85–91.

Scotlandi, K., Remondini, D., Castellani, G., Manara, M. C., Nardi, F., Cantiani, L., Francesconi, M., Mercuri, M., Caccuri, A. M., Serra, M., Knuutila, S., and Picci, P. (2009). Overcoming resistance to conventional drugs in ewing sarcoma and identification of molecular predictors of outcome. *J Clin Oncol*, 27(13):2209–2216.

Shao, H., Chung, J., Balaj, L., Charest, A., Bigner, D. D., Carter, B. S., Hochberg, F. H., Breakefield, X. O., Weissleder, R., and Lee, H. (2012). Protein typing of circulating microvesicles allows real-time monitoring of glioblastoma therapy. *Nature medicine*, 18(12):1835–40.

Sheldon, H., Heikamp, E., Turley, H., Dragovic, R., Thomas, P., Oon, C. E., Leek, R., Edelmann, M., Kessler, B., Sainson, R. C. A., Sargent, I., Li, J.-L., and Harris, A. L. (2010). New mechanism for notch signaling to endothelium at a distance by delta-like 4 incorporation into exosomes. *Blood*, 116(13):2385–94.

Silva, J., Garcia, V., Rodriguez, M., Compte, M., Cisneros, E., Veguillas, P., Garcia, J. M., Dominguez, G., Campos-Martin, Y., Cuevas, J., Peña, C., Herrera, M., Diaz, R., Mohammed, N., and Bonilla, F. (2012). Analysis of exosome release and its prognostic value in human colorectal cancer. *Genes Chromosomes Cancer*, 51(4):409–18.

Silva, J., García, V., Zaballos, Á., Provencio, M., Lombardía, L., Almonacid, L., García, J. M., Domínguez, G., Peña, C., Diaz, R., Herrera, M., Varela, A., and Bonilla, F. (2011). Vesicle-related micrornas in plasma of nonsmall cell lung cancer patients and correlation with survival. *Eur Respir J*, 37(3):617–23.

Skog, J., Wurdinger, T., van Rijn, S., Meijer, D. H., Gainche, L., Sena-Esteves, M., Curry, W. T., J., Carter, B. S., Krichevsky, A. M., and Breakefield, X. O. (2008). Glioblastoma microvesicles transport rna and proteins that promote tumour growth and provide diagnostic biomarkers. *Nat Cell Biol*, 10(12):1470–6.

Smalley, D. M., Sheman, N. E., Nelson, K., and Theodorescu, D. (2008). Isolation and identification of potential urinary microparticle biomarkers of bladder cancer. *J Proteome Res*, 7(5):2088–96.

Smith, R., Owen, L. A., Trem, D. J., Wong, J. S., Whangbo, J. S., Golub, T. R., and Lessnick, S. L. (2006). Expression profiling of ews/fli identifies nkx2.2 as a critical target gene in ewing's sarcoma. *Cancer Cell*, 9(5):405–16.

Sorensen, P. H., Lessnick, S. L., Lopez-Terrada, D., Liu, X. F., Triche, T. J., and Denny, C. T. (1994). A second ewing's sarcoma translocation, t(21;22), fuses the ews gene to another ets-family transcription factor, erg. *Nat Genet*, 6(2):146–51.

Specht, K., Sung, Y.-S., Zhang, L., Richter, G. H. S., Fletcher, C. D., and Antonescu, C. R. (2014). Distinct transcriptional signature and immunoprofile of cic-dux4 fusion-positive round cell tumors compared to ewsr1-rearranged ewing sarcomas: Further evidence toward distinct pathologic entities. *Genes Chromosomes Cancer*, 53(7):622–33.

Staege, M. S., Hutter, C., Neumann, I., Foja, S., Hattenhorst, U. E., Hansen, G., Afar, D., and Burdach, S. E. (2004). Dna microarrays reveal relationship of ewing family tumors to both endothelial and fetal neural crest-derived cells and define novel targets. *Cancer Res*, 64(22):8213–21.

Stahl, M., Ranft, A., and Paulussen, M. (2011). Risk of recurrence and survival after relapse in patients with Ewing sarcoma. *Pediatric blood & ...*, (September 2010):549–553.

Surdez, D., Benetkiewicz, M., Perrin, V., Han, Z.-Y., Pierron, G., Ballet, S., Lamoureux, F., Rédini, F., Decouvelaere, A.-V., Daudigeos-Dubus, E., Geoerger, B., de Pinieux, G., Delattre, O., and Tirode, F. (2012). Targeting the ewsr1-fli1 oncogene-induced protein kinase pkc-b abolishes ewing sarcoma growth. *Cancer Res*, 72(17):4494–503.

Szajnik, M., Czystowska, M., Szczepanski, M. J., Mandapathil, M., and Whiteside, T. L. (2010). Tumor-derived microvesicles induce, expand and up-regulate biological activities of human regulatory t cells (treg). *PLoS One*, 5(7):e11469.

Szczepanski, M. J., Szajnik, M., Welsh, A., Whiteside, T. L., and Boyiadzis, M. (2011). Blast-derived microvesicles in sera from patients with acute myeloid leukemia suppress natural killer cell function via membrane-associated transforming growth factor-beta1. *Haematologica*, 96(9):1302–9.

Takeshita, N., Hoshino, I., Mori, M., Akutsu, Y., Hanari, N., Yoneyama, Y., Ikeda, N., Isozaki, Y., Maruyama, T., Akanuma, N., Komatsu, A., Jitsukawa, M., and Matsubara, H. (2013). Serum microrna expression profile: mir-1246 as a novel diagnostic and prognostic biomarker for oesophageal squamous cell carcinoma. *Br J Cancer*, 108(3):644–52.

Tanaka, Y., Kamohara, H., Kinoshita, K., Kurashige, J., Ishimoto, T., Iwatsuki, M., Watanabe, M., and Baba, H. (2013). Clinical impact of serum exosomal microrna-21 as a clinical biomarker in human esophageal squamous cell carcinoma. *Cancer*, 119(6):1159–67.

Tavoosidana, G., Ronquist, G., Darmanis, S., Yan, J., Carlsson, L., Wu, D., Conze, T., Ek, P., Semjonow, A., Eltze, E., Larsson, A., Landegren, U. D., and Kamali-Moghaddam, M. (2011). Multiple recognition assay reveals prostasomes as promising plasma biomarkers for prostate cancer. *Proc Natl Acad Sci U S A*, 108(21):8809–14.

Taylor, D. D. and Gercel-Taylor, C. (2008). Microrna signatures of tumor-derived exosomes as diagnostic biomarkers of ovarian cancer. *Gynecol Oncol*, 110(1):13–21.

Taylor, D. D. and Gercel-Taylor, C. (2013). The origin, function, and diagnostic potential of rna within extracellular vesicles present in human biological fluids. *Front Genet*, 4:142.

Taylor, D. D., Zacharias, W., and Gercel-Taylor, C. (2011). Exosome isolation for proteomic analyses and rna profiling. *Methods Mol Biol*, 728:235–46.

Thébaud, B. and Stewart, D. J. (2012). Exosomes: cell garbage can, therapeutic carrier, or trojan horse? *Circulation*, 126(22):2553–5.

Thery, C., Amigorena, S., Raposo, G., and Clayton, A. (2006). Isolation and characterization of exosomes from cell culture supernatants and biological fluids. *Curr Protoc Cell Biol*, Chapter 3:Unit 3 22.

Tickner, J. A., Urquhart, A. J., Stephenson, S.-A., Richard, D. J., and O'Byrne, K. J. (2014). Functions and Therapeutic Roles of Exosomes in Cancer. *Frontiers in oncology*, 4:127.

Tirode, F., Laud-Duval, K., Prieur, A., Delorme, B., Charbord, P., and Delattre, O. (2007). Mesenchymal stem cell features of ewing tumors. *Cancer Cell*, 11(5):421–9.

Toomey, E. C., Schiffman, J. D., and Lessnick, S. L. (2010). Recent advances in the molecular pathogenesis of ewing's sarcoma. *Oncogene*, 29(32):4504–16.

Trajkovic, K., Hsu, C., Chiantia, S., Rajendran, L., Wenzel, D., Wieland, F., Schwille, P., Brügger, B., and Simons, M. (2008). Ceramide triggers budding of exosome vesicles into multivesicular endosomes. *Science*, 319(5867):1244–1247.

Tsugita, M., Yamada, N., Noguchi, S., Yamada, K., Moritake, H., Shimizu, K., Akao, Y., and Ohno, T. (2013). Ewing Sarcoma Cells Secrete EWS/Fli-1 Fusion mRNA via Microvesicles. *PLoS ONE*, 8(10):e77416.

Tsui, N. B., Ng, E. K., and Lo, Y. M. (2002). Stability of endogenous and added rna in blood specimens, serum, and plasma. *Clin Chem*, 48(10):1647–53.

Uggeri, J., Gatti, R., Belletti, S., Scandroglio, R., Corradini, R., Rotoli, B. M., and Orlandini, G. (2004). Calcein-am is a detector of intracellular oxidative activity. *Histochem Cell Biol*, 122(5):499–505.

Umezu, T., Ohyashiki, K., Kuroda, M., and Ohyashiki, J. H. (2012). Leukemia cell to endothelial cell communication via exosomal mirnas. *Oncogene*.

Vader, P., Breakefield, X. O., and Wood, M. J. a. (2014). Extracellular vesicles: emerging targets for cancer therapy. *Trends in molecular medicine*, pages 1–9.

Valadi, H., Ekstrom, K., Bossios, A., Sjostrand, M., Lee, J. J., and Lotvall, J. O. (2007). Exosome-mediated transfer of mrnas and micrornas is a novel mechanism of genetic exchange between cells. *Nat Cell Biol*, 9(6):654–9.

Valenti, M. T., Dalle Carbonare, L., Donatelli, L., Bertoldo, F., Giovanazzi, B., Caliari, F., and Lo Cascio, V. (2009). STEAP mRNA detection in serum of patients with solid tumours. *Cancer letters*, 273(1):122–6.

van der Pol, E., Böing, A. N., Harrison, P., Sturk, A., and Nieuwland, R. (2012). Classification, functions, and clinical relevance of extracellular vesicles. *Pharmacol Rev*, 64(3):676–705.

Vermeulen, J., Ballet, S., Oberlin, O., Peter, M., Pierron, G., Longavenne, E., Laurence, V., Kanold, J., Chastagner, P., Lejars, O., Blay, J. Y., Marec-Berard, P., Michon, J., Delattre, O., and Schleiermacher, G. (2006). Incidence and prognostic value of tumour cells detected by rt-pcr in peripheral blood stem cell collections from patients with ewing tumour. *Br J Cancer*, 95(10):1326–33.

von Levetzow, C., Jiang, X., Gwye, Y., von Levetzow, G., Hung, L., Cooper, A., Hsu, J. H.-R., and Lawlor, E. R. (2011). Modeling initiation of ewing sarcoma in human neural crest cells. *PLoS One*, 6(4):e19305.

Webber, J., Steadman, R., Mason, M. D., Tabi, Z., and Clayton, A. (2010). Cancer exosomes trigger fibroblast to myofibroblast differentiation. *Cancer Res*, 70(23):9621–30.

Webber, J. P., Spary, L. K., Sanders, a. J., Chowdhury, R., Jiang, W. G., Steadman, R., Wymant, J., Jones, a. T., Kynaston, H., Mason, M. D., Tabi, Z., and Clayton, a. (2014). Differentiation of tumour-promoting stromal myofibroblasts by cancer exosomes. *Oncogene*, (August 2013):1–13.

Welton, J. L., Khanna, S., Giles, P. J., Brennan, P., Brewis, I. A., Staffurth, J., Mason, M. D., and Clayton, A. (2010). Proteomics analysis of bladder cancer exosomes. *Mol Cell Proteomics*, 9(6):1324–38.

Wieckowski, E. U., Visus, C., Szajnik, M., Szczepanski, M. J., Storkus, W. J., and Whiteside, T. L. (2009). Tumor-derived microvesicles promote regulatory t cell expansion and induce apoptosis in tumor-reactive activated cd8+ t lymphocytes. *J Immunol*, 183(6):3720–30.

Williams, D. B. (2006). Beyond lectins: the calnexin/calreticulin chaperone system of the endoplasmic reticulum. *J Cell Sci*, 119(Pt 4):615–23.

Yoshioka, Y., Kosaka, N., Konishi, Y., Ohta, H., Okamoto, H., Sonoda, H., Nonaka, R., Yamamoto, H., Ishii, H., Mori, M., Furuta, K., Nakajima, T., Hayashi, H., Sugisaki, H., Higashimoto, H., Kato, T., Takeshita, F., and Ochiya, T. (2014). Ultra-sensitive liquid biopsy of circulating extracellular vesicles using ExoScreen. *Nature communications*, 5:3591.

Young, J. M., Whiddon, J. L., Yao, Z., Kasinathan, B., Snider, L., Geng, L. N., Balog, J., Tawil, R., van der Maarel, S. M., and Tapscott, S. J. (2013). DUX4 binding to retroelements creates promoters that are active in FSHD muscle and testis. *PLoS genetics*, 9(11):e1003947.

Yu, S., Liu, C., Su, K., Wang, J., Liu, Y., Zhang, L., Li, C., Cong, Y., Kimberly, R., Grizzle, W. E., Falkson, C., and Zhang, H.-G. (2007). Tumor exosomes inhibit differentiation of bone marrow dendritic cells. *J Immunol*, 178(11):6867–75.

Zeelenberg, I. S., Ostrowski, M., Krumeich, S., Bobrie, A., Jancic, C., Boissonnas, A., Delcayre, A., Le Pecq, J.-B., Combadière, B., Amigorena, S., and Théry, C. (2008). Targeting tumor antigens to secreted membrane vesicles in vivo induces efficient antitumor immune responses. *Cancer research*, 68(4):1228–35.

Zhuang, G., Wu, X., Jiang, Z., Kasman, I., Yao, J., Guan, Y., Oeh, J., Modrusan, Z., Bais, C., Sampath, D., and Ferrara, N. (2012). Tumour-secreted mir-9 promotes endothelial cell migration and angiogenesis by activating the jak-stat pathway. *EMBO J*, 31(17):3513–23.

Zomer, A., Vendrig, T., Hopmans, E. S., van Eijndhoven, M., Middeldorp, J. M., and Pegtel, D. M. (2010). Exosomes: Fit to deliver small RNA. *Communicative & integrative biology*, 3(5):447–50.

Appendix

I Form sheet

NEO-IDENT-Studie zur Serumanalyse bei Ewing-Tumor-Patienten

Im Rahmen der NEO-IDENT-Studie sollen neue **Tumormarker für Ewing-Tumore** ermittelt werden. Dafür wird Patientenseren vor und nach Therapie benötigt. Die Blutabnahme ist durch die Ethikkommission abgesichert.

Procedere:
Bitte **drei 9ml-EDTA-Röhrchen**, also 27ml Blut, abnehmen (unbedingt in EDTA-Röhrchen verwenden, nicht Heparin o.a.) und möglichst schnell ins Labor Dr. Richter, Forschungszentrum für krebskranke Kinder, schicken.

Patient:

Patientenetikett

Tumorlokalisation: _____

Metastasierung: _____

Vor Therapiebeginn	**Nach Induktionstherapie / vor OP**	**Nach Abschluss der Konsolidierungstherapie**
☐ 3 x 9ml EDTA-Röhrchen abgenommen	☐ 3 x 9ml EDTA-Röhrchen abgenommen	☐ 3 x 9ml EDTA-Röhrchen abgenommen
_____ Datum. Unterschrift	_____ Datum, Unterschrift	_____ Datum, Unterschrift

Ansprechpartner:

Isabella Miller
Telefon: 0151-11770095
Isabella.Miller@lrz.tu-muenchen.de

Dr. Uwe Thiel
Telefon: -5525
Uwe.Thiel@lrz.tu-muenchen.de

Colette Berns
Telefon: -3216

Dr. Thomas Grünewald
Thomas.Gruenewald@lrz.tum.de

Bitte melden Sie sich, sobald Sie erfahren, dass ein Ewing-Tumor-Patient kommt, damit wir das Vorgehen abstimmen können.

II Questionnaire

Klinik und Poliklinik für Kinder- und Jugendmedizin
Klinikum Rechts der Isar der
Technischen Universität München
Anstalt des öffentlichen Rechts

Kinderklinik München Schwabing

Direktor: Prof. Dr. Stefan Burdach

Gesundheitsfragebogen für volljährige einwilligungsfähige Patientinnen und Patienten

Betrifft: Blut- und Gewebeentnahme für die **NEO-IDENT**-Studie
bei Patienten ***ohne Krebserkrankung und ohne immunsuppressive Therapie***

Name: Geburtsdatum: Geschlecht: m/w

Sind Sie zur Zeit völlig gesund?

Litten Sie innerhalb der letzten 4 Wochen an einer infektiösen Erkrankung (z.B. Erkältung)?

Nehmen Sie regelmäßig Medikamente ein (auch Kontrazeptiva)? Wenn ja, welche?

Wurde bei Ihnen jemals eine onkologische Erkrankung (gutartig/bösartig) diagnostiziert oder behandelt? Wenn ja, welche?

Haben Sie eine chronische Erkrankung, wegen welcher Sie sich in Behandlung befinden (z.B. Bluthochdruck, Diabetes mellitus, chronisch entzündliche Darmerkrankungen, Asthma, Schilddrüsenerkrankungen)?

Leiden Sie unter Gehirn- oder Nervenerkrankungen/Anfallsleiden?

Bestehen bei Ihnen angeborene Erkrankungen?

Haben Sie Allergien? Wenn ja, welche?

Sind Sie schwanger?

Rauchen Sie? Wenn ja, wie viel?

Befinden Sie sich zur Zeit in ärztlicher Behandlung? Wenn ja, aus welchem Grund?

Hiermit versichere ich, dass ich alle Fragen wahrheitsgemäß beantwortet und nichts verschwiegen habe, was zur Beurteilung meines Gesundheitszustandes von Bedeutung ist.

Ort, Datum Unterschrift

III Volunteer data

No.	Age	Sex	Smoker	Allergies
1	22	f	n	y
2	30	m	n	y
3	23	f	n	n
4	23	f	n	y
5	25	m	n	n
6	30	f	y	y
7	31	m	n	n
8	23	f	n	n
9	32	m	n	n
10	26	m	n	n
11	28	m	n	y
12	23	m	n	n
13	21	f	y	n
14	26	m	n	n
15	57	m	n	n
16	28	m	n	n
17	23	f	y	y
18	26	m	y	n
19	31	m	n	y
20	24	m	n	n
21	29	m	n	y
22	26	m	n	n
23	27	m	n	y

IV Patient data

No.	Age	Sex	Site	Recurrence	lung metastasis	bone met	Therapy at test
1	24	f	Fibula	y	y	y	CTx
2	18	m	Multiple	y	y	y	CTx
3	14	m	Humerus	y	n	y	CTx
4	7	m	Spine	y	y	y	CTx
5	7	m	Os ischium	ID	y	y	n
6	18	m	Tibia	y	y	y	CTx
7	16	m	Spine	ID	n	n	n

V List of miRNAs identified by microarray analyses

Probe Set ID	Gene Description	FC SK-N-MC	FC SB-KMS-KS1	FC A673	Mean linear FC
7950490	microRNA 326	6.74	9.28	9.57	8.53
8149705	microRNA 320a	4.48	5.15	6.31	5.31
8163729	microRNA 147	4.70	4.69	6.22	5.20
7987097	microRNA 211	2.87	4.17	8.07	5.04
7903717	microRNA 197	2.39	5.77	6.44	4.87
8034698	microRNA 23a	3.30	4.20	7.09	4.86
8006321	microRNA 193a	4.26	3.50	6.65	4.80
7950195	microRNA 139	3.81	4.73	5.52	4.69
7953590	microRNA 200c	3.52	1.47	8.84	4.61
7922326	microRNA 214	2.90	4.09	6.07	4.35
8156569	microRNA 23b	2.95	1.78	7.34	4.03
8175706	microRNA 105-1	3.06	1.56	7.19	3.94
7939463	microRNA 129-2	2.31	1.02	8.21	3.85
8026212	microRNA 181c	2.89	4.58	3.35	3.61
8137707	microRNA 339	3.33	1.19	5.57	3.36
8071312	microRNA 185	2.54	1.49	5.90	3.31
7993337	microRNA 365-1	1.58	2.29	6.00	3.29
7949275	microRNA 194-2	2.52	3.68	3.59	3.27
8156523	microRNA let-7d	1.75	3.14	4.76	3.21
8073822	microRNA let-7a-3	2.99	1.19	5.25	3.14
8049682	microRNA 149	1.97	2.95	4.50	3.14
8024896	microRNA 7-3	2.79	1.65	4.90	3.11
8073824	microRNA let-7b	4.10	1.50	3.72	3.11
8038393	microRNA 150	2.69	1.67	4.69	3.01
8022912	microRNA 187	1.50	2.54	4.96	3.00
8067277	microRNA 296	1.47	2.05	5.40	2.97
7981326	microRNA 1247	2.27	1.76	4.85	2.96
8160439	microRNA 31	3.31	3.18	2.35	2.94
8175708	microRNA 105-2	2.77	1.61	4.44	2.94
8016482	microRNA 196a-1	4.02	2.00	2.72	2.91
8109157	microRNA 143	1.24	2.54	4.48	2.75
8175455	microRNA 504	1.42	2.26	4.38	2.69
8115730	microRNA 218-2	1.41	1.75	4.81	2.66
7956737	microRNA let-7i	2.67	1.99	3.24	2.63

Probe Set ID	Gene Description	FC SK-N-MC	FC SB-KMS-KS1	FC A673	Mean linear FC
7950490	microRNA 326	6.74	9.28	9.57	8.53
8167623	microRNA 188	1.88	2.96	2.93	2.59
8012004	microRNA 195	2.10	2.54	3.12	2.59
8037640	microRNA 330	2.06	1.22	4.45	2.58
8087250	microRNA 425	1.67	1.71	4.24	2.54
7912250	microRNA 34a	2.08	2.00	3.53	2.54
8175261	microRNA 503	2.14	2.21	3.25	2.54
8030846	microRNA 125a	3.85	1.09	2.52	2.49
7921012	microRNA 9-1	2.09	1.54	3.76	2.46
8157802	microRNA 181b-2	1.46	1.29	4.58	2.44
7976804	microRNA 127	2.44	1.60	3.17	2.41
8135907	microRNA 129-1	1.41	2.82	2.97	2.40
7945460	microRNA 210	1.59	1.45	4.06	2.37
7976844	microRNA 134	1.87	1.81	3.36	2.35
8011220	microRNA 212	2.20	1.50	3.24	2.31
8030844	microRNA let-7e	2.08	1.57	3.25	2.30
7900490	microRNA 30c-1	1.67	2.08	2.92	2.22
8164438	microRNA 219-2	1.33	2.88	2.31	2.17
8175587	microRNA 509-1	1.19	2.95	2.36	2.17
8030842	microRNA 99b	0.93	1.58	3.90	2.14
7952313	microRNA let-7a-2	1.23	1.24	3.88	2.11
8034696	microRNA 27a	2.46	1.28	2.53	2.09
7940044	microRNA 130a	1.09	0.92	4.21	2.07
7909422	microRNA 205	1.53	1.61	3.07	2.07
8079165	microRNA 138-1	2.20	1.40	2.38	1.99
8031029	microRNA 520c	0.86	1.59	3.52	1.99
8078663	microRNA 26a-1	1.42	1.66	2.89	1.99
7953592	microRNA 141	1.80	1.09	3.03	1.97
8141419	microRNA 25	1.51	1.64	2.60	1.92
8067942	microRNA 99a	1.40	2.05	2.20	1.88
8006119	microRNA 423	1.93	1.41	2.20	1.85
7934959	microRNA 107	1.36	1.45	2.51	1.77
8020419	microRNA 320c-1	1.95	2.11	1.25	1.77
8011218	microRNA 132	1.32	2.05	1.89	1.76
8078527	microRNA 128-2	1.14	1.33	2.75	1.74
8141421	microRNA 93	1.64	1.20	2.38	1.74

Probe Set ID	Gene Description	FC SK-N-MC	FC SB-KMS-KS1	FC A673	Mean linear FC
7950490	microRNA 326	6.74	9.28	9.57	8.53
8144149	microRNA 153-2	1.56	1.74	1.88	1.73
8157800	microRNA 181a-2	1.56	1.33	2.29	1.73
8149277	microRNA 124-1	1.17	0.96	3.04	1.72
8059211	microRNA 153-1	1.18	1.25	2.69	1.70
8167971	microRNA 223	1.57	1.41	2.12	1.70
7922328	microRNA 199a-2	2.16	1.47	1.47	1.70
8068022	microRNA 155	1.88	1.24	1.95	1.69
8060734	microRNA 103-2	0.98	1.25	2.80	1.68
8157444	microRNA 455	1.35	1.20	2.47	1.67
8127498	microRNA 30c-2	1.54	1.54	1.92	1.67
7949273	microRNA 192	1.69	1.17	2.11	1.66
8087252	microRNA 191	1.32	1.46	2.19	1.65
8052374	microRNA 216a	1.26	1.25	2.45	1.65
8146643	microRNA 124-2	2.61	1.18	1.16	1.65
8120206	microRNA 206	1.31	1.49	2.14	1.65
8164396	microRNA 199b	1.29	1.21	2.38	1.63
7964592	microRNA 26a-2	1.27	1.27	2.24	1.59
8109159	microRNA 145	1.00	1.08	2.62	1.57
8048317	microRNA 26b	1.64	1.14	1.87	1.55
7985871	microRNA 9-3	1.70	1.23	1.72	1.55
7923175	microRNA 181a-1	1.37	1.70	1.55	1.54
8087881	microRNA let-7g	1.38	1.50	1.75	1.54
8161695	microRNA 204	1.55	1.50	1.56	1.54
8071564	microRNA 130b	1.52	1.08	1.95	1.52
7985236	microRNA 184	1.23	1.24	2.07	1.51
8153065	microRNA 30b	1.57	1.47	1.46	1.50
7912248	microRNA 34a	1.31	1.28	1.91	1.50
7985765	microRNA 7-2	1.08	1.22	2.18	1.49
8031035	microRNA 516b-1	1.05	1.05	2.33	1.48
8031039	microRNA 519a-2	1.12	1.71	1.59	1.47
8156519	microRNA let-7a-1	1.72	1.43	1.22	1.46
8156571	microRNA 27b	1.97	1.04	1.29	1.43
7976846	microRNA 485	1.34	1.21	1.74	1.43
8045453	microRNA 128-1	1.15	1.21	1.91	1.42
7976842	microRNA 382	1.57	1.33	1.35	1.42

Probe Set ID	Gene Description	FC SK-N-MC	FC SB-KMS-KS1	FC A673	Mean linear FC
7950490	microRNA 326	6.74	9.28	9.57	8.53
8016400	microRNA 152	1.35	1.26	1.60	1.40
8031045	microRNA 519a-2	1.13	1.22	1.85	1.40
7976854	microRNA 412	1.17	1.31	1.71	1.40
7955906	microRNA 148b	1.36	1.23	1.59	1.39
7917944	microRNA 137	1.76	1.05	1.34	1.38
8138668	microRNA 148a	1.35	1.26	1.50	1.37
7957608	microRNA 492	1.39	1.20	1.48	1.36
8087883	microRNA 135a-1	1.39	1.25	1.42	1.35
7976832	microRNA 323	1.38	1.16	1.52	1.35
8142880	microRNA 182	1.29	1.21	1.55	1.35
8142882	microRNA 96	1.35	1.18	1.50	1.34
8021416	microRNA 122	1.17	1.52	1.33	1.34
7943736	microRNA 34b	1.39	1.06	1.57	1.34
7896859	microRNA 200b	1.41	1.16	1.45	1.34
8173005	microRNA 98	1.26	1.24	1.52	1.34
8175248	microRNA 92a-2	1.18	1.26	1.57	1.34
8031027	microRNA 519a-2	0.98	1.16	1.87	1.33
7955863	microRNA 196a-2	1.03	1.12	1.85	1.33
8120208	microRNA 133b	1.36	1.27	1.37	1.33
8142884	microRNA 183	1.43	1.33	1.24	1.33
8031031	microRNA 516b-2	1.09	1.41	1.48	1.33
8109649	microRNA 146a	1.06	1.17	1.74	1.33
7937148	microRNA 202	1.18	1.22	1.57	1.32
7976806	microRNA 136	1.13	1.31	1.51	1.32
7957631	microRNA 331	1.18	1.11	1.65	1.32
7952307	microRNA 125b-1	1.22	1.56	1.15	1.31
7952315	microRNA 100	1.27	1.41	1.25	1.31
8034694	microRNA 24-2	1.14	1.20	1.57	1.31
7976834	microRNA 494	1.30	1.11	1.50	1.30
7896861	microRNA 200a	1.17	1.21	1.53	1.30
7977214	microRNA 203	1.30	1.22	1.37	1.30
8094340	microRNA 218-1	1.35	1.03	1.52	1.30
8154176	microRNA 101-2	1.22	1.32	1.33	1.29
7923976	microRNA 29b-2	1.31	1.22	1.35	1.29
8046553	microRNA 10b	1.24	1.26	1.37	1.29

Probe Set ID	Gene Description	FC SK-N-MC	FC SB-KMS-KS1	FC A673	Mean linear FC
7950490	microRNA 326	6.74	9.28	9.57	8.53
7997008	microRNA 140	1.01	1.03	1.82	1.28
8159371	microRNA 126	1.08	1.03	1.74	1.28
7969574	microRNA 622	1.07	2.54	0.23	1.28
8141423	microRNA 106b	1.20	1.26	1.36	1.27
7971659	microRNA 16-1	1.29	1.21	1.32	1.27
8118632	microRNA 219-1	1.49	1.07	1.25	1.27
8016980	microRNA 142	1.10	1.21	1.42	1.24
8115689	microRNA 103-1	1.12	1.07	1.53	1.24
8031037	microRNA 517c	1.10	1.33	1.28	1.24
8008885	microRNA 21	1.43	1.05	1.21	1.23
8067946	microRNA 125b-2	1.09	1.40	1.21	1.23
7984077	microRNA 190	1.17	1.18	1.33	1.23
7957735	microRNA 135a-2	1.16	1.36	1.15	1.22
8064029	microRNA 124-3	1.15	1.07	1.42	1.21
8017139	microRNA 301a	1.25	1.18	1.21	1.21
8067944	microRNA let-7c	1.22	1.28	1.12	1.21
7896863	microRNA 429	1.28	1.32	1.02	1.21
8013784	microRNA 451	0.94	1.30	1.35	1.20
8156573	microRNA 24-1	1.26	1.16	1.17	1.20
7995866	microRNA 138-2	1.16	1.16	1.27	1.20
7943738	microRNA 34c	1.29	1.17	1.11	1.19
8175250	microRNA 19b-2	0.95	1.31	1.29	1.18
7978019	microRNA 208a	1.22	1.17	1.15	1.18
8084755	microRNA 28	1.00	1.03	1.50	1.18
8022500	microRNA 1-2	1.14	1.04	1.34	1.18
8156521	microRNA let-7f-1	1.04	1.19	1.29	1.17
8073544	microRNA 33a	1.14	1.06	1.32	1.17
7976850	microRNA 154	1.16	1.13	1.22	1.17
8175252	microRNA 106a	1.08	1.18	1.25	1.17
7976856	microRNA 410	0.98	1.16	1.36	1.17
7976852	microRNA 377	0.97	1.16	1.38	1.17
7923974	microRNA 29c	1.36	0.96	1.19	1.17
8016455	microRNA 10a	1.38	1.11	1.00	1.16
8175683	microRNA 224	1.04	1.07	1.38	1.16
8022498	microRNA 133a-1	0.97	1.15	1.32	1.15

Probe Set ID	Gene Description	FC SK-N-MC	FC SB-KMS-KS1	FC A673	Mean linear FC
7950490	microRNA 326	6.74	9.28	9.57	8.53
7916777	microRNA 101-1	1.17	1.20	1.06	1.14
7976838	microRNA 376c	1.00	1.25	1.16	1.14
8099302	microRNA 95	0.97	1.10	1.33	1.13
8083739	microRNA 16-2	1.04	1.03	1.33	1.13
7924403	microRNA 194-1	1.09	0.99	1.32	1.13
7924401	microRNA 215	1.06	0.96	1.37	1.13
8172266	microRNA 221	1.06	1.18	1.15	1.13
7976840	microRNA 487a	1.15	1.08	1.15	1.13
8102406	microRNA 302b	1.04	1.13	1.22	1.13
8052372	microRNA 217	1.21	1.11	1.02	1.12
8153067	microRNA 30d	1.05	1.04	1.25	1.11
8063921	microRNA 1-1	1.12	1.05	1.16	1.11
8173007	microRNA let-7f-2	1.15	1.09	1.07	1.10
7976830	microRNA 299	1.02	1.09	1.18	1.10
8083737	microRNA 15b	1.29	1.12	0.86	1.09
8127500	microRNA 30a	1.08	0.99	1.18	1.08
8172268	microRNA 222	1.01	1.05	1.20	1.08
8142975	microRNA 29a	1.12	0.98	1.15	1.08
8142977	microRNA 29b-1	1.02	0.92	1.29	1.08
7976836	microRNA 495	1.03	1.17	1.02	1.07
8163107	microRNA 32	1.00	1.36	0.85	1.07
8013786	microRNA 144	0.99	1.03	1.18	1.06
8102404	microRNA 302a	1.00	1.01	1.19	1.06
8034099	microRNA 199a-1	1.07	1.03	1.09	1.06
8113037	microRNA 9-2	1.08	1.08	0.98	1.05
7969576	MIR17 host gene	1.25	1.04	0.83	1.04
7923173	microRNA 181b-1	1.26	1.26	0.58	1.03
7900488	microRNA 30e	1.07	1.07	0.83	0.99
8059026	microRNA 375	0.71	0.75	1.42	0.96
7971661	microRNA 15a	0.94	1.04	0.80	0.93
7916984	microRNA 186	0.73	0.86	1.00	0.86

VI List of the 120 highest expressed transcripts in ES cell line derived exosomes

Probe Set ID	Gene Symbol	Exo SK-N-MC	Exo SB-KMS-KS1	Exo A673	Mean Exo
7919438	RN28S1	2375.41	4086.18	5362.00	3941.20
8149218	RN7SK	1607.19	2670.20	2560.66	2279.35
8112560	COX1	2482.95	1471.29	1922.48	1958.91
8165669	RNU1-1	1542.72	1903.79	2393.26	1946.59
8141166	REXO1L1	1776.06	343.12	3499.67	1872.95
8076511	CYTB	2282.31	934.11	2049.46	1755.29
7966996	FTH1	663.35	2728.45	1284.86	1558.89
8094130	NBPF1	989.27	1133.40	2207.86	1443.51
8098740	RN7SL1	654.41	1848.11	1548.73	1350.42
7942824	COX2	1558.82	870.04	1446.59	1291.82
7904974	NBPF3	827.62	1078.70	1918.65	1274.99
7919412	NBPF10	792.99	931.40	1925.45	1216.61
7960896	GAPDH	538.73	1860.29	1241.03	1213.35
8149228	NBPF14	757.77	915.70	1919.95	1197.81
8000205	NBPF11	961.60	975.36	1611.55	1182.83
7895422	RNU2-1	717.97	643.02	1927.16	1096.05
8149153	NBPF9	670.29	833.62	1584.63	1029.52
8175537	ND1	1298.70	452.62	1268.66	1006.66
7975457	SNORA3	754.30	704.68	1544.16	1001.05
7994026	ND5	1317.36	593.76	798.04	903.05
8005471	EEF1A1	344.72	1442.48	853.70	880.30
8071272	ND4	922.05	451.61	1116.48	830.05
7893438	TOB2	1053.89	223.88	1211.11	829.63
8038086	IGHA1	521.23	530.38	1271.26	774.29
7916562	ZBTB34	605.23	514.98	1182.54	767.58
8094116	PTMA	277.17	1202.27	699.67	726.37
7892853	RPL10	206.38	1202.23	721.18	709.93
7982282	RPL8	336.34	913.35	680.93	643.54
7892667	UBC	271.60	1238.64	354.93	621.72
7895556	RPS2	291.90	896.97	641.01	609.96
7919854	RPL41	284.20	951.07	556.97	597.41
7945645	GAGE12B	306.54	241.68	1171.30	573.17
8091806	ACTB	185.37	819.69	630.04	545.03

Probe Set ID	Gene Symbol	Exo SK-N-MC	Exo SB-KMS-KS1	Exo A673	Mean Exo
8149216	SNORA71D	248.78	892.79	454.76	532.11
7982307	RPLP0	155.79	1021.45	391.96	523.07
7893374	RPL23A	474.63	661.48	429.40	521.84
8031992	HIST1H1E	102.28	1064.72	389.70	518.90
8151935	RPL5	139.27	1169.58	238.25	515.70
7896511	USP17L6P	199.56	178.05	1155.22	510.94
8043502	RPL13AP5	192.95	667.89	645.78	502.21
8149161	MT2A	242.31	185.23	975.81	467.79
8151607	GUSBP3	180.20	514.52	701.37	465.36
8015206	SMA5	179.14	502.83	701.37	461.11
7982356	RPS28	183.54	512.34	662.12	452.67
7895969	YBX1	82.86	825.57	439.78	449.40
8015208	SNORD13	541.67	386.53	390.73	439.64
7960898	RPL5	138.72	941.01	216.33	432.02
8177669	KRTAP4-7	380.41	210.53	688.49	426.48
7995340	TUBB	98.71	804.15	369.36	424.07
7894098	SIAE	214.42	199.07	850.18	421.22
7893649	RPS11	246.67	648.15	318.56	404.46
8030351	GUSBP1	131.60	439.71	634.35	401.88
8067978	RPL18A	202.50	433.73	560.60	398.94
7958197	KRTAP4-12	386.64	203.55	606.59	398.93
7945652	KRTAP4-11	343.16	188.82	661.53	397.84
8005166	KRTAP5-1	219.47	116.44	827.71	387.87
7981730	OR7E87P	219.16	209.36	730.43	386.32
8007115	HMGN2	357.73	546.22	234.90	379.62
7945344	REXO1L2P	277.59	57.52	794.22	376.44
7905523	RPL13A	237.14	588.97	294.30	373.47
8015230	FLJ45340	188.14	123.00	779.54	363.56
8013348	C15orf51	284.80	113.36	690.95	363.04
8104621	EEF1G	149.01	518.04	417.71	361.59
7919436	KRTAP4-9	315.94	178.59	579.89	358.14
7986522	LOC349196	338.00	154.22	571.17	354.46
7895651	RPL18	122.80	655.25	284.49	354.18
7948679	HIST2H2BC	188.97	586.05	286.70	353.91
7919625	IGKV1-5	147.33	166.61	717.88	343.94
7899187	GP1BB	319.35	93.86	608.75	340.65

Probe Set ID	Gene Symbol	Exo SK-N-MC	Exo SB-KMS-KS1	Exo A673	Mean Exo
8110861	KRTAP5-3	203.14	149.27	664.53	338.98
7892898	RPL18AP3	160.44	470.84	380.24	337.18
8139458	PPIAL4A	230.81	433.10	344.38	336.09
7893929	UBB	178.33	522.67	281.26	327.42
7952325	POTEF	232.91	323.45	424.85	327.07
8165648	MRPL36	206.52	231.95	535.16	324.54
8151623	HAPLN4	186.16	126.14	644.47	318.92
8029129	OR7E14P	223.23	133.92	594.82	317.32
7933976	SLC25A6	125.40	642.75	166.65	311.60
8000676	POTEE	232.80	397.73	302.83	311.12
8117995	DUX4L4	102.28	35.00	782.57	306.61
7942267	RPS20	168.08	499.98	245.19	304.42
8165703	RPPH1	268.25	166.63	471.80	302.23
8117377	ACTG1	98.66	634.05	173.22	301.98
8007141	OR7E5P	211.72	184.35	484.04	293.37
8151609	GNB2L1	124.65	646.65	106.79	292.70
7986517	LOC100288034	119.04	59.13	697.94	292.04
8095362	C7orf11	234.13	71.75	569.02	291.64
7904465	USP17	106.89	99.91	657.59	288.13
8069142	NPIPL3	213.94	258.40	387.72	286.68
7986520	KRTAP5-7	167.24	91.99	599.75	286.33
7892896	RPL12	112.87	480.12	254.61	282.53
7982269	RPS3	58.35	519.56	268.29	282.07
8061364	C1orf152	84.51	237.43	523.75	281.90
8086752	CXorf18	249.94	267.34	325.67	280.98
8043438	KRTAP10-4	125.69	101.25	600.80	275.91
8144420	LOC100132217	139.90	88.79	594.97	274.55
7937483	RPS19	212.86	465.79	144.97	274.54
8026868	EIF1	139.40	567.93	112.20	273.18
8026440	IGLJ3	201.02	195.49	422.16	272.89
8144414	HSPA8	50.33	564.22	199.75	271.44
8116520	LOC613037	193.48	158.90	454.45	268.94
7938683	LOC100128364	118.81	49.53	629.70	266.01
7948113	LOC441268	170.66	185.07	431.17	262.30
7987025	SH3KBP1	152.81	36.51	590.53	259.95
8063473	NBPF15	182.11	225.37	367.18	258.22

Probe Set ID	Gene Symbol	Exo SK-N-MC	Exo SB-KMS-KS1	Exo A673	Mean Exo
7942586	NBPF16	171.00	228.31	369.47	256.26
8015218	DUX4	192.24	65.62	486.19	248.02
7900585	COX3	183.93	75.92	478.21	246.02
8035646	LCE1D	170.06	92.13	467.99	243.40
8022320	PPIA	129.79	370.33	224.94	241.68
7894678	RPL30	109.94	518.22	90.26	239.47
7982248	UIMC1	376.46	32.10	304.73	237.77
7967025	SNORA52	190.17	157.79	361.36	236.44
8073309	LRRFIP1	139.48	103.40	465.32	236.07
8055151	KRTAP5-10	105.17	85.94	510.12	233.74
8071274	KRTAP2-1	188.34	92.07	406.76	229.06
7986509	HIST2H2BA	148.12	362.72	160.88	223.91
8105991	CKS1B	89.91	189.63	389.22	222.92
8144412	HNRNPA1	84.09	259.86	320.99	221.65

VII List of upregulated transcripts in exosomes compared to their parental cells

Probeset ID	Gene Symbol	SK-N-MC		SB-KMS-KS1		A673		mean
		Exo	Cell	Exo	Cell	Exo	Cell	log2 FC
8151605	REXO1L1	1776.06	62.35	343.12	17.95	3499.67	43.94	5.5
8139458	LOC100128364	118.81	4.94	49.53	4.45	629.7	12.73	5.17
8148962	OR4F21	95.53	5.42	81.78	4.04	340.16	9.11	4.8
7896744	OR4F16	96.18	5.44	82.06	4.04	340.16	9.11	4.8
8167560	GAGE12J	34.39	3.18	43.31	3.52	330.88	10.4	4.58
8139943	SPDYE7P	63.24	7.53	22.54	4.35	451.67	11	4.55
8071049	LOC51152	58.56	3.62	22.67	3.41	232.65	6.51	4.53
8094134	USP17L6P	199.56	14.45	178.05	29.84	1155.22	29.43	4.38
7940182	OR4D10	50.88	6.18	46.43	5.95	294.65	7.85	4.29
7919580	LOC440570	70.17	5.87	45.4	4.35	247.26	9.02	4.24
7944867	SIAE	214.42	12.48	199.07	22.3	850.18	36.07	4.16
8176570	DUX4L4	102.28	14.26	35	7.8	782.57	29.54	4.16
7982084	SNORD115-11	20.6	4.95	18.67	3.46	227.29	6.97	4.11
7981724	IGHD	144.4	9.24	107.54	7.89	373.6	19.38	4.1
8135031	MUC12	71.47	5.91	18.09	3.91	309.47	13.66	4.09

Probeset ID	Gene Symbol	SK-N-MC		SB-KMS-KS1		A673		mean
		Exo	Cell	Exo	Cell	Exo	Cell	log2 FC
8094130	USP17	106.89	11.94	99.91	15.63	657.59	23.49	4.08
8015230	KRTAP4-12	386.64	19.97	203.55	12.91	606.59	49.47	3.86
7898353	LOC388692	49.02	3.2	22.08	4.78	147.78	7.86	3.79
7981722	IGHA1	521.23	47.64	530.38	44.09	1271.26	77.13	3.78
8015218	KRTAP4-7	380.41	24.01	210.53	13.59	688.49	57.35	3.75
8167573	GAGE12B	306.54	54.04	241.68	14.83	1171.3	60.96	3.73
8073309	LOC100288034	119.04	9.08	59.13	9.27	697.94	51.09	3.66
8071272	GP1BB	223.62	19.63	77.33	14.58	539.09	33.13	3.64
8144420	LOC349196	274.61	22.5	136.53	28.2	537.41	27.56	3.6
8015221	KRTAP4-11	343.16	22.49	188.82	13.69	661.53	63.09	3.59
7960896	OR7E87P	219.16	21.93	209.36	24.17	730.43	50.73	3.58
8149208	OR7E125P	88.62	8.47	52.59	7.69	283.43	21.32	3.5
7981730	IGLJ3	201.02	24.22	195.49	18.62	422.16	29.9	3.49
7912802	LOC100132147	60.33	6.61	54.75	4.67	140.65	12.44	3.43
8144422	OR7E154P	89.84	9.44	52.78	7.77	291.71	23.86	3.4
8007115	KRTAP4-9	315.94	20.54	178.59	14.79	579.89	66.33	3.4
8144440	FAM90A18	80.49	7.8	37.34	8.7	156.19	9.8	3.38
8144424	FAM90A13	80.49	7.8	37.34	8.7	156.19	9.8	3.38
8144448	FAM90A10	85.98	7.94	34.8	8.43	133.14	7.98	3.38
8064382	SRXN1	35.54	3.77	21.73	3.23	124.81	11.51	3.3
7904429	HSD3BP4	48.05	5.15	15.42	3.69	127.32	11.02	3.26
8167577	GAGE12G	49.28	6.58	40.92	5.76	165.43	14.29	3.26
7956876	LLPH	27.74	4.04	16.43	3.07	114.24	9.65	3.24
8167482	GAGE12I	47.31	6.53	40.45	5.61	159.69	14.37	3.22
8123760	LY86-AS	72.99	8.63	39.23	7.42	264.97	24.39	3.22
7925743	OR2T12	32.84	5.54	25.92	3.94	149.82	13.06	3.21
7942267	KRTAP5-10	105.17	19.45	85.94	11.35	510.12	47.27	3.17
7950490	MIR326	251.3	37.27	323.97	34.91	676.05	70.64	3.13
7945645	KRTAP5-1	219.47	36.97	116.44	22.95	827.71	77.6	3.08
7986741	GOLGA6L1	29.49	4.52	20.24	3.39	106.27	10.7	3.07
8133582	SPDYE8P	31.34	5.12	38.96	6.37	126.89	12.49	3.04
8070789	KRTAP12-4	43.03	9.6	33.86	5.74	223.54	21.59	3.02
8043438	IGKV1-5	147.33	25.16	166.61	30.71	717.88	71.56	3.02
7945652	KRTAP5-3	203.14	34.94	149.27	18.95	664.53	74.07	2.99
8007130	KRTAP9-8	20.32	4.99	19.03	3.89	125.21	12.95	2.92
7924682	LEFTY2	110.08	14.61	58.95	13.42	360.83	42.99	2.9

Probeset ID	Gene Symbol	SK-N-MC		SB-KMS-KS1		A673		mean
		Exo	Cell	Exo	Cell	Exo	Cell	log2 FC
7906017	POU5F1P4	45.68	7.25	30.2	4.2	88.76	11.7	2.83
8155521	FAM27A	121.68	15.24	113.74	16.42	299.75	49.17	2.73
7982284	LOC653075	80.27	15.44	90.81	18.52	274.54	33.55	2.72
8070777	KRTAP10-2	75.85	9.53	48.58	8.92	162.44	25.95	2.69
7981718	IGHM	65.67	11.49	55.86	9.04	133.48	21.79	2.59
7950078	KRTAP5-11	53.47	10.49	36.5	8.18	214.05	32.69	2.57
8069156	KRTAP10-11	21.61	5.39	18.47	4.07	130.21	19.97	2.53
8163729	MIR147	18.38	3.91	20.07	4.28	86.47	13.89	2.5
8149705	MIR320A	51.53	11.5	47.95	9.31	163.54	25.92	2.49
7911241	OR2L8	19.73	4.71	22.66	3.25	48.43	8.59	2.46
8020354	OR4K15	11.73	2.64	17.27	3.03	44.49	7.8	2.45
7915841	KNCN	43.6	7.99	26.38	6.34	156.87	28.16	2.42
7897991	PRAMEF7	36.14	4.92	22.4	4.52	56.99	12.43	2.4
8137330	ABCB8	64.95	15.29	78.13	12.58	349.37	70.83	2.32
7948113	OR7E5P	211.72	41.45	184.35	37.84	484.04	98.79	2.31

Acknowledgement

First of all, I would like to thank my supervisor Univ.-Prof. Dr. med. Stefan Burdach for committing me the work on such an innovative and exciting topic with great confidence and for conducting the process of this thesis with his encouraging questions and proposals. Furthermore, I want to thank PD Dr. rer. nat. Günther Richter for his continuos support with regards to all the organizational, thematic and technical questions around this project. Most notably, I thank my mentor Dr. med. Thomas Grünewald, PhD, who introduced me into the world of experimental research and spread his enthusiasm out over me. I particularly thank for his openness in discussions and the high degree of independence he taught me to develop during this project.

This project was only accomplishable due to the support of my outstanding collaboration partners. I thank Maria Lebar and Arne Kaumann from Max Planck Institute of Psychiatry for their unique cooperativeness. Moreover, I owe my gratitude to Prof. Dr. Ulrich Welsch and Sabine Tost for their kind support in performing electron microscopy. Sincere thanks I yield Graça Raposo, PhD, whose help was essential for displaying exosomes with the electron microscope and who gave advice to the publication manuscript with her sensational expertise. Particularly, I want to thank the patients and their parents taking part in this study, my colleagues in the clinic, who acquired the samples, and the generous healthy donors.

Furthermore, I thank my colleagues Dr. rer. nat. Stefanie Plehm, Dr. med. Uwe Thiel, Caroline Wernicke and Franziska Blaeschke, who helped me with their friendship and great knowledge to overcome all experimental and emotional obstacles. I am very grateful to Alice Altissimo, Maximilian Poidinger and Justus Geilhufe, who helped me to correct this manuscript. Deeply I thank Simon Früh, Max Schmidtlein and Martin Geilhufe for strengthening me with their sincere friendship and for sharing all these delighting moments in and out of the kitchen. For their unconditional love and company I warmly thank my family, Gertrud Miller, Viktoria Miller and Martin Geilhufe.

Finally, I owe words of thanks to the Dr. Sepp und Hanne Sturm Gedächtnisstiftung, who enabled the realization of this project by its generous financial support.

Publications

Original articles (peer-reviewed)

Miller IV, Raposo G, Welsch U, Prazeres da Costa O, Thiel U, Lebar M, Maurer M, Bender HU, Richter GH, Burdach S, Grunewald TG
"First identification of Ewing's sarcoma-derived extracellular vesicles and exploration of their biological and potential diagnostic implications."
Biology of the Cell 2013;105:289–303.

Miller IV, Grunewald TG
"Tumour-derived exosomes: Tiny envelopes for big stories."
Biology of the Cell 2015;107(9):287-305.

Contributions to congresses (poster presentation)

2012 May Miller IV, Thiel U, Maurer M, von Luettichau I, Welsch U, Richter GH, Burdach S, Grunewald TG
"First identification of Ewing's sarcoma derived exosomes and their diagnostic implications"
Molecular Diagnostics Europe, London/UK

2013 Jun Miller IV, Raposo G, Welsch U, Prazeres da Costa O, Thiel U, Lebar M, Maurer M, Bender HU, Richter GH, Burdach S, Grunewald TG
"First identification of Ewing's sarcoma derived exosomes and their diagnostic implications"
Paediatric Cancer Research at the Interface, Vienna/Austria